

# Detection of Explosive Materials

**Brydie Anne Moore**

A thesis presented for the degree of  
Master of Science by Research



School of Chemistry  
University of East Anglia  
September 2015

This copy of the thesis has been supplied on condition that anyone who consults it is understood to recognise that its copyright rests with the author and that use of any information derived there from must be in accordance with current UK Copyright Law. In addition, any quotation or extract must include full attribution.

## **Declaration**

I declare that the work contained in this thesis submitted by me for the Degree of Master of Science by Research is my work, except where due reference is made to other authors, and has not previously been submitted by me for a degree at this or any other university.

Brydie Anne Moore

## **Acknowledgements**

I would like to begin by thanking Professor David Russell for his irreplaceable help, support and guidance over the past year. Without which, I would not have achieved as much as I have with my research. I would also like to say a special thank you to Maria-José, Paula and Beth. I have really enjoyed working alongside you. You are all such talented scientists and I have learnt so much from you. All of you are always more than happy to help, I really couldn't have asked for a better group. I wish David, and all the group, the best in all you do.

I would like to thank Intelligent Fingerprinting for funding this research. I would like to thank Dr Jerry Walker, without his help this opportunity would not have been possible. I would also like to thank Dr Mark Hudson for his help throughout my time as an employee of Intelligent Fingerprinting. I learnt valuable skills that will stay with me for the rest of my scientific career. I would also like to say a special thank you to Stephan, Tanya, Smita, Rachel, Simon, Paul, Jalpa and Sam for their support and guidance. They have all had a huge influence on the scientist I am today, and have provided invaluable support over the past two years.

Last but certainly not least, I would like to say a massive thank you to my family. Thank you for putting up with me, rain or shine. I would certainly not have achieved half as much as I have already without your continuous encouragement and support. You all deserve the very best!

## Abstract

Explosive materials are increasingly being exploited by criminal organisations, with harmful, devastating and destructive effects on targeted societies; highlighting the demand for sensitive, reliable and quick explosive detection methods that can be used in a range of environments. Immunoassays are one type of test that can provide these qualities. Immunoassays use antibodies to detect a molecule of interest (analyte). A common type of user-friendly immunoassay that has been employed for a wide-range of applications is the lateral flow immunoassay (LFIA). A LFIA simplifies the immunoassay procedure, applying the principle (discussed in detail later) to perform along a single axis by utilising a porous membrane. This type of test is quick, sensitive and relatively easy to use, which means it is accessible by non-specialised personnel. This research uses a competitive immunoassay format, which arises from competitive binding between a free form and a bound form of the analyte. Successful detection of explosive material: 2,4,6-trinitrotoluene (TNT) has been demonstrated via a competitive immunoassay technique. Through optimisation of reagents and conditions, the limit of detection is  $0.03 \mu\text{g ml}^{-1}$  (300 pg per fingerprint deposit) on a plate assay format. Initial steps have been taken to apply this mechanism to the LFIA format to produce a test. However, further research is required before a functioning device is ready for commercial value.



# Contents

<b>1</b>	<b>Introduction</b>	<b>1</b>
1.1	Fingerprints . . . . .	1
1.1.1	Fingerprint Formation . . . . .	1
1.1.2	Fingerprint Composition . . . . .	3
1.2	Explosive Materials . . . . .	4
1.2.1	Classification of Explosives . . . . .	4
1.2.2	TNT . . . . .	7
1.2.3	Current Detection Methods of Explosives in Fingerprints . . . . .	7
1.3	Immunoassays . . . . .	14
1.3.1	Antigens . . . . .	14
1.3.2	Antibodies . . . . .	15
1.3.3	Antibody-Antigen Interaction . . . . .	18
1.3.4	Immunoassay Classification . . . . .	19
1.4	Fluorescence . . . . .	23
1.5	Thesis Outline . . . . .	27
<b>2</b>	<b>Experimental</b>	<b>29</b>
2.1	Buffers . . . . .	29
2.2	Plate Assays . . . . .	30
2.2.1	Direct Binding Plate Assay . . . . .	30
2.2.2	Competitive Plate Assay . . . . .	31
2.2.3	Quenching Studies . . . . .	32

2.2.4	Competitive Plate Assay with TNT Spiked Fingerprints . . . . .	32
2.3	Antibody Labelling . . . . .	35
2.4	Lateral Flow Immunoassay . . . . .	37
2.4.1	Material Preparation . . . . .	37
2.4.2	Direct Wick Assembly and Testing . . . . .	38
2.4.3	Lateral Flow Immunoassay Assembly and Testing . . . . .	42
2.5	Equations . . . . .	44
<b>3</b>	<b>Detection of TNT using a Competitive Immunoassay Immobilised on a 384 Well Plate</b>	<b>46</b>
3.1	Introduction . . . . .	48
3.2	Aims of the Research Described in this Chapter . . . . .	50
3.3	Results and Discussion . . . . .	51
3.3.1	Unlabelled Anti-TNT Antibody Binding Specificity . . . . .	51
3.3.2	Anti-TNT Antibody Labelling . . . . .	56
3.3.3	Labelling Effects on the Anti-TNT Antibody Binding Specificity . . . . .	62
3.3.4	Fluorescence Quenching Effects by TNT . . . . .	63
3.3.5	TNT Solubilisation Buffer Optimisation . . . . .	65
3.3.6	Plate Immunoassay Optimisation . . . . .	72
3.3.7	Competitive Plate Assay using TNT Spiked Fingerprints . . . . .	74
3.4	Conclusions . . . . .	75
<b>4</b>	<b>Developing a Lateral Flow Immunoassay Test Using a Competitive Binding Format</b>	<b>78</b>
4.1	Introduction . . . . .	79
4.2	Aims of the Research Described in this Chapter . . . . .	84
4.3	Results and Discussion . . . . .	84
4.3.1	Direct Wick Studies . . . . .	84
4.3.2	LFIA Studies . . . . .	98
4.4	Conclusions . . . . .	101

**5 Conclusions and Future Work** **103**  
5.1 Conclusions . . . . . 103  
5.2 Future Work . . . . . 106

**6 References** **108**

**109**

# Chapter 1

## Introduction

The aim of the research described in this thesis was to detect explosive materials in fingerprints with a competitive immunoassay technique. This chapter will begin with a description of the formation and composition of fingerprints. Next, the classification of explosive materials will be discussed, looking at the current techniques being developed to detect explosive materials in fingerprints. The final part of this chapter will focus on the competitive fluoroimmunoassay technique used in this research, with a description of fluorescence.

### 1.1 Fingerprints

Fingerprints have vast potential in forensic analysis as they are thought to be unique to an individual<sup>[1]</sup>. Fingerprints are therefore a valuable tool for linking identification to criminal activity, whether that be locating an individual to a crime or detecting an illegal substance handled or metabolised by an individual.

#### 1.1.1 Fingerprint Formation

Fingerprints are impressions of a friction ridge pattern located on the fingertips, formed from sweat secretions that are deposited upon contact with a surface<sup>[2]</sup>. The friction ridge pattern is a thickened layer of skin which begins development

in the womb. It is both genetically and environmentally influenced by factors, such as the fetus' position within the womb<sup>[1]</sup>. This results in even identical twins, who share the same DNA, having differing fingerprints<sup>[3]</sup>. The friction ridge pattern begins development in the womb at around seven to ten weeks. By the nineteenth week, the pattern becomes permanent, unchanging throughout an individual's life<sup>[4]</sup>. The friction ridge skin covers the surface of the palms, fingers, soles and toes. It forms a complex pattern involving arches, loops and whorls as seen in Figure 1.1<sup>[5]</sup>. Although other patterns do occur, they are more rare. As demonstrated in Kücken and Newell<sup>[1]</sup>, loops can be classified by an arch, which opens towards the thumb or the finger. The former is given the term radial and the latter is termed ulnar. Loops are accompanied by one triradius, which is the meeting of three ridge patterns at  $120^\circ$ . A whorl pattern consists of a spiral with the addition of two triradii<sup>[1]</sup>. Defects in the patterns are referred to as minutiae<sup>[6]</sup> and can consist of dislocations, islands and incipient ridges<sup>[1]</sup>. There can be up to 70 minutiae per fingerprint<sup>[7]</sup>. It is the minutiae in the patterns that are exclusive to an individual, which allows for discrimination between different fingerprints for identification purposes<sup>[1]</sup>.

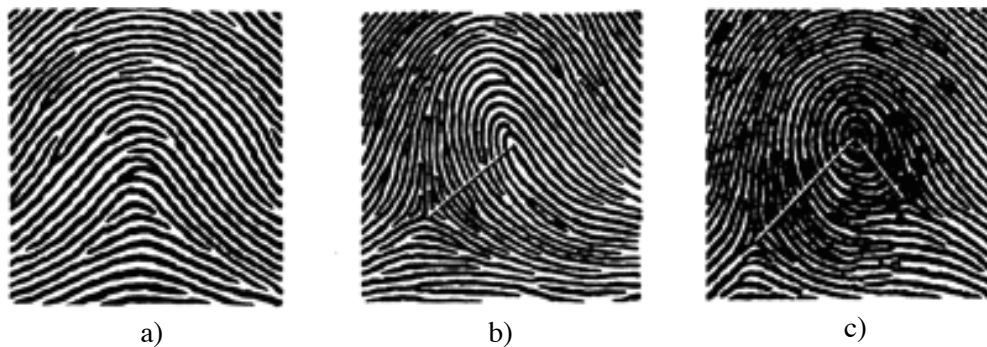


*Figure 1.1: Fingertip ridge patterns: a) arch; b) loop; and c) whorl. Image from Kahn<sup>[8]</sup>.*

### 1.1.2 Fingerprint Composition

As well as identifying an individual through fingerprints, it is also possible to detect substances ingested or handled through the fingerprint depositions. As stated previously, fingerprint deposits are composed of an individual's sweat secretions. The sweat is secreted from pores within the fingertip ridges. There are three main types of sweat secreted from the body, which include eccrine, apocrine and sebaceous. Each type of sweat has a different composition and is secreted in varying locations. The eccrine glands are concentrated in the hands and feet, although they can be found in most parts of the body. Eccrine sweat is composed of ~98% water, where the remaining ~2% is composed of both organic ( *e.g.*, amino acids, lipids, glucose) and inorganic ( *e.g.*, chloride, iron, calcium) components<sup>[2]</sup>. The apocrine glands are present from birth but do not become activated until puberty. They are primarily located in the axilla and genital areas of the body<sup>[9]</sup>. The sebaceous glands are located all over the body, apart from the hands and feet<sup>[10]</sup>. Sebaceous sweat is called sebum, which is a waxy substance that helps waterproof, as well as hydrate, the skin<sup>[11]</sup>. The sebum is mainly composed of lipids, lipid esters and sterols<sup>[2]</sup>.

As fingertip ridges are lined with eccrine sweat pores, deposited fingerprints are mainly composed of eccrine secretions. Fingerprints often contain varying levels of sebaceous secretions from contact of the hands with the hair and face; as well as excreted metabolites from the body, and contaminants that the hands have come into contact with<sup>[2]</sup>. Fingerprint composition can also vary dependent on factors such as diet/contaminants<sup>[12]</sup>, gender<sup>[13]</sup>, age<sup>[14]</sup>, and contact pressure/time of fingerprint deposition<sup>[15]</sup>. Therefore, fingerprints are useful for identification purposes as well as detecting substances that an individual has ingested (from excreted metabolites) or handled.

The ability to detect suspicious contaminants in fingerprints provides a non-

invasive method to link a handled substance with the identification of a handler. There have already been methods demonstrated that detect drugs of abuse in fingerprint deposits<sup>[16]</sup>. However, there is a pressing need to be able to detect explosive materials due to criminal activity that exploits explosive substances. The strong advantage of being able to detect explosive materials in fingerprints is that it offers a method to identify those who have handled explosive substances, in the hope of preventing catastrophic and devastating events from occurring.

## 1.2 Explosive Materials

### 1.2.1 Classification of Explosives

Explosive materials are energetic molecules that rapidly decompose through a self-propagation mechanism upon initiation by stimuli, such as sparks and friction<sup>[17]</sup>. This process results in the sudden release of heat and gases as more stable products are formed<sup>[18]</sup>. The blast is the build up of pressure that occurs when large quantities of gas are produced which require a much bigger volume than the starting material<sup>[19]</sup>. Explosive materials can detonate or deflagrate depending on the strength of the shock wave generated by the ignition source<sup>[19]</sup>.

Explosive materials are commonly classified by their characteristics. Firstly, they can be divided by their burn rates into high ( $\sim\text{km s}^{-1}$ ) or low explosives ( $\sim\text{cm s}^{-1}$ ). High explosives are further categorised by their stability into primary, secondary and tertiary explosives, with primary explosives being the most sensitive to initiation. Low explosives are composed of propellants and pyrotechnics. Propellants are used to propel or accelerate compounds in rockets and guns, for example gunpowder<sup>[20]</sup>. Pyrotechnics, like all explosive materials, undergo exothermic reactions and release heat, light, sound and gas. Common uses of pyrotechnics are for fireworks, flares and matches<sup>[21]</sup>. Explosives can also be classified by their chemical structure. The majority of explosives fall into one of the categories

of nitroaromatics, nitroamines, nitrate esters, peroxides or acid salts. Table 1.1 summarises these properties of common explosives. Note that high explosives detonate, whereas low explosives deflagrate. The explosive material that was the focus of this research is 2,4,6-trinitrotoluene (TNT), a high explosive.



Table 1.1: Explosive Material Classification Summary <sup>a</sup>

Explosive Material	Classification			Chemical Group
	Abbreviation	High or Low	Primary, Secondary or Tertiary	
Triacetone triperoxide	TATP	High	Primary	Peroxide
Lead Azide	-	High	Primary	Inorganic
2,4,6-trinitrotoluene	TNT	High	Secondary	Nitroaromatic
2,4-dinitrotoluene	DNT	High	Secondary	Nitroaromatic
2,4,6-trinitrophenol (picric acid)	TNP	High	Secondary	Nitroaromatic
Ethylene glycol dinitrate	EGDN	High	Secondary	Nitrate ester
Pentaerythritol tetranitrate	PETN	High	Secondary	Nitrate ester
Tetranitro-triazacyclohexane	RDX	High	Secondary	Nitramine
Tetranitro-N-methylaniline	Tetryl	High	Secondary	Nitramine
Tetranitro-tetraazacyclooctane (octagon)	HMX	High	Secondary	Nitramine
Nitromethane	NM	High	Secondary	Aliphatic nitro
Ammonium nitrate	AN	High	Tertiary	Acid Salt
Blackpowder	-	Low	Propellant	Mixture of compounds ( <i>primarily KNO<sub>2</sub></i> )

<sup>a</sup>Table adapted from Singh<sup>[18]</sup> and Senesac and Thundat<sup>[17]</sup>.

### 1.2.2 TNT

The nitroaromatic molecule: TNT, is a secondary high explosive. The structure is shown in Figure 1.2. It has a low molecular weight of  $227.13 \text{ g mol}^{-1}$  and relatively low solubility in water of  $130 \text{ mg L}^{-1}$ . TNT was originally used as a yellow dye for industrial applications, since 1863. Its explosive properties were not discovered until 1891 by Carl Haeussermann, primarily due to its insensitivity to detonation<sup>[22]</sup>. However, it is now the most commonly used explosive in the military. This is because of its insensitivity and low melting temperature ( $83^\circ\text{C}$ ). This allows for a molten solution to be poured for ammunition production. TNT is also highly toxic to a diverse range of organisms, and an environmental contaminant. TNT is toxic to humans *via* inhalation, ingestion and absorption through the skin. It is metabolised by the liver, primarily into: 2-amino-4,6-dinitrotoluene and 4-amino-2,6-dinitrotoluene. Exposure to TNT has resulted in many adverse health effects, including anaemia, headaches, nausea and liver disease, as well as damaging effects to reproductive functioning<sup>[23]</sup>. TNT is also suspected to be a carcinogen<sup>[24]</sup>.

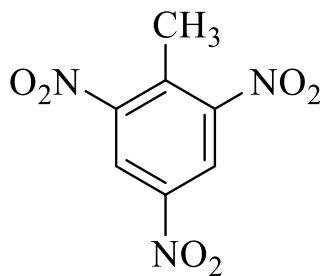


Figure 1.2: The structure of TNT.

### 1.2.3 Current Detection Methods of Explosives in Fingerprints

The criminal use of explosive materials may involve a variety of substances<sup>[25]</sup>. This requires detection methods to be able to differentiate between a wide range

of explosive materials with high sensitivity, as there are often only trace levels of tested residue. The use of latent fingerprints for the detection of explosive material can identify trace levels of substance as well as the handler. This link is critical for determining responsibility for a criminal activity, and is not provided by many other techniques. However, latent fingerprints are invisible to the naked eye, and require treatment for visualisation and detection of substances. With this in mind, detection of explosives in latent fingerprints has been explored using many different methods. An ideal detection method would be quick, low-cost, non-invasive, non-destructive to the print, transportable, and exhibit high sensitivity and reliability. The need for these techniques to be highly sensitive is emphasised by the variability in quantity and distribution of material between different fingerprints<sup>[26]</sup><sup>[27]</sup>. If these techniques will be used for prosecution applications, reliability and accuracy are essential.

## Mass Spectrometry

Mass spectrometry (MS) is a technique which measures the mass-to-charge ratio and relative abundance of ions<sup>[28]</sup>. Briefly, MS requires a sample to be ionised; a mass analyser to separate the species according to their mass-to-charge ratio; and a detector that converts the energy from the incoming particles into a signal that can be interpreted by a computer of the spectrometer. There are many variations of the MS technique, with different ion sources, mass analysers and detectors available. The different MS methods have their own strengths and weaknesses, but all provide a large amount of chemical information along with high chemical sensitivity. This has resulted in different types of MS being used for explosive detection in fingerprints<sup>[29]</sup>, including: desorption electrospray ionization (DESI); direct analysis in real time-MS (DART-MS); and surface-assisted laser desorption/ionization-time of flight-MS (SALDI-TOF-MS). In 2008, Ifa et al.<sup>[29]</sup> used DESI to detect RDX in a deposited fingerprint, whilst also providing an image of the fingerprint. The results were obtained, with images having a resolution of 150  $\mu\text{m}$ , *i.e.*, one pixel corresponds to a 150  $\mu\text{m}$  by 150  $\mu\text{m}$  area of the sample. The conditions pro-

vided a limit of detection at 5  $\mu\text{g}$  of RDX. In 2012, Rowell et al.<sup>[30]</sup> performed a comparative study between DART-MS and SALDI-TOF-MS for the detection of explosive contaminants in lifted and non-lifted fingerprints. A range of explosive materials were tested, including TNT, RDX, PETN, HMX, TATP, TNG and Tetryl. A novel approach was taken to locate and enhance the explosive materials in the fingerprints by applying magnetisable-doped silica-based sub-micron particles. The particles were added after dusting the prints and then lifted with tape, ready for analysis. In non-lifted fingerprints, both DART-MS and SALDI-TOF-MS successfully detected the explosive contaminants in the prints, with a detection limit of 10-100 ng. However, only SALDI-TOF-MS could detect the explosive residues in the lifted fingerprints. This was due to the high background level from the tape that prevented substance discrimination. Clemons et al.<sup>[31]</sup> used a DART-MS method in conjunction with direct analyte-probed nanoextraction (DAPNe-DART-MS). This was used to detect the explosive materials TNT and RDX at a sample particle size of  $\sim 20 \mu\text{m}$ . Hence, this method provided sensitive analysis whilst keeping the fingerprint intact. One of the most sensitive techniques for material determination is mass spectrometry (MS) coupled with gas chromatography (GC-MS)<sup>[32]</sup>. However, GC-MS, as well as most types of MS, is a difficult technique to apply to security environments as they are expensive, not portable and often require trained personnel to operate the equipment.

## **Ion Mobility Spectrometry**

Ion mobility spectrometry (IMS) is the most widespread technique employed for explosive residue detection in airports<sup>[33]</sup>. A range of handheld IMS devices already exist, for example Quantum Sniffer QS-H150 (Implant Sciences Corporation), MicroHound (Sandia National Laboratories) and Mobile Trace (Morpho Detection)<sup>[34]</sup>. Developments in IMS have resulted in the technique having strong advantages, including rapid data acquisition, high sensitivity and portability. In 2014, Staymates et al.<sup>[35]</sup> demonstrated detection of RDX in lifted fingerprints using IMS. This novel technique also has the advantage of ensuring the fingerprint

was kept intact for imaging and identification. Although, improvements on the solution used to lift the fingerprints is necessary to reduce background signal for increased discrimination between materials. Although IMS has its advantages, it can be difficult to quantify the results and false positives can be observed from contaminants or other molecules within the sample matrix<sup>[36]</sup>.

## **Vibrational Spectroscopy**

Vibrational spectroscopy measures the vibrational energy levels associated with the chemical bonds in the structure. Molecules contain different vibrational motions, or modes, that can be affected by a number of different factors, including atom and bond orientation, atomic mass, bond order and hydrogen bonds. The patterns of vibrations relate to molecular symmetry, molecular shape, and strength of each bond. Hence, vibrational spectroscopy can provide large amounts of chemical information. The main types of analytical techniques that use vibrational spectroscopy are Infrared spectroscopy (IR) and Raman spectroscopy.

IR is the most commonly used of the two techniques. For a molecule to be IR active, the molecule must exhibit a change in molecular dipole moment during vibration<sup>[37]</sup>. Primarily, molecules with non-polar bonds and non-symmetric vibrations are detected with IR. Generally, IR involves a sample being irradiated with radiation from the IR region of the electromagnetic spectrum. The molecules within a substance absorb wavelengths of light whose energies correspond to particular molecular vibrations within the molecule. The different absorbance intensities at different wavelengths of light are measured to provide a characteristic IR spectrum for a given molecule. This is known as a molecule's "fingerprint" region, as the absorbance pattern is unique to a molecule. Like most spectroscopy techniques, there are variations in the methods and each with their own strengths and weaknesses. In 2014, Fernández de la Ossa et al.<sup>[38]</sup> used near infrared hyperspectral imaging (NIR-HSI) technique to detect numerous explosive materials (ammonium nitrate, dynamite, blackpowder, single-base and double-base smoke-

less gun powder) in fingerprints. The method had a quick analysis time, preserved the fingerprint integrity, and also didn't require sample preparation. However, the small test area could prove problematic and the sensitivity still required investigation. In the same year, Fernández de la Ossa et al.<sup>[39]</sup> also demonstrated NIR-HSI to detect dynamite and ammonium nitrate. This technique provided 100% specificity with a spatial detection limit of 300  $\mu\text{m}$ . Another type of IR is Fourier transformation-IR (FT-IR), which can have improved sensitivity and reduced measurement time compared to IR, as all IR wavelengths are measured simultaneously<sup>[40]</sup>. The intensities are interpreted by a mathematical technique called the Fourier transformation, processed by a computer linked to the spectrometer. Bhargava et al.<sup>[41]</sup> employed a FTIR spectroscopic imaging technique, which is neither invasive nor destructive of the latent fingerprint. Detection of the explosive material (RDX) was demonstrated along with an imaged and preserved fingerprint. Chen et al.<sup>[42]</sup> also demonstrated detection of RDX ( $\sim 0.1 \text{ ng pixel}^{-1}$ ) within contaminated fingerprint deposits using FTIR imaging. FTIR does not require sample preparation, which maintains the integrity of the fingerprint. The prints are high enough quality to be used for matching in databases. Mou and Rabalais<sup>[43]</sup> demonstrate a technique that couples an attenuated total reflection microscope to FTIR (ATR-FTIR) for the detection of TNT, TNB and ammonium nitrate. This method allowed for the discrimination between fingerprint and explosive residue, as small as 20  $\mu\text{m}$ . This technique is also non-invasive.

In Raman spectroscopy, a molecule must exhibit a change in its polarisability to be Raman active. This involves an alteration in the size, shape or orientation of the electron cloud that surrounds the molecule. A sample is irradiated with visible light where the molecules then absorb and reemit. Some of this energy is absorbed by the molecular vibrations, causing a small portion to reemit at a different frequency than the incident light. Light can be scattered either elastically or inelastically. The former refers to Rayleigh scattering and is the most common of the two. The latter is known as Raman scattering and involves the transfer

of energy between the molecule and photons. These molecules may return to a higher or lower vibrational energy level. Hence, the Raman scattered light will either have lost (Stokes shift) or gained (anti-Stokes shift) energy, in comparison to the incident light<sup>[40]</sup>. Raman spectroscopy has the advantage of being able to maintain sample integrity as the method only requires illumination of the sample along with minimal sample preparation, and hence, is classed as a non-destructive technique<sup>[44]</sup>. The technique can analyse matter in any state and has already been shown possible to be used as a portable device<sup>[45]</sup>. Malka et al.<sup>[46]</sup> show a portable technique that can provide Raman spectra of contaminated fingerprints (ammonium nitrate, urea, urea nitrate, 2,4 and 3,4 DNT, potassium nitrate, TNT, RDX, HMX and PETN) along with an image of the deposited fingerprint. The method proved to be a highly sensitive technique, with a limit of detection being  $\sim 1$  ng. The primary challenge Raman spectroscopy faces is the high fluorescence background signal that can occur with certain incident light wavelengths<sup>[45]</sup>.

### **Laser Induced Breakdown Spectroscopy**

Laser induced breakdown spectroscopy (LIBS) is an atomic emission spectroscopy technique, which can provide the composition of a molecule. Through high energy laser pulses applied to a sample, a plasma of ionised matter is formed. The light emission from the plasma provide characteristic spectra, which can provide the composition of the sample<sup>[47]</sup>. The advantages of LIBS are that no sample preparation is required, it is sensitive, has fast analysis, can be used for any type of matter and can be used as a stand-off technique in explosive material detection. Stand-off techniques provide safety by allowing distance between those operating the detection equipment and the sample<sup>[25]</sup>. In 2006, López-Moreno et al.<sup>[48]</sup> were the first to demonstrate the use of a LIBS sensor for stand-off detection for a variety of different explosive substances, including TNT, RDX and C4 in fingerprint deposits. The sensor could detect  $\sim 5$   $\mu\text{g}$  in a fingerprint deposit at a 30 m range. However, a limitation of LIBS is its difficulty in discriminating between explosive residues and materials of similar composition. There have been different

approaches to address this problem, including De Lucia et al.<sup>[49]</sup> who employed a double-pulse LIBS method that aims to reduce the influence that atmospheric nitrogen and oxygen have on the signal; and Moros et al.<sup>[50]</sup> that present a mathematical algorithm. In 2011, Abdelhamid et al.<sup>[51]</sup> use optical catapulting-LIBS (OC-LIBS) to detect TNT, DNT and MNT. OC-LIBS also provides a means to discriminate between explosive and non-explosive residues; however, the method requires access to the back of the sample. Lucena et al.<sup>[25]</sup> goes on to develop a LIBS technique, which involves scanning and locating a surface (aluminium or glass) that contains fingerprint deposits contaminated with different explosive residues (DNT, TNT, chloratite, RDX and PETN). This method provided 100% sensitivity for the recognition of explosive contaminated fingerprints at 31 m. It was highlighted that environmental problems such as weathering affect the quality of the print. LIBS offers many advantages but faces challenges in variability, due to differences in energy of the laser with each pulse. The analysed sample area is typically a few micrometres across and down, and so can be misrepresentative of the bulk of the sample when in solid form.

### **Colorimetric Sensors**

Colorimetric sensors are based on a colour change of a solution in the presence of the molecule of interest. By measuring the absorbance of the solution, it is possible to determine the concentration of the molecule of interest using the Beer-Lambert law. Dorozhkin et al.<sup>[52]</sup> demonstrate a specific colorimetric test for field detection of nitrogen dioxide based explosive compounds on different surfaces, including fingerprints. The molecule (cymantree) which senses the nitrogen dioxide turns a deep blue colour upon exposure to the nitrogen dioxide and UV irradiation. More recently in 2015, Cross et al.<sup>[32]</sup> developed a colorimetric method that involves the pre-treatment of a glass surface to detect urea nitrate. This test has the advantage of using a molecule (9,10-diphenylanthracene) that enhances the visualisation of the fingerprint. The test involves two different solutions that can detect the urea nitrate by turning a yellow (p-dimethylaminobenzaldehyde) or



red (p-dimethylaminocinnamaldehyde) colour when in contact with urea nitrate. Thus, the method provides a quick and simple test for the detection of deposited prints that are contaminated with urea nitrate. Although colorimetric sensors can provide easy to use devices for non-specialised personnel as well as a cheap alternative to many other detection systems, colorimetric sensors can lack sensitivity from interference from other molecules or the matrix<sup>[52]</sup>.

The technique used in this research is a competitive immunoassay, which will be described in detail below (Section 1.3). There have been no studies reported that demonstrate the detection of explosive residue in fingerprints, using an immunoassay technique. However, Chapter 3 discusses the literature for the detection of explosives with immunoassays, in general.

## 1.3 Immunoassays

Immunoassays are a type of analytical test that detect the presence or quantity of a molecule of interest (analyte), with the use of antibodies. The test applies a mechanism that is central to an animal's immune system, based on a high affinity interaction of an antibody and its substrate, an antigen. To appreciate this technique, it is important to understand the two terms: 'antigen' and 'antibody' and their interaction.

### 1.3.1 Antigens

An antigen is a substance that is recognised as non-self or foreign in an animal. For example, an antigen could be a protein present on a pathogenic microorganism. The antigen generally contains a short sequence of amino acids which is responsible for antibody-antigen binding, called the epitope or antigenic determinant<sup>[53]</sup>; however, any chemical species can be an antigen. This accounts for the ability of the immunoassay technique to detect a vast range of analytes<sup>[54]</sup>. Technically,

antigens that evoke an immune response and consequently antibody production are termed immunogens<sup>[55]</sup>. Hence, an immunogen is an antigen, but an antigen is not necessarily an immunogen. In an immunoassay, the analyte replaces the term antigen to refer to the substrate that the antibody is detecting and binding to.

### 1.3.2 Antibodies

#### Antibody Classification

Antibodies are produced in the body to bind to the antigen that has elicited the response, which is important for identifying and eradicating the foreign substance, such as pathogens. Hence, this mechanism has to be a highly specific interaction to prevent incorrect binding. Antibodies are large glycoprotein immunoglobulins (Igs)<sup>[56]</sup>. There are different classes of Igs; for example, humans have five classes: IgA, IgD, IgE, IgG and IgM. All classes are composed of heavy (~50 kDa) and light (~25 kDa) polypeptide chains, along with variable and constant regions for a given species. Each Ig class has a different biological function which is determined by their heavy chains. This is due to the constant regions being located at the carboxyl termini of the heavy chains, and is the area responsible for binding to effector targets<sup>[57]</sup>.

For scientific research purposes, antibodies can either be monoclonal or polyclonal. This is dependent on how they were raised, and consequently provides different characteristics and advantages. Polyclonal antibodies are acquired by injecting the antigen, *i.e.*, the analyte (or analyte-carrier conjugate for small molecules), into an animal. Blood is taken from the animal and once antibody concentrations are at appropriate levels, purified antisera (sera containing antibodies) are obtained from these collections<sup>[53]</sup>. This results in antibodies from different cell lineages recognising the same antigen, by binding to different epitopes. Polyclonal antibodies are cheap and relatively quick to produce, however they lack specificity and

are not very reproducible. Monoclonal antibodies are produced from hybridoma cells from the same cell lineage, resulting in identical clones. Hence, monoclonal antibodies all recognise the same epitope on the analyte<sup>[58]</sup>. This means monoclonal antibodies share the same specificity and are reproducible, although they are more expensive and take longer to produce compared to polyclonal antibodies. Note that even though monoclonal antibodies have the same specificity, it does not necessarily mean that monoclonal antibodies have higher specificity. For example, a monoclonal anti-TNT antibody may bind to toluene, dinitrotoluene and trinitrotoluene (TNT) if the antibody recognises the toluene structure that is common to all three molecules. Primary antibodies bind to the analyte; and secondary antibodies bind to the primary antibody. The primary antibody that is raised against a substance is termed 'anti-substance antibody', with respect to immunoassays it will be anti-analyte antibody, *e.g.*, anti-TNT antibody.

### **Antibody Structure**

The most commonly used antibody and Ig class in immunoassays is the IgG, primarily due to its bioavailability in sera. The IgG is composed of four polypeptide chains: two identical heavy polypeptide chains and two identical light polypeptide chains. The chains are linked by disulphide bridges. The chains are formed from repeating units of ~110 amino acids in length, which fold to form the globular Ig domain. There are multiple Ig domains which make up the Ig structure, and provide the characteristic Y-structure. This Ig domain consists of two layers of beta-pleated sheets consisting of around five anti-parallel polypeptide chains that are connected by a disulphide bridge. There are small loops which join the strands that are next to each other, and it is these loops which consist of some of the most highly variable sequences in the IgG structure. These loops are thus responsible for antigen recognition<sup>[59]</sup>. The actual sequence of amino acids on the antibody which binds the antigen is called the paratope. This is a complementary sequence to the epitope on the antigen. The fragment antigen binding (Fab fragment) region encompasses all regions involving antigen recognition, *i.e.*, the paratope and

hypervariable loops. There are two Fab fragments on an IgG molecule, and they are located at the amino termini of the heavy and light chains. Hence, one antibody has the potential to bind to two antigens. At the carboxyl termini of the heavy chains, or the 'tail' of the antibody, lies the fragment crystallizable (Fc) region. The Fc region is constant between Igs of the same class within a species. As stated previously, it is this region of the antibody which determines its biological function<sup>[57]</sup>. Figure 1.3 summarises the structure of an IgG antibody.

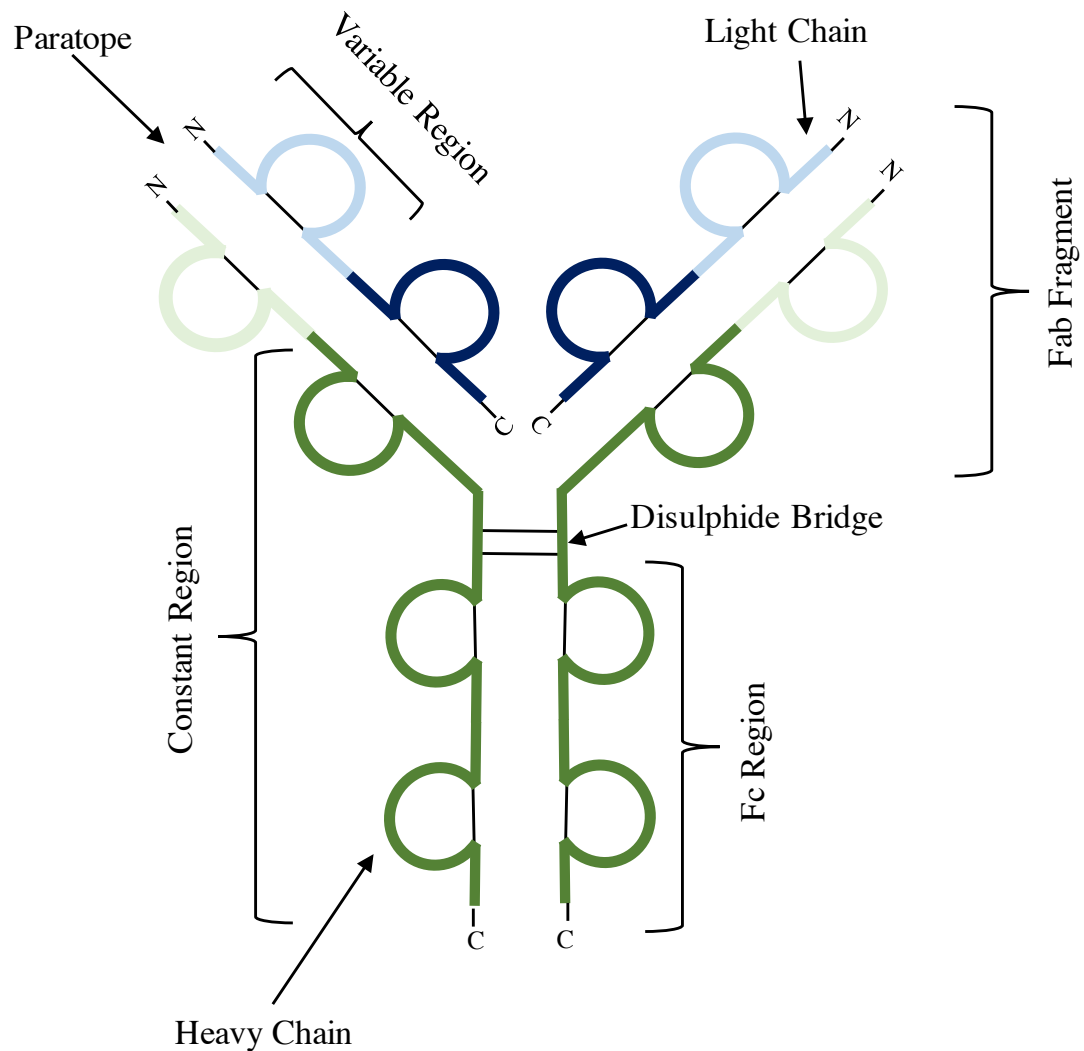


Figure 1.3: The structure of an antibody (IgG). Heavy chains are shown in green and light chains are shown in blue. Constant regions are dark green (heavy chains) and dark blue (light chains); whereas, variable regions are light green (heavy chains) and light blue (light chains). Black lines represent disulphide bonds. Adapted from Janeway et al.<sup>[57]</sup>

### 1.3.3 Antibody-Antigen Interaction

The primary antibody-antigen interaction is a rapid process that involves the binding between the complementary epitope and paratope, providing specificity. It is a high affinity interaction ( $10^5$  to  $10^{12}$  association constant)<sup>[58]</sup> requiring extreme pH or salt concentrations to break it<sup>[56]</sup>. However, it involves fairly weak,

non-covalent interactions, which suggests that the interaction occurs over a large area of the Fab region. For multivalent antigens, secondary binding does occur, *i.e.*, multiple antibodies bound to one analyte, forming aggregations. However, this does not apply to the small analyte (TNT) used in this research.

### 1.3.4 Immunoassay Classification

Methods vary between different immunoassays but all require an immobilised component, labelled component and free analyte sample. There are numerous ways immunoassays can be classified, though, most simply is to define them by non-competitive or competitive. Non-competitive assays produce a signal which is *directly* proportional to the amount of analyte in the sample; whereas, competitive assays result in a signal that is *inversely* proportional to the amount of analyte present in the sample<sup>[60]</sup>. The assays can be further categorised into homogenous and heterogeneous. Immunoassays involve the binding between an antibody and an analyte, and consequently there are often unbound elements. In order to obtain a measurement from the immunoassay, the unbound analyte may need to be separated from the bound analyte (heterogeneous) or can be measured without separation (homogenous). Immunoassays are also classified by the type of label used. The most common types of label used are fluorescent, enzyme, radioactive and chemiluminescent<sup>[56]</sup>.

The format used in this research is a competitive fluoroimmunoassay, *i.e.*, detection through the use of a fluorescent label. In this research, the anti-TNT antibody is either unlabelled or labelled with the fluorescent dye: Alexa Fluor 488 (AF488). The anti-TNT antibody is primarily used in its labelled form; however, a labelled secondary antibody is required if the anti-TNT antibody is not labelled. Note that the primary and secondary antibody are both labelled with the same fluorescent dye (see Section 1.4). Competitive immunoassays are primarily used in the detection of small molecular weight substances, such as TNT.

This is due to the method requiring the analyte to be bound by only one antibody; as opposed to non-competitive immunoassays, which require multiple antibodies binding to one analyte, *i.e.*, sandwich immunoassays<sup>[61]</sup>. Multiple antibody binding is problematic for small molecules due to accessibility difficulties, and often small analytes may be univalent (one epitope). In this research the competitive immunoassay is performed on a plate and a lateral flow immunoassay (LFIA) format. The following components are required for both formats: an immobilised, bound form of the analyte; a free form of the analyte; and an AF488 labelled antibody (primary or secondary). The bound analyte is achieved by conjugating the analyte to a large protein, which in this case is bovine serum albumin (BSA).

The competitive plate immunoassay for both labelled and unlabelled anti-TNT antibody is illustrated in Figure 1.4. The bound form of the TNT (BSA-TNT) is first immobilised on the solid surface material, *i.e.*, the wells of a 384 well plate. A sample, containing the free analyte (TNT) is added to the system, along with anti-TNT antibody (primary antibody). The free TNT and the anti-TNT antibody interact with one another, resulting in the anti-TNT antibody binding the TNT. As the free TNT concentration is increased, the more anti-TNT antibody binding sites are occupied by the free TNT. This reduces the amount of antibody available to bind to the immobilised BSA-TNT. The system is washed, which means that any anti-TNT that is not bound to the BSA-TNT will be removed. With labelled anti-TNT antibody, the wells can then be immediately measured for fluorescence intensity. If unlabelled anti-TNT antibody is used, a labelled secondary antibody is added. The secondary antibody binds to any anti-TNT antibody that is bound to the BSA-TNT, as any other anti-TNT antibody will have been removed from the washing step. The more labelled antibody (primary or secondary) bound to the BSA-TNT, the higher the fluorescence intensity. Therefore, as the free TNT concentration increases, the less antibody available to bind to the BSA-TNT, and the lower the fluorescence intensity. Hence, the fluorescence signal emitted is *inversely* proportional to the amount of free TNT in the sample.

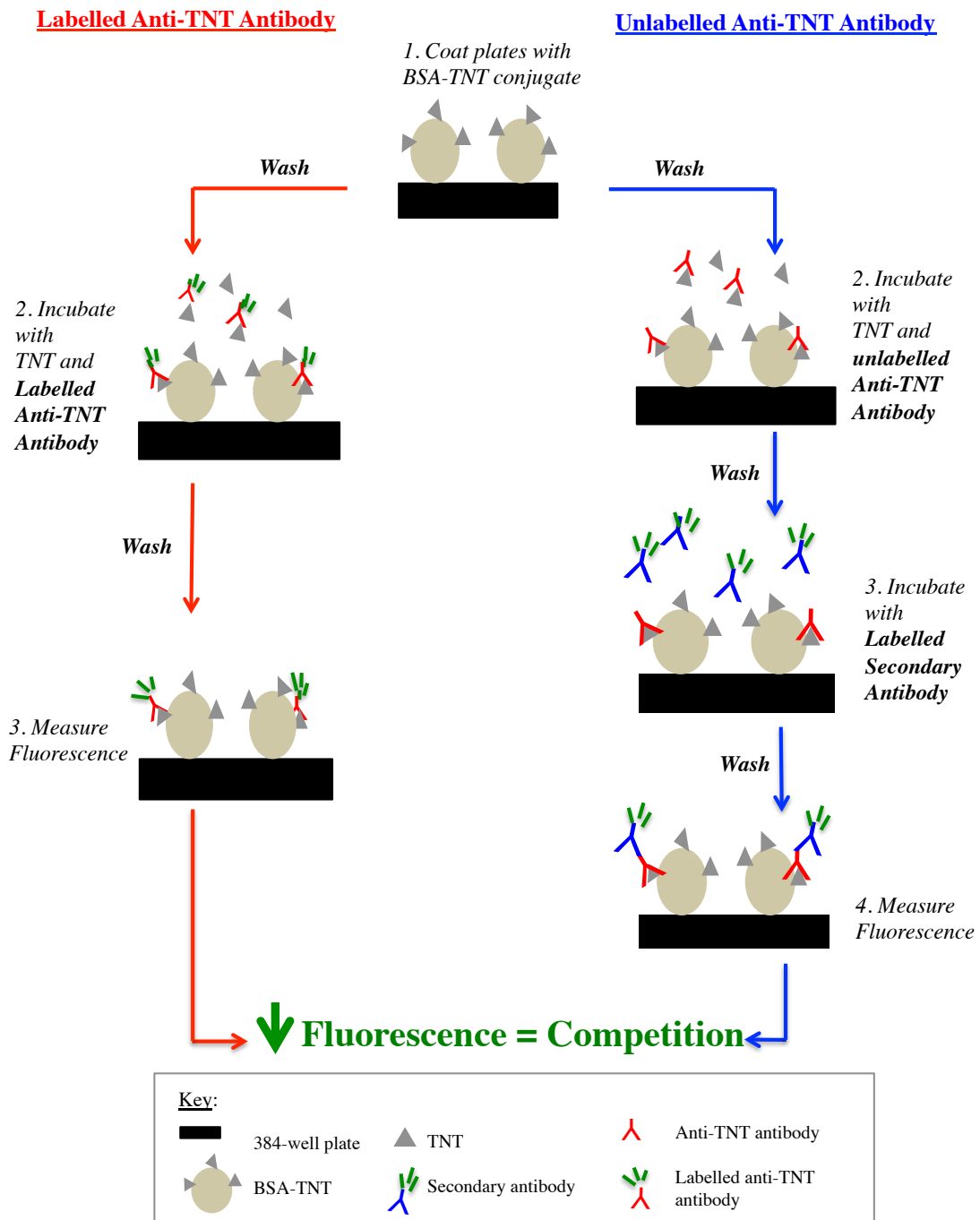


Figure 1.4: Summary of the competitive plate assay with labelled (red arrows) and unlabelled (blue arrows) anti-TNT antibody. The plate is washed three times with 100  $\mu$ l of 10 mM phosphate buffer with 80 mM NaCl and 0.22 mM Tween 20, pH 7.4 (PBST). The plate is incubated at 37°C.



The same competitive immunoassay principle involved in the plate immunoassay was applied to the LFIA. In the LFIA format, BSA-TNT is deposited onto nitrocellulose instead of the wells of a plate. The deposited BSA-TNT is referred to as the test line. A second line, called the control line, is deposited with horse anti-mouse secondary antibody. This is unlabelled and is deposited further up the strip from the test line. The control line binds anti-TNT antibody as a check that the test has functioned properly, *i.e.*, antibody has passed over the test and control lines. The nitrocellulose with deposited lines is referred to as the test strip. The anti-TNT antibody is deposited onto material that is termed the conjugate pad. The sample pad is the material where the fingerprint, and consequently the free TNT, are deposited. A solubilisation buffer is required, which solubilises the analyte (TNT) and antibody (anti-TNT antibody) as it wicks through the assembled test. The term 'wick' is used to describe the movement of a solution by capillary action. To ensure movement of the solution through the test, an adsorbent pad is assembled at the end of the test strip to draw the liquid through<sup>[62]</sup>. The preparation and assembly of the materials used in the LFIA are described in Section 2.4. Once the components have been assembled, solubilisation buffer (see Section 2.1) is added to the sample pad. The free TNT is solubilised as the solution moves through the sample pad. The solubilisation buffer, which contains the solubilised TNT, then moves into the conjugate pad, which contains the AF488 labelled anti-TNT antibody. The solution solubilises the anti-TNT antibody. The free TNT and anti-TNT antibody can then interact as they move along the test strip, resulting in the antibody binding the TNT. The test and control lines are at the end of the test strip, just before the adsorbant pad. As in the plate assay, the anti-TNT antibody can not bind to the BSA-TNT (test line) when bound to the free TNT. Therefore, the higher the concentration of free TNT in the sample, the lower the concentration of labelled anti-TNT antibody available to bind to the test line, and the lower the fluorescent signal. Thus the plate assay and LFIA have exactly the same response to free TNT in the sample, which is that the fluorescence signal is inversely proportional to the concentration of free TNT in

the sample.

## 1.4 Fluorescence

As stated above, in this research the technique employed is a competitive fluoroimmunoassay, where the antibody is labelled with a fluorescent dye (AF488). The fluorescence signal is measured, which provides a relative intensity that is indirectly proportional to the amount of TNT in the sample. Fluorescence is described as the emission of photons "associated with electrons moving from an excited state to a ground state"<sup>[40]</sup>. Molecules which exhibit fluorescence are called fluorophores. At room temperature electrons typically exist in only the lowest electronic energy level, referred to as the molecular ground state. A molecule can be excited, *i.e.*, promoted to an electronic state of higher energy, by absorption of the energy of a photon<sup>[63]</sup>. A large amount of energy is required for an electron to undergo an electronic transition, typically requiring the energy from UV or visible light. The molecular electronic transitions are governed by selection rules outlined by a set of quantum mechanical equations. The selection rules result in 'allowed' electronic transitions; although forbidden transitions do occur, but with much lower probability<sup>[40]</sup>. Fluorescence involves allowed transitions between singlet electronic states. Singlet electronic states refers to two electrons which have opposite spin orientation, or 'paired' electrons<sup>[63]</sup>. Therefore, in an excited singlet electronic state, the excited electron remains paired (opposing spin) to an electron in the ground state<sup>[64]</sup>.

A Jablonski diagram is shown in Figure 1.5 and is often used to illustrate the fluorescence process. As seen in stage (1), an electron in the ground singlet state, denoted  $S_0$ , absorbs energy from a photon of incident radiation at a given wavelength. This results in an electron being promoted to the first ( $S_1$ ) or higher energy excited singlet state ( $S_n$ ) (as seen in stage (2)). The molecule can be excited to higher vibrational levels within an excited electronic state<sup>[40]</sup>. Following

Kasha's rule, an electron in  $S_n$  ( $n>1$ ) rapidly ( $10^{-22}$  s) undergoes non-radiative relaxation to the lowest excited electronic state ( $S_1$ )<sup>[64]</sup>. Vibrational relaxation (stage (3)) involves the electron dissipating to a lower vibrational energy level through the release of kinetic energy. Internal conversion is non-radiative change in state (conserves energy), for example from  $S_2$  to a higher vibrational level of  $S_1$ , followed by vibrational relaxation. Once the electron is in the lowest vibrational energy level of the lowest excited electronic energy level ( $S_1$ ), the electron can then drop down to  $S_0$  by releasing energy through the emission of a photon (stage (5)), or decay non-radiatively. As energy must be conserved, the energy of the photon emitted is of lower energy (longer wavelength) than the photon absorbed, as some energy is released through processes such as vibrational relaxation in the excited states. This is known as the Stokes shift<sup>[64]</sup>. The wavelengths emitted from a molecule during fluorescence are defined in the emission spectrum. The wavelengths absorbed by a molecule are referred as the excitation spectrum.

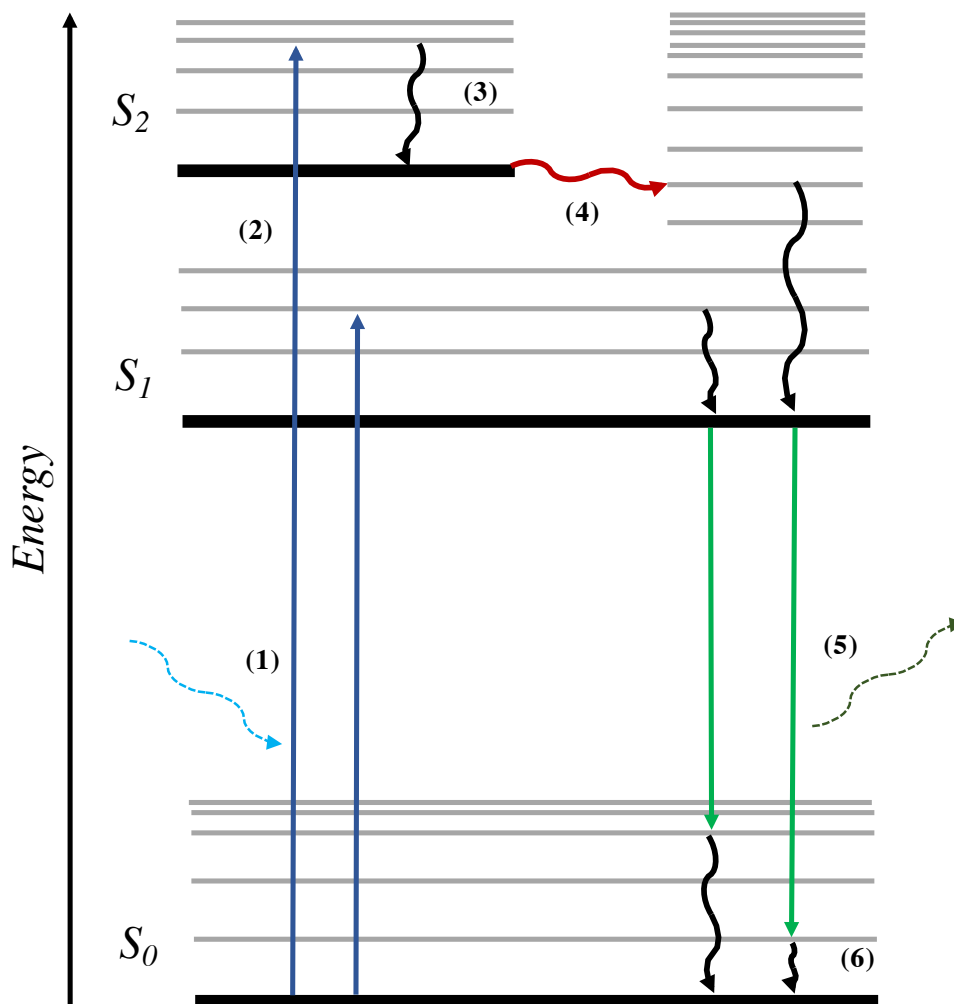


Figure 1.5: A Jablonski's diagram to illustrate the fluorescence process. Electronic energy levels are shown as solid, black, horizontal lines; vibrational energy levels are shown as solid, grey, horizontal lines. Absorbance is shown as solid, blue, vertical arrows; fluorescence is shown as solid, green, vertical arrows. Vibrational relaxation is shown as solid, black curved arrows; internal conversion is shown as solid, red, curved arrows. Excitation light is shown as blue, dashed, curved arrows; emitted light is shown as green, dashed, curved arrows. Adapted from Lakowicz<sup>[64]</sup>.

In this research, the anti-TNT antibody is labelled with the fluorescent dye: Alexa Fluor<sup>®</sup> 488 (AF488) tetrafluorophenyl (TFP) ester. The advantage of using a fluorescent label is that it provides high sensitivity. This is a result of fluorescence having no background interference from other molecules, *i.e.*, TNT. The AF488 TFP ester reacts with the  $\epsilon$ -amino group on lysine residues of the anti-TNT anti-

body, shown in Figure 1.6. The reaction is determined by the concentration and reactivity of the reagents. The class and basicity of an amino acid can affect its reactivity. The lysine residues are both aliphatic and relatively basic, which makes them reactive with the AF488 TFP ester. Hence, this reaction is also pH dependent as there are fewer free base aliphatic amines at pH values below eight<sup>[65]</sup>. The absorption and emission spectra of the AF488 dye is shown in Figure 1.7.

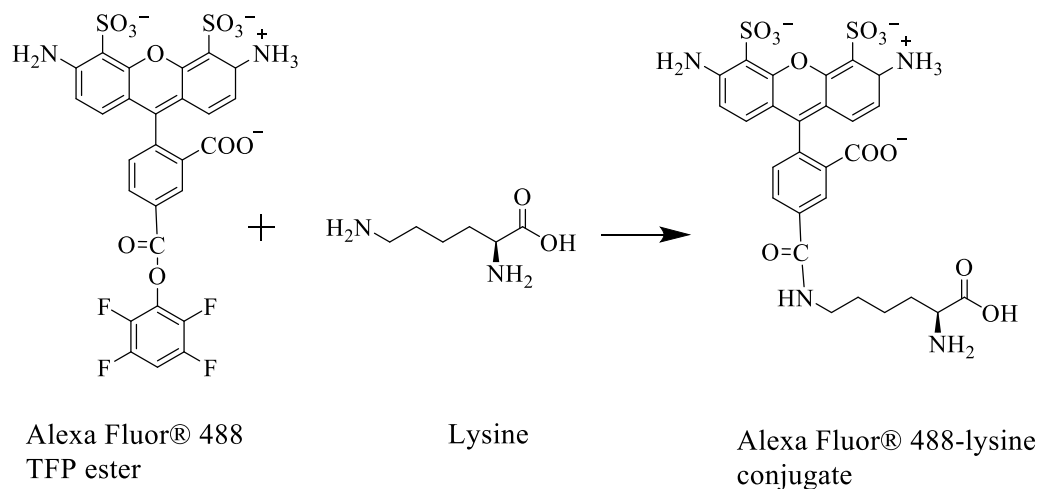


Figure 1.6: A scheme showing the reaction between the AF488 TFP ester and lysine. Adapted from Johnson and Spence<sup>[65]</sup>.

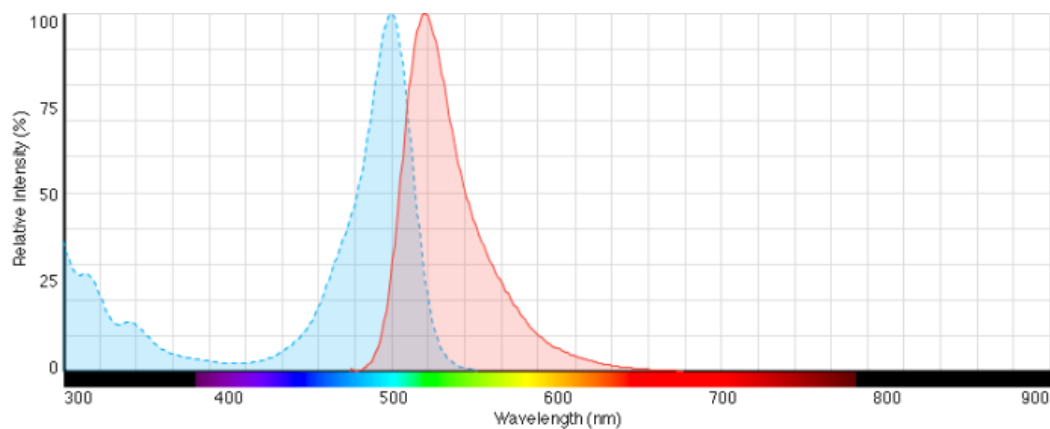


Figure 1.7: Absorbance (blue, dotted line) and emission (red, solid line) spectra of the AF488 dye<sup>[66]</sup>.

## 1.5 Thesis Outline

The main two aims of this research are firstly to demonstrate that TNT can be detected with a competitive fluoroimmunoassay technique. The second aim is to develop the technique into a lateral flow immunoassay test, for the detection of TNT in fingerprints. The different materials and methods used throughout this research will be described in Chapter 2.

The research in Chapter 3 investigates the first aim, which is to demonstrate that TNT can be detected using a competitive immunoassay format. This research utilises a 384 well plate to immobilise the relevant immunoassay chemistry onto the surface of the wells (plate immunoassay). The chapter begins by outlining the importance of TNT detection, followed by an explanation of the plate immunoassay technique used in the research, the relative advantages of the plate immunoassay and current literature that detects TNT with immunoassays. Chapter 3 then discusses the research performed, beginning with studies that focus on the binding specificity of the unlabelled anti-TNT to the bound form of TNT, *i.e.*, BSA-TNT conjugate and the free form of TNT. Next, the labelling of the anti-TNT antibody with the fluorescent dye (AF488) was optimised, finding the optimal number of moles of labelled dye to mole of anti-TNT antibody. To find the maximum sensitivity of the assay, the composition of the solubilisation buffer and the concentrations of the BSA-TNT and anti-TNT antibody were optimised. Finally, the effect of the presence of a fingerprint was tested in the optimised competitive plate immunoassay. The chapter then provides a section on the conclusions reached from the findings of the research described in Chapter 3.

In Chapter 4, the research focuses on the second aim of the research, which is to develop a competitive LFIA test for the detection of TNT in fingerprints. The chapter begins with an introduction to the advantages and uses of a LFIA technique for the detection of TNT in fingerprints. This is followed by a description

of the LFIA technique used in the research described in Chapter 4, the relative advantages of the LFIA over the plate immunoassay, and current literature that employs LFIA mechanism for explosive detection. The chapter then discusses the results from the direct wick and LFIA studies. The first studies focus on using the direct wick technique. This is due to the direct wick having a more simple design than the LFIA, reducing interference from the different materials in the LFIA. Firstly, the optimised plate immunoassay conditions are applied to the direct wick format. From these results it was clear that the direct wick conditions required further optimisation. Therefore, the nitrocellulose was treated with different solutions to block non-specific binding of the anti-TNT antibody and/or TNT, and to enhance wicking of the solution through the strip. Different TNT concentrations were then tested to find the sensitivity of the assay. At this point, there was no competition observed. Therefore, the plate immunoassay was tested using direct wick conditions, alongside a direct wick experiment. This was to test that the competitive immunoassay developed in Chapter 3 could function under the same temperature and time constraints as in the direct wick method. Different BSA-TNT concentrations are then tested to improve the sensitivity of the direct wick assay. Once, the optimal BSA-TNT concentration was selected this concentration was carried forward to be tested with a range of TNT concentrations. The conditions were then applied to the LFIA. The chapter then concludes the findings from the research conducted within Chapter 4.

Chapter 5 discusses the conclusions from the research carried out in Chapters 3 and 4. Chapter 5 then outlines some possibilities for future work based on the conclusions of this research.

# Chapter 2

## Experimental

This chapter provides the different materials and methods used in this research. The methods used within this research are adapted from protocols designed by Intelligent Fingerprinting.

### 2.1 Buffers

In this research, there are various experiments which test different buffer compositions to optimise conditions of a given assay. The following chemicals that made up the different solutions were obtained from Sigma Aldrich: sodium chloride (NaCl), Tween 20, Tween 80, polyvinylpyrrolidone (PVP) and methanol. The bovine serum albumin (BSA) was obtained from Fitzgerald Industries International. The composition of the main buffers used in this research are summarised in Table 2.1. Any variations of the buffers will be stated within the relevant text. For example, in Section 4.1, the nitrocellulose blocking buffer has different compositions tested during optimisation. However, the final, optimised nitrocellulose blocking condition is stated below in Table 2.1.



Table 2.1: Summary of the buffer compositions used in this research.

Abbreviation	Composition	pH
SBB	100 mM Sodium Bicarbonate Buffer	8.02 or 9.5
PBS	10 mM Phosphate Buffer, 150 mM NaCl	7.4
PBST	10 mM Phosphate Buffer, 80 mM NaCl, 0.22 mM Tween 20	7.4
Solubilisation Buffer	10 mM Phosphate Buffer, 40 mM NaCl, 0.12 mM Tween 20	7.4
Nitrocellulose Blocking Buffer	10 mM Phosphate Buffer, 3% PVP	7.4

## 2.2 Plate Assays

### 2.2.1 Direct Binding Plate Assay

The bovine serum albumin-analyte conjugate (BSA-TNT, received as a gift from DSTL) was prepared by diluting to a desired concentration (variable in experiments) in 100 mM sodium bicarbonate buffer, pH 8.02 (SBB). The wells of the Nunc<sup>®</sup> MaxiSorp<sup>™</sup> 384 well plates (Fisher Scientific) were coated with the BSA-TNT and incubated for 2 hours in the LTE Incubator IP60 UF 60L (Scientific Laboratory Supplies Ltd) at 37°C. Wells were washed 3 times with 100 µl of PBST (10 mM phosphate buffer, 80 mM NaCl, 0.22 mM Tween 20, pH 7.4). Either 10 µl of the labelled (with Alexa Fluor<sup>®</sup> 488) or unlabelled primary mouse monoclonal anti-TNT antibody (DSTL), which was diluted in PBS (10 mM phosphate buffer, 150 mM NaCl, pH 7.4), was added to the wells. The plate was incubated for a

further 1 hour at 37°C and washed 3 times with 100 µl of PBST. For plate assays which used unlabelled primary anti-TNT antibodies, the Alexa Fluor<sup>®</sup> 488 goat anti-mouse IgG (H+L) secondary antibody (Life Technologies) was added to the wells and incubated for 1 hour at 37°C. The plate was then washed with 100 µl of PBST, 3 times. To the washed wells, 50 µl of PBST was added and then analysed using a BMG LABTECH CLARIOstar<sup>®</sup> High Performance Multimode Microplate Reader, at excitation and emission wavelengths of 485 nm and 530 nm, respectively. The results were analysed in Microsoft Excel and normalised to the fluorescence reading at 100 µg ml<sup>-1</sup> of anti-TNT antibody.

### **2.2.2 Competitive Plate Assay**

The competitive plate assay follows the same layout as the direct binding plate assay. The BSA-TNT was prepared by diluting to a desired concentration (variable in experiments) in 100 mM sodium bicarbonate buffer pH 8.02 (SBB). The wells of the Nunc<sup>®</sup> MaxiSorp<sup>™</sup> 384 well plates (Fisher Scientific) were coated with 10 µl of the BSA-TNT (variable concentration between experiments) and incubated for 2 hours in the LTE Incubator IP60 UF 60L (Scientific Laboratory Supplies Ltd) at 37°C. Wells were washed 3 times with 100 µl of PBST (10 mM phosphate buffer, 80 mM NaCl, 0.22 mM Tween 20, pH 7.4). The TNT reference solution (Thames Restek) was added to the wells. Note that the TNT reference solution was diluted in a range of buffers, stated within the relevant text. This was followed by the addition of either the labelled (with Alexa Fluor<sup>®</sup> 488) or unlabelled anti-TNT antibody (DSTL), which was diluted in PBS (10 mM phosphate buffer, 150 mM NaCl, pH 7.4). The plate was incubated for a further 1 hour at 37°C and washed 3 times with 100 of µl PBST. For plate assays which used unlabelled primary anti-TNT antibodies, the Alexa Fluor<sup>®</sup> 488 goat anti-mouse IgG (H+L) secondary antibody (Life Technologies) was added to the wells and incubated for 1 hour at 37°C. The plate was then washed with 100 µl of PBST, 3 times. To the washed wells, 50 µl of PBST was added and then analysed using a BMG

LABTECH CLARIOstar<sup>®</sup> High Performance Multimode Microplate Reader, at excitation and emission wavelengths of 485 nm and 530 nm, respectively. The results were analysed in Microsoft Excel and normalised the highest fluorescence reading at 0  $\mu\text{g ml}^{-1}$  of TNT. The average was taken of the normalised values for each condition and displayed in the relevant figures in Chapter 3.

### **2.2.3 Quenching Studies**

Starting with the same format as the competitive plate assay, the BSA-TNT was prepared by diluting to 1  $\mu\text{g ml}^{-1}$  in SBB (100 mM sodium bicarbonate buffer, pH 8.02). The wells of the Nunc<sup>®</sup> MaxiSorp<sup>™</sup> 384 well plates (Fisher Scientific) were coated with the BSA-TNT and incubated for 2 hours in the LTE Incubator IP60 UF 60L (Scientific Laboratory Supplies Ltd). Wells were washed 3 times with 100  $\mu\text{l}$  of PBST (10 mM phosphate buffer, 80 mM NaCl, 0.22 mM Tween 20, pH 7.4). Labelled anti-TNT antibody was diluted to 25  $\mu\text{g ml}^{-1}$  in PBS (10 mM phosphate buffer, 150 mM NaCl, pH 7.4) and added to the coated wells. The plate was incubated for 1 hour at 37°C before the wells were washed with 100  $\mu\text{l}$  of PBST, 3 times. To the wells, 10  $\mu\text{l}$  of the TNT reference solution was added and the plate was immediately read in a BMG LABTECH CLARIOstar<sup>®</sup> High Performance Multimode Microplate Reader, at excitation and emission wavelengths of 485 nm and 530 nm, respectively. Results were analysed in Microsoft Excel and normalised to the fluorescence reading at 0  $\mu\text{g ml}^{-1}$  TNT. The average was taken of the normalised values for each condition and displayed in the relevant figures in Chapter 3.

### **2.2.4 Competitive Plate Assay with TNT Spiked Fingerprints**

This method differs from the competitive plate assay outlined above in Section 2.2.2, as the TNT reference solutions include the addition of fingerprint deposits.

## **Fingerprint Deposition**

First of all, two sets of fingerprints were deposited onto glass microscope slides (Fisher Scientific). Each glass slide had a single finger or thumb pressed onto the centre of the glass slide. The presence of the fingerprint deposit can be seen by eye. Therefore, after each fingerprint deposition, the slide was checked to ensure successful fingerprint deposition.

## **Fingerprint Extraction**

A 20  $\mu$ l drop of solubilisation buffer (10 mM phosphate buffer, 40 mM NaCl, 0.12 mM Tween 20, pH 7.4) was pipetted onto the fingerprint and a cover slip (Fisher Scientific) was placed on top of the drop of solubilisation buffer and fingerprint for 2 mins. The cover slip was then lifted, to  $\sim 45^\circ$  angle, maintaining contact between the glass slide and one edge of the cover slip. The cover slip was then rubbed over the fingerprint 10 times to encourage extraction of the fingerprint from the slide. The liquid that contains the solubilisation buffer and fingerprint is then pipetted into a 1.5 ml tube.

## **TNT Spiked Fingerprints**

There are two sets of fingerprints in this technique: the first set is spiked with TNT *before* fingerprint extraction, and the second set is spiked with TNT *after* fingerprint extraction. Spiking refers to a known concentration of TNT being added to the fingerprint deposit. A series of TNT reference solutions were prepared in solubilisation buffer (10 mM phosphate buffer, 40 mM NaCl, 0.12 mM Tween 20, pH 7.4). To the first set of deposited fingerprints, 10  $\mu$ l of the TNT reference solution was added on top of the deposited fingerprints, i.e. the fingerprint deposits were 'spiked' with TNT. The glass slides were placed in the LTE Incubator IP60 UF 60L (Scientific Laboratory Supplies Ltd) at  $37^\circ\text{C}$ , for 1 hour. The slides were removed from the incubator. The spiked fingerprints were then extracted as detailed above (Section 2.2.4).

The second set of fingerprints were deposited on the glass slides and immediately incubated for 1 hour at 37°C, in the LTE Incubator IP60 UF 60L (Scientific Laboratory Supplies Ltd). The slides were removed from the incubator and extracted, as described above (Section 2.2.4). The TNT reference solutions were then added to the extracted fingerprint solutions. Hence, the fingerprints were spiked with TNT *after* extraction.

Note that a control set of TNT reference solutions were prepared without any fingerprint addition. The different TNT-containing solutions (with and without extracted fingerprints) could then be used in the competitive plate assay format.

### **Testing of the TNT Spiked Fingerprints**

The TNT spiked fingerprints were tested in the competitive plate assay format. As described before, wells of the Nunc<sup>®</sup> MaxiSorp<sup>™</sup> 384 well plates (Fisher Scientific) were coated with 10 µl of 1 µg ml<sup>-1</sup> of BSA-TNT (diluted in 100 mM sodium bicarbonate buffer, pH 8.02) and incubated for 2 hours in the LTE Incubator IP60 UF 60L (Scientific Laboratory Supplies Ltd) at 37°C. Wells were washed 3 times with 100 µl of PBST (10 mM phosphate buffer, 80 mM NaCl, 0.22 mM Tween 20, pH 7.4). The various TNT reference solutions, which included: fingerprints spiked with TNT *before* extraction; fingerprints spiked with TNT *after* extraction; and TNT reference solutions without any fingerprint addition, were added to the wells (10 µl). This was followed by the addition of 10 µl of 6.25 µg ml<sup>-1</sup> labelled anti-TNT antibody solution (DSTL), which was diluted in PBS (10 mM phosphate buffer, 150 mM NaCl, pH 7.4). The plate was incubated for a further 1 hour at 37°C and washed 3 times with 100 µl of PBST. To the washed wells, 50 µl of PBST was added and then analysed using a BMG LABTECH CLARIOstar<sup>®</sup> High Performance Multimode Microplate Reader, at excitation and emission wavelengths of 485 nm and 530 nm, respectively. The results were analysed in Microsoft Excel and normalised to the fluorescence reading at 0 µg ml<sup>-1</sup>. The average was taken

of the normalised values for each condition and displayed in the relevant figures in Chapter 3. The half maximal inhibitory concentration ( $IC_{50}$ ) of the solutions, with and without fingerprints, were calculated using SigmaPlot.

## 2.3 Antibody Labelling

The anti-TNT antibody labelling method is based on the 'Invitrogen Alexa Fluor<sup>®</sup> 488 Protein Labeling Kit' manual<sup>[67]</sup>. The labelled antibody purification method is based on the instructions provided with the PD-10 columns (GE Healthcare Life Sciences)<sup>[68]</sup>. Corning<sup>®</sup> Spin-X<sup>®</sup> UF 10K concentrators (Sigma Aldrich) were equilibrated prior to use with 500  $\mu$ l of SBB (100 mM sodium bicarbonate buffer, either pH 8.02 or 9.5) and spun for 12 mins at 5,000 g on the MSE Micro Centaur Pulse centrifuge. The anti-TNT antibody (DSTL) was concentrated by adding 500  $\mu$ l of antibody to equilibrated concentrator tubes and spun for 18 mins at 10,000 g. The concentration of the antibody was determined before and after concentration by placing the solutions in the UV-Vis Hitachi U-3000 Spectrophotometer and recording the absorbance at 280 nm, using the UV Solutions software. The concentration was then calculated using Equation 2.2 (see Section 2.5). The antibody concentrate was resuspended in SBB to make a final concentration of 2 mg ml<sup>-1</sup>. The dye, Alexa Fluor<sup>®</sup> 488 TFP ester (Life Technologies), was solubilised in dimethyl sulfoxide (DMSO). Note that the concentration of the Alexa Fluor<sup>®</sup> 488 TFP ester varied between 0.5 mg ml<sup>-1</sup> and 10 mg ml<sup>-1</sup>, and will be noted in the relevant text. The variable concentration of dye added provided different numbers of dye molecules labelled to the anti-TNT antibody. The concentrated antibody solution was added to the dye, mixed thoroughly and then incubated at room temperature in the dark, for 1 hour. The antibody-dye solution was then purified with PD-10 columns (GE Healthcare Life Sciences). The PD-10 columns were firstly equilibrated with 10 ml of SBB. Once all the solution had run through the column, 450  $\mu$ l of the antibody-dye solution was added. After the antibody dye solution had moved into the column, a further 2 ml of SBB was

added. After ~2 mins, a colour gradient could be observed as the antibody dye solution began to separate into: labelled antibody; flow through between labelled antibody and unbound dye (flow between); and unbound dye (see Figure 2.1). A further 4 ml of SBB was added and then the various fractions (labelled antibody, flow between, unbound dye) were collected in 1.5 ml tubes. The collected fractions were separately ran on the UV-Vis Hitachi U-3000 Spectrophotometer. The absorbances at 280 nm and 494 nm were recorded, using the UV Solutions software, for analysis of the composition of the solutions (see Section 2.5).

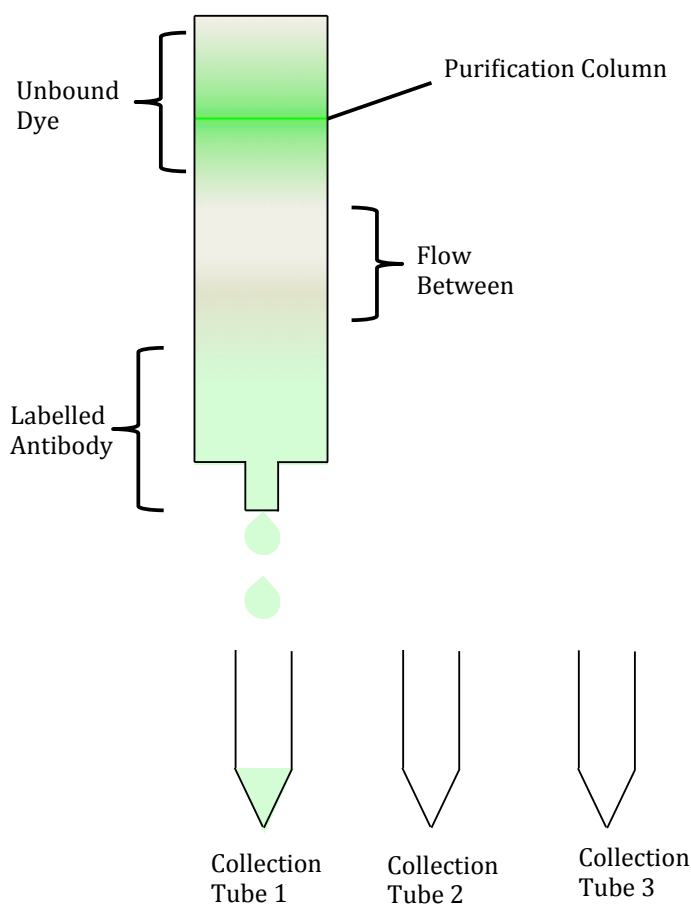


*Figure 2.1: A schematic diagram demonstrating the collection of the different fractions of the antibody-dye solution during purification. The labelled antibody was collected in Tube 1; the flow between labelled anti-TNT antibody and unbound dye (referred to as 'flow between') was collected in Tube 2; and the unbound dye was collected in Tube 3.*

## 2.4 Lateral Flow Immunoassay

### 2.4.1 Material Preparation

#### Test Strips

A BioDot XYZ3060 Dispense Platform was primed with 10 cycles of ethanol (Sigma Aldrich), followed by 10 cycles of 0.05% BioTerge AS-40, 10 cycles of the SBB (100 mM sodium bicarbonate buffer, pH 8.02) and 3 cycles of either horse anti-mouse IgG antibody (Vector Laboratories Ltd) or BSA-TNT (DSTL) for the control and test line, respectively. Nitrocellulose (Immunopore RP, GE Healthcare Life Sciences) was cut into 25 mm by 300 mm strips. The control (horse anti-mouse antibody) and test (BSA-TNT) lines were deposited onto the nitrocellulose at a deposition rate of  $800 \text{ nl cm}^{-1}$  using the primed BioDot XYZ3060 Dispense Platform. Note that the control line was dispensed from line 1 and the test line was dispensed from line 3, providing a 3 mm distance between the deposited lines. The nitrocellulose was placed on top of a sheet of lint-free tissue inside a plastic box that contained silica gel (Sigma Aldrich). The nitrocellulose was left to dry overnight in the closed box, at room temperature. The tissue and silica gel were removed from the box and 75 ml of the nitrocellulose blocking solution (10 mM phosphate buffer, 3% PVP, pH 7.4) was poured over a strip of nitrocellulose and 'rocked' on a Stuart Scientific Mini-Orbital Shaker S05, for 20 mins. The nitrocellulose was removed from the solution and placed on a fresh sheet of lint-free tissue inside a new plastic box that contained silica gel. The box was placed in the LTE Incubator IP60 UF 60L (Scientific Laboratory Supplies Ltd) to dry the nitrocellulose at  $37^{\circ}\text{C}$ , overnight. The nitrocellulose was then cut into 4 mm by 25 mm test strips using a guillotine (BioDot CM4000 Guillotine Cutter).

#### Conjugate Pads

Either Fusion 5 (GE Healthcare Life Sciences) or Grade 8964 (Ahlstrom) were used as the conjugate pad material. The conjugate pad material was cut with



a guillotine (BioDot CM4000 Guillotine Cutter) into 4 mm by 10 mm sections. Labelled anti-TNT antibody was prepared in PBS (10 mM phosphate buffer, 150 mM NaCl, pH 7.4) to a concentration of 6.25  $\mu\text{g ml}^{-1}$ . The conjugate pads were stood vertically in the wells of a Nunc<sup>®</sup> MaxiSorp<sup>™</sup> 384 well plate (Fisher Scientific). Using a pipette, 10  $\mu\text{l}$  of the labelled anti-TNT antibody solution was deposited on the top of each conjugate pad, moving from left to right as the solution was added. The 'loaded' conjugate pads were left to dry overnight at 37°C in a LTE Incubator IP60 UF 60L (Scientific Laboratory Supplies Ltd).

### **Sample Pads**

Either Fusion 5 (GE Healthcare Life Sciences) or Ahlstrom Grade 8964 was used for the sample pad material. The sample pads were backed (by Adhesive Research). TNT reference solutions were prepared in solubilisation buffer (10 mM phosphate buffer, 40 mM NaCl, 0.12 mM Tween 20, pH 7.4). The sample pads were spiked with 10  $\mu\text{l}$  of TNT standard solution, by adding the solution to the centre of the sample pad. The sample pads were dried for 1 hour at 37°C in a LTE Incubator IP60 UF 60L (Scientific Laboratory Supplies Ltd).

### **Wick**

In the direct wick experiments, the material used for the wick was Ahlstrom Grade 319 that was cut into 8 mm by 8 mm sections, using the guillotine (BioDot CM4000 Guillotine Cutter). In the lateral flow immunoassay, the material used for the wick was Ahlstrom Grade 320 that was cut into 3 mm by 22 mm sections with the guillotine.

## **2.4.2 Direct Wick Assembly and Testing**

Nitrocellulose test strips were prepared as described in Section 2.4.1. The test strips were then cut to a point at the bottom of the strip i.e. at the opposite end to where the test and control lines were deposited. A wick (see Section 2.4.1) was

placed at the top of a test strip and clipped in place (see Figure 2.2). Labelled anti-TNT antibody solution was prepared in PBS (10 mM phosphate buffer, 150 mM NaCl, pH7.4) to a concentration of  $6.25 \mu\text{g ml}^{-1}$ . The TNT reference solutions were prepared in solubilisation buffer (10 mM phosphate buffer, 40 mM NaCl, 0.12 mM Tween 20, pH 7.4). The antibody and TNT solutions were added to a separate vial, in equal volumes to form the 'premixed solutions'. A 20  $\mu\text{l}$  drop of the premixed solution was positioned at the centre of the base of a 2 ml self-standing microcentrifuge tube (Simport<sup>®</sup>). The 2 ml tube was then laid along its side. The bottom, pointed end of the assembled strip was then placed into the drop so that the solution could wick through the strip. Once all the solution had been absorbed through the test strip, a further 20  $\mu\text{l}$  of solubilisation buffer was added at the base of the 2 ml self-standing tube. After all the solubilisation buffer had been absorbed, the wick was removed and the test strip was placed in the ESEQuant Lateral Flow Reader (Qiagen), where the fluorescence was measured at excitation and emission wavelengths of 470 nm and 520 nm, respectively. Immediately after, the test strip was fluorescently imaged using an Optical Breadboard Imaging Device designed by EG Technology (see Figure 2.3), with an exposure of 1 sec. The results were processed in Microsoft Excel.

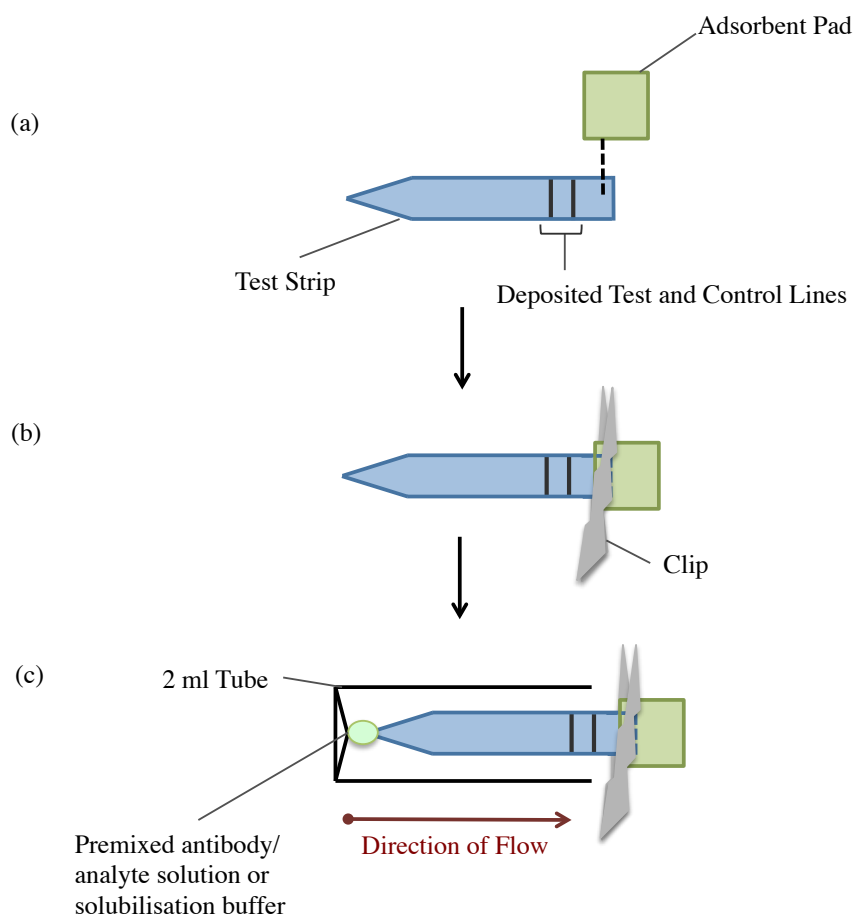
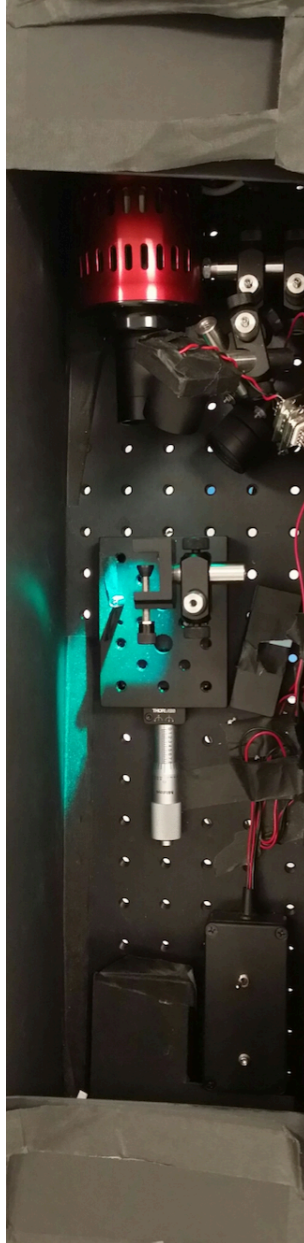


Figure 2.2: A schematic diagram summarising the direct wick experiment. A) shows the different components required; B) shows the assembled components that are clipped into place; C) shows the experiment at set up. Note that 20  $\mu\text{l}$  of premixed antibody/analyte solution is allowed to wick through the test strip first before a further 20  $\mu\text{l}$  of solubilisation buffer (10 mM phosphate buffer, 40 mM NaCl, 0.12 mM Tween 20, pH 7.4) is added.



*Figure 2.3: The Optical Breadboard Imaging Device designed by EG Technology that was used to take images of the nitrocellulose test strips.*

### **2.4.3 Lateral Flow Immunoassay Assembly and Testing**

The prepared components, outlined in Section 2.4.1, were assembled together as shown in Figure 2.4. Note that the components were backed (by Adhesive Research) to provide support and ease of handling during assembly and testing. To a reagent reservoir (Sigma Aldrich), 1 ml of solubilisation buffer (10 mM phosphate buffer, 40 mM NaCl, 0.12 mM Tween 20, pH 7.4) was added. The exposed bottom edge of the sample pad was immersed into the solubilisation buffer, so that the cassette was aligned vertically. The solution was allowed to wick through the system for 8 mins. The cassette was then placed in the ESEQuant Lateral Flow Reader (Qiagen), where the fluorescence of the test and control line was measured. The excitation and emission wavelengths were 470 nm and 520 nm, respectively. The test strips were then fluorescently imaged using an Optical Breadboard Imaging Device (designed by EG Technology), with an exposure of 1 second. Results were analysed in Microsoft Excel.

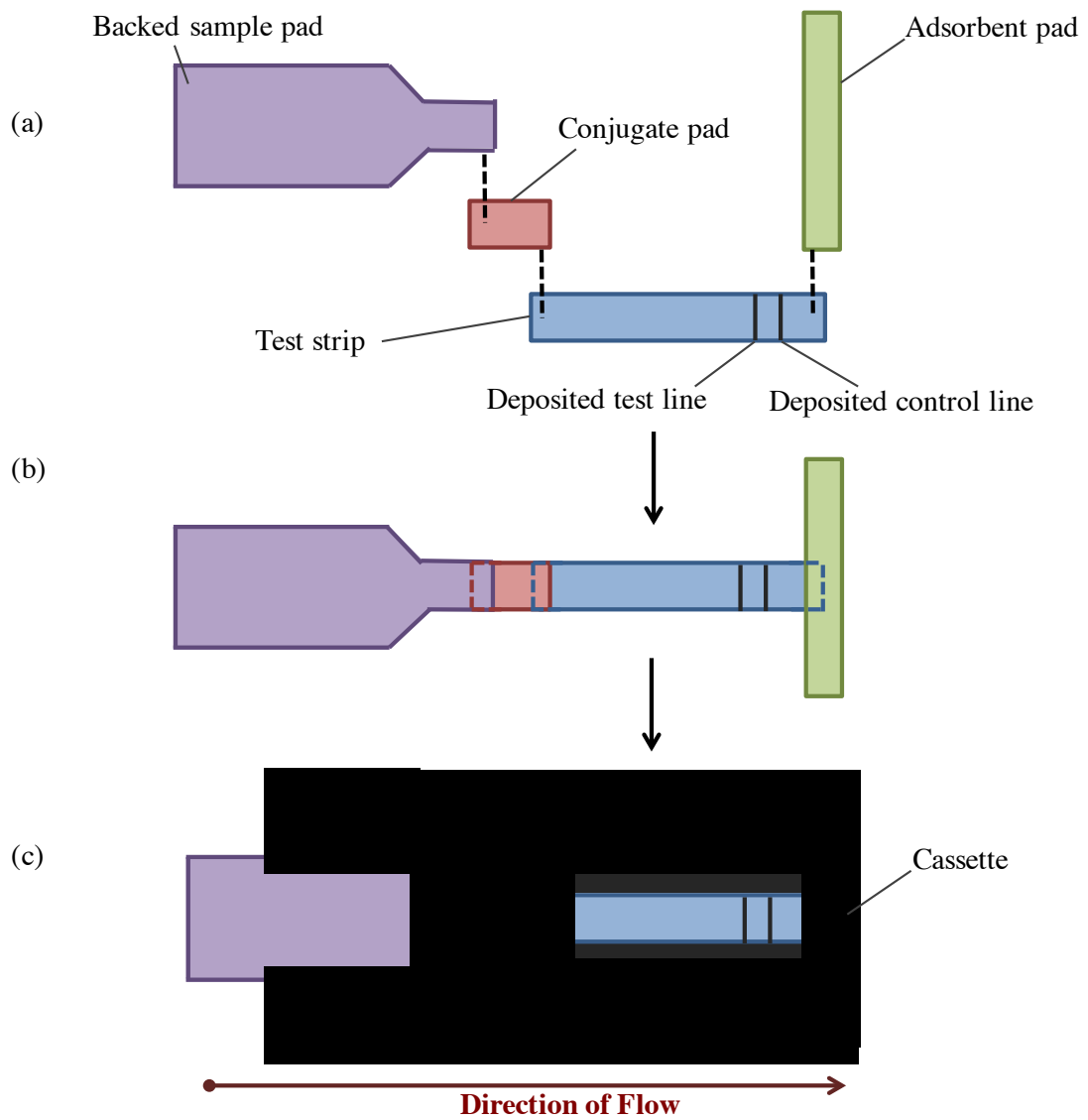


Figure 2.4: Summary of the assembly of the lateral flow components. A) shows the labelled individual components, before assembly; B) shows the assembled components; and C) shows the assembled components within the cassette. Note that the components are not to scale.

## 2.5 Equations

The following equation was used to determine the limit of detection, where relevant:

$$\text{Limit of detection} = 3 * \left[ \frac{S_{\text{Blank}}}{n} \right] \quad (2.1)$$

The following equations were used to determine antibody concentration before antibody labelling:

$$[\text{Antibody}], M = \left[ \frac{A_{280}}{(\epsilon_{\text{Antibody}} \times l)} \right] \times DF \quad (2.2)$$

$A_{280}$  = absorbance at 280 nm, *variable*

$\epsilon_{\text{Antibody}}$  = extinction coefficient of antibody,  $208,000 \text{ L mol}^{-1} \text{ cm}^{-1}$  [67]

$l$  = path length,  $1 \text{ cm}$

DF = dilution factor, *variable*

$$[\text{Antibody}], g L^{-1} = [\text{Antibody}], M \times MW_{\text{Antibody}} \quad (2.3)$$

[Antibody], M = antibody concentration from Equation 2.2, *variable*

$MW_{\text{Antibody}}$  = molecular weight of antibody,  $150,000 \text{ g mol}^{-1}$  [67]

The following equations were used to determine antibody concentration after antibody labelling:

$$[\text{Labelled Antibody}], M = \left[ \frac{(A_{280} - (A_{494} \times CF))}{(\epsilon \times l)} \right] \times DF \quad (2.4)$$

$A_{280}$  = absorbance at 280 nm, *variable*

$A_{494}$  = absorbance at 494 nm, *variable*

$\epsilon_{\text{Antibody}}$  = extinction coefficient of antibody,  $208,000 \text{ L mol}^{-1} \text{ cm}^{-1}$  [67]

$l$  = path length,  $1 \text{ cm}$

CF = correction factor of dye absorbing at 280 nm,  $0.11$  [67]

DF = dilution factor, *variable*

$$[\text{LabelledAntibody}], g L^{-1} = [\text{LabelledAntibody}], M \times MW_{\text{Antibody}} \quad (2.5)$$

[Labelled Antibody], M = antibody concentration from Equation 2.4, *variable*

$MW_{\text{Antibody}}$  = molecular weight of antibody,  $150,000 g mol^{-1}$  [67]

The following equation was used to determine the molar dye to protein ratio:

$$\text{Molar ratio of dye : antibody} = \left[ \frac{A_{494}}{([\text{LabelledAntibody}], M \times \epsilon_{\text{Dye}} \times l)} \right] \quad (2.6)$$

$A_{494}$  = absorbance at 494 nm, *variable*

$\epsilon_{\text{Dye}}$  = extinction coefficient of dye,  $71,000 \text{ L mol}^{-1} \text{ cm}^{-1}$  [67]

$l$  = path length,  $1 \text{ cm}$

[Labelled Antibody], M = antibody concentration from Equation 2.4, *variable*

DF = dilution factor, *variable*

Equations were obtained from the Alexa Fluor<sup>®</sup> 488 antibody labelling kit (Life Technologies) manual [67].



## Chapter 3

# Detection of TNT using a Competitive Immunoassay Immobilised on a 384 Well Plate

TNT is one of the most commonly used high explosives<sup>[69]</sup> due to its low sensitivity to detonation by shocks and friction<sup>[70]</sup>. TNT is an explosive material utilised in criminal activity, and has demanded quick, sensitive and reliable detection methods to prevent catastrophic events from occurring<sup>[71]</sup>. Immunoassays use antibodies that are specific to the analyte (TNT, in this instance) to detect the presence of the analyte in a sample. The antibody-analyte binding is a high affinity and highly specific interaction, providing a sensitive assay without sample preparation. With reference to TNT, the TNT molecule has a low molecular mass of  $227.13 \text{ g mol}^{-1}$ . As described in Chapter 1, this results in the competitive format being the choice of immunoassay for the detection of TNT, as it only requires the binding of one antibody to the TNT. A non-competitive format requires the binding of two antibodies to the analyte, which is often physically not possible to low molecular mass analytes.

The primary aim of the research described in this chapter is to demonstrate that

TNT can be detected in a competitive immunoassay format. All immunoassays were performed using a 384 well plate, and are subsequently referred to as 'plate immunoassays'. The presence of TNT was detected by measuring the fluorescence signal using a CLARIOstar Plate Reader. Note, in the competitive immunoassay format the TNT concentration is indirectly proportional to the fluorescence intensity. Firstly, the specificity of the anti-TNT antibody was tested, demonstrating the ability of the antibody to specifically recognise both the free form of the TNT and the bound form (BSA-TNT conjugate) of TNT. Next, the number of moles of labelled fluorescent dye (AF488) per mole of anti-TNT antibody was optimised. The binding specificity of the antibody was also assessed after labelling, as labelling can disrupt the structure, and consequently, the specificity of the antibody. Any quenching effects on the fluorescence signal emitted by the AF488 dye bound to the anti-TNT antibody by TNT were examined, again in a plate assay. The buffer that was used to solubilise the TNT, named the 'solubilisation buffer', was then optimised to contain the concentrations of the buffer components for optimal sensitivity in the competitive plate assay. The anti-TNT antibody and the BSA-TNT conjugate (BSA-TNT) concentrations were also optimised in the plate assay. Finally, as the end goal of the research was to produce a competitive immunoassay based test to detect TNT in fingerprint deposits, the effect of fingerprint addition in the system was tested to ensure the sensitivity of the assay was not affected by the fingerprint presence, *i.e.*, by non-specific binding between the antibody to the components in the fingerprints.

This chapter will firstly discuss the importance of the detection of TNT, followed by the advantages of using the competitive immunoassay immobilised on a 384 well plate for initial TNT detection studies. The advantages of using fingerprints and plate immunoassay techniques that have been published in the literature have also been discussed. Finally, the research results are discussed and then some conclusions drawn from the research presented in this chapter.

## 3.1 Introduction

TNT is the most commonly used explosive<sup>[72]</sup>, due to its relative high stability and low sensitivity to detonation. The low melting point allows TNT to be melted, which makes it easily poured into ammunition without risk of explosion. The stability of TNT is also appealing to criminal organisations, as it is safer to handle compared to other high explosives. The use of explosive materials in criminal activity<sup>[73]</sup>, such as terrorism, has created a demand for sensitive, reliable and quick detection tests to be used for security measures in environments such as airports. It is critical to be able to detect TNT or to identify people or items that have been in contact with TNT, in the hope of preventing catastrophic, criminal events from occurring. TNT and its metabolites are also toxic to a wide range of organisms, from humans to aquatic life<sup>[23]</sup>. Therefore, TNT not only poses a threat to life from the primary destructive effects from the explosion but also from long term effects by contaminating the surrounding environment. In situations where people may be exposed to TNT, a technique to be able to detect TNT would be necessary to ensure those exposed are not in contact with dangerous levels of TNT. For example, monitoring workers in ammunition factories.

The fluoroimmunoassay used in the research described in this chapter was immobilised on a 384 well plate, referred to as a plate immunoassay. As described in Chapter 1, a bound form of TNT (BSA-TNT) was immobilised onto the wells of the plate. Anti-TNT antibody and a sample containing TNT are added to the wells. There was competitive binding of the anti-TNT antibody between the bound form and free form of TNT. As the TNT in the sample was increased, less anti-TNT antibody was available for binding to the BSA-TNT. Either the anti-TNT antibody was labelled, or a labelled secondary anti-TNT antibody was required. Higher concentrations of TNT in the sample, result in lower amount of labelled antibody bound to the BSA-TNT, and a lower fluorescent intensity was measured in the plate reader. The fluorescent dye used in this research was

the Alexa Fluor<sup>®</sup> 488, selected for its high photostability, pH stability over the range of 4 to 10 and its high fluorescent yield. Generally, lower background signals are observed when using a fluorescent dye, which improves sensitivity of the assay.

The plate immunoassay offers many advantages for initial studies. Firstly, the high number of wells (384) in the plate allows for a large amount of samples and conditions to be tested simultaneously, ideal for optimisation studies. The antibody-analyte interaction in the plate immunoassay takes place in the wells of the plate. Whereas, the LFIA, utilises multiple materials for the different components of the test (see Chapter 4). Therefore, the plate immunoassay does not have the additional challenges posed from material interference as in the LFIA. Hence the plate assay allows for the fundamental principle of a competitive immunoassay to be tested, *i.e.*, whether TNT can be detected in a competitive immunoassay format with the reagents that have been selected. The conditions of the reagents of the immunoassay can also be optimised, which provides the optimum sensitivity of the assay that can be achieved with the selected conditions.

The competitive immunoassay used in this research aims to detect TNT in fingerprint deposits. Detection of TNT in fingerprints offers a strong advantage as it allows for the contaminated sample (fingerprint deposit) to be linked with the identity of the handler. For example, techniques that detect TNT in swabbed samples from luggage may identify the presence of TNT but do not account for situations where luggage, or the contents of the luggage, may have been swapped. Detection of TNT in fingerprints also has the added advantage of being a non-invasive procedure.

As described in Chapter 1, there are various techniques in development for the detection of TNT and explosive materials in fingerprints. To date, there have been no literature reports demonstrating the detection of TNT in fingerprint deposits through an immunoassay technique. The primary focus of the literature

has been to develop immunoassays which detect TNT in swab samples, such as samples from luggage at airports; hand swabs; or environmental samples, such as TNT contaminated soil or water. The large majority of literature on fluoroimmunoassays is based on a flow through format, *i.e.*, LFIA, which will be discussed in Chapter 4. With regards to plate immunoassays, Fetterolf et al.<sup>[74]</sup> was the first to demonstrate detection of TNT in hand swab samples, with a sensitivity of 50 pg. The study used an enzyme-linked immunosorbent assay (ELISA). The ELISA format is similar to the protocol in this research, with a protein-TNT conjugate immobilised on a plate and incubated with TNT and anti-TNT antibody. The difference with the ELISA method is that it employs a secondary antibody conjugated to an enzyme. The secondary antibody-enzyme conjugate binds to any anti-TNT antibody that is bound to the immobilised TNT. Finally, an enzyme substrate is added to the system where it is bound by the enzyme. This binding reaction results in a colour change that is indirectly proportional to the concentration of free TNT in the sample. Hence, the reported ELISA is a colorimetric method, *i.e.*, absorbance is measured; whereas the method in this research employs an antibody labelled with a fluorescent dye.

## **3.2 Aims of the Research Described in this Chapter**

Firstly, the aim of the research in this chapter is to demonstrate that it is possible to detect TNT in a competitive immunoassay format. Secondly, the research aims to find the optimal conditions of the different reagents to determine the sensitivity of the immunoassay. Thirdly, the research described in this chapter aims to investigate the effect of the presence of a fingerprint deposit on the immunoassay sensitivity.

## 3.3 Results and Discussion

### 3.3.1 Unlabelled Anti-TNT Antibody Binding Specificity

All testing performed with the unlabelled anti-TNT antibody required an AF488 labelled secondary antibody, to provide a signal for detection. The first step was to determine that the anti-TNT antibody recognised the bound form of the analyte, *i.e.*, BSA-TNT. This study was performed in a direct binding plate assay and the results are shown in Figure 3.1. Figure 3.1 demonstrates that the anti-TNT antibody recognises the BSA-TNT as when the antibody concentration is increased, an increase in the fluorescence intensity is observed. The fluorescence intensity is dependent on the amount of labelled secondary antibody bound, which in turn is dependent on the amount of anti-TNT antibody bound to the BSA-TNT. Hence, the more anti-TNT antibody bound to the BSA-TNT, the higher the fluorescence intensity. Eventually the binding does become saturated and the fluorescence intensity plateaus. This can be seen in Figure 3.1 as the steepness of the slope reduces after  $25 \mu\text{g ml}^{-1}$  of the anti-TNT antibody.

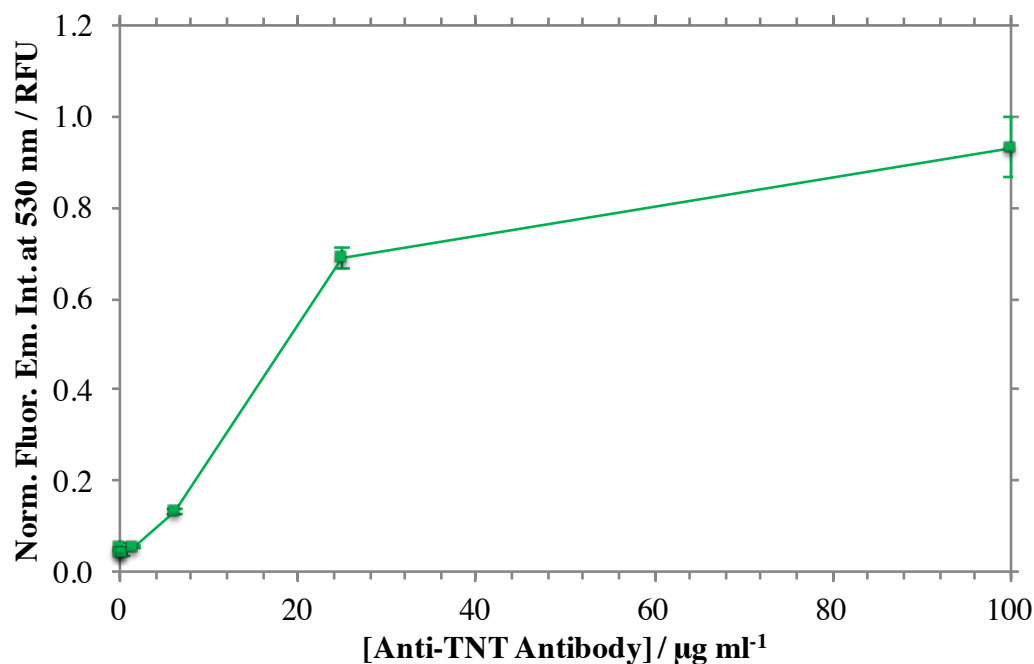


Figure 3.1: Direct binding assay assessing the anti-TNT antibody binding to the BSA-TNT. Wells were coated with  $1 \mu\text{g ml}^{-1}$  of BSA-TNT. The anti-TNT antibody concentration used was  $0\text{-}100 \mu\text{g ml}^{-1}$ . The secondary antibody concentration used was  $50 \mu\text{g ml}^{-1}$ . Error bars represent standard deviation,  $n=3$ .

As the results shown in Figure 3.1 demonstrated that the anti-TNT antibody recognises the bound TNT (BSA-TNT), the next step was to assess the ability of the anti-TNT antibody to bind to the free TNT (TNT). This study was performed in a competitive plate assay. For a competitive plate assay, the fluorescence intensity is indirectly proportional to the concentration of TNT. As the TNT concentration is increased, more anti-TNT antibody is occupied by the free TNT. Hence, fewer antibodies bind to the BSA-TNT and therefore there are fewer sites for the labelled secondary antibody to bind to. However, as shown in Figure 3.2, there was no decrease in fluorescence intensity when the TNT concentration was increased. This result could be due to a number of reasons. Firstly, it may be that the anti-TNT antibody is in such excess that the anti-TNT antibody can bind all the TNT available in the sample, and there still be enough unoccupied anti-TNT antibody remaining to bind to the BSA-TNT. Secondly, there may be non-specific binding from the secondary antibody, *i.e.*, the secondary antibody is

in such excess that it is binding to other components. This would result in the secondary antibody masking any competition that may occur. Thirdly, the antibody may be recognising the BSA of the BSA-TNT conjugate, rather than the TNT. The latter will be discussed in Section 3.3.3. All of these possibilities were examined. Note that the anti-TNT antibody concentration used for the following studies was  $25 \mu\text{g ml}^{-1}$ . This was because the  $25 \mu\text{g ml}^{-1}$  concentration provided a similar fluorescent intensity as the  $100 \mu\text{g ml}^{-1}$  anti-TNT antibody concentration, as shown in Figure 3.2. Lower anti-TNT antibody concentrations can increase sensitivity of the assay as a lower TNT concentration is required to occupy the anti-TNT antibody sites, and consequently to show reduced fluorescence signals, *i.e.*, competition. However, at too low a concentration of anti-TNT antibody the fluorescence intensity can be too low for detection. Therefore, it was thought that  $25 \mu\text{g ml}^{-1}$  of anti-TNT antibody concentration should be used as this concentration produces a similar fluorescence signal as that of the  $100 \mu\text{g ml}^{-1}$ , as shown in Figure 3.2, but with the possibility of a greater sensitivity for the TNT.



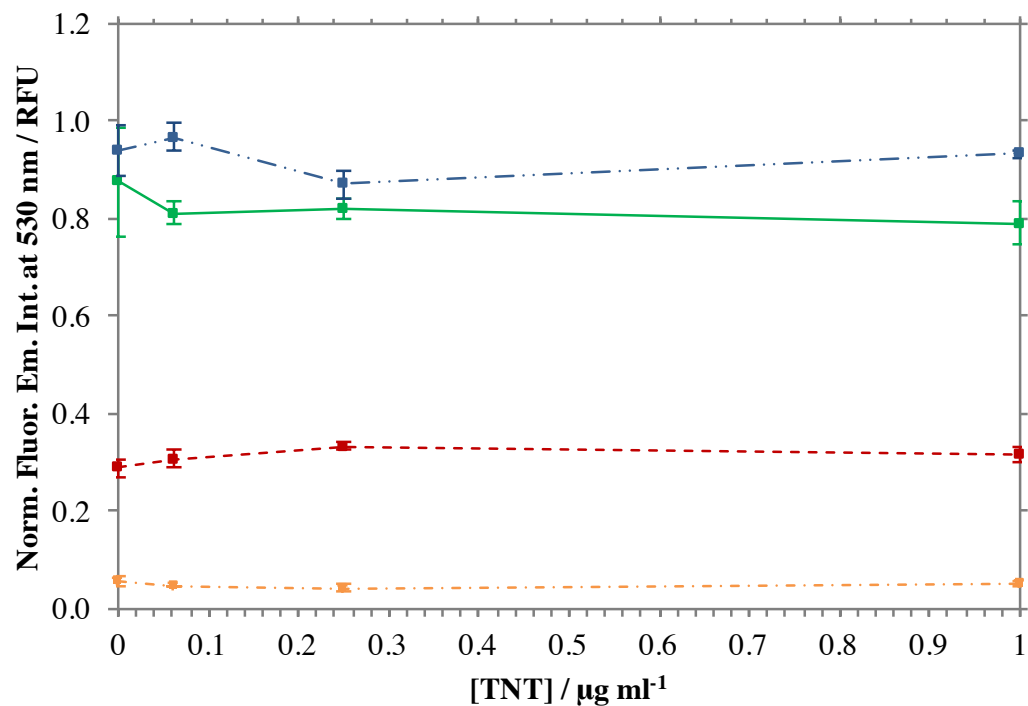


Figure 3.2: Competitive plate immunoassay testing the effect of anti-TNT concentration on the sensitivity of the assay. The anti-TNT antibody concentrations used were: 0  $\mu\text{g ml}^{-1}$  (orange, dash dot line); 6.25  $\mu\text{g ml}^{-1}$  (red, dashed line); 25  $\mu\text{g ml}^{-1}$  (green, solid line) and 100  $\mu\text{g ml}^{-1}$  (blue, dash dot dot line). TNT concentration ranged between 0-1  $\mu\text{g ml}^{-1}$ . The secondary antibody concentration used was 50  $\mu\text{g ml}^{-1}$ . Error bars represent standard deviation,  $n=3$ .

Firstly, the TNT concentration was increased 10-fold to determine whether competition could be seen. As shown in Figure 3.3, increasing the TNT concentration did not show a decrease in the fluorescence intensity and hence, the immunoassay did not show competition. Next, different secondary antibody concentrations were tested to assess whether the secondary antibody was in such excess that it was non-specifically binding to the wells. As can be seen in Figure 3.4, both concentrations of secondary antibody maintained relatively constant fluorescence intensities, regardless of TNT concentration. This implies that reducing the secondary antibody concentration did not increase the assay sensitivity, nor display any signs of competition. However, to completely rule out non-specific binding by the secondary antibody, the anti-TNT antibody was labelled with the AF488 dye. Removal of the secondary antibody would also simplify the immunoassay by reducing the number of steps in the immunoassay procedure, which could reduce error.

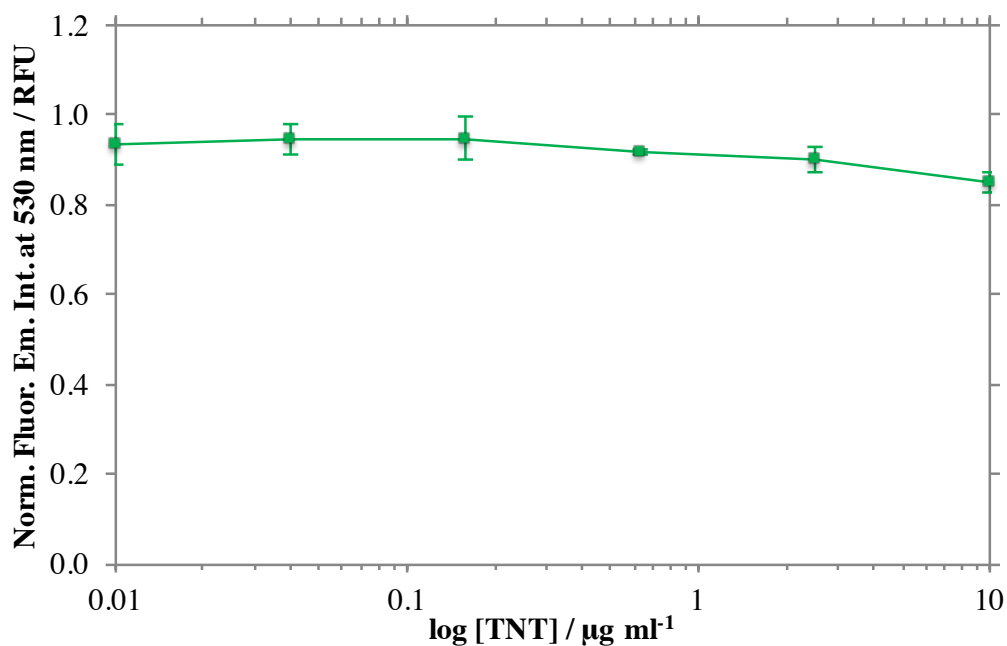


Figure 3.3: A competitive plate immunoassay to determine whether an increased TNT ( $0\text{-}10 \mu\text{g ml}^{-1}$ ) concentration would improve sensitivity. The anti-TNT antibody concentration was  $25 \mu\text{g ml}^{-1}$  and the secondary antibody concentration was  $50 \mu\text{g ml}^{-1}$ . Error bars represent standard deviation,  $n=3$ .

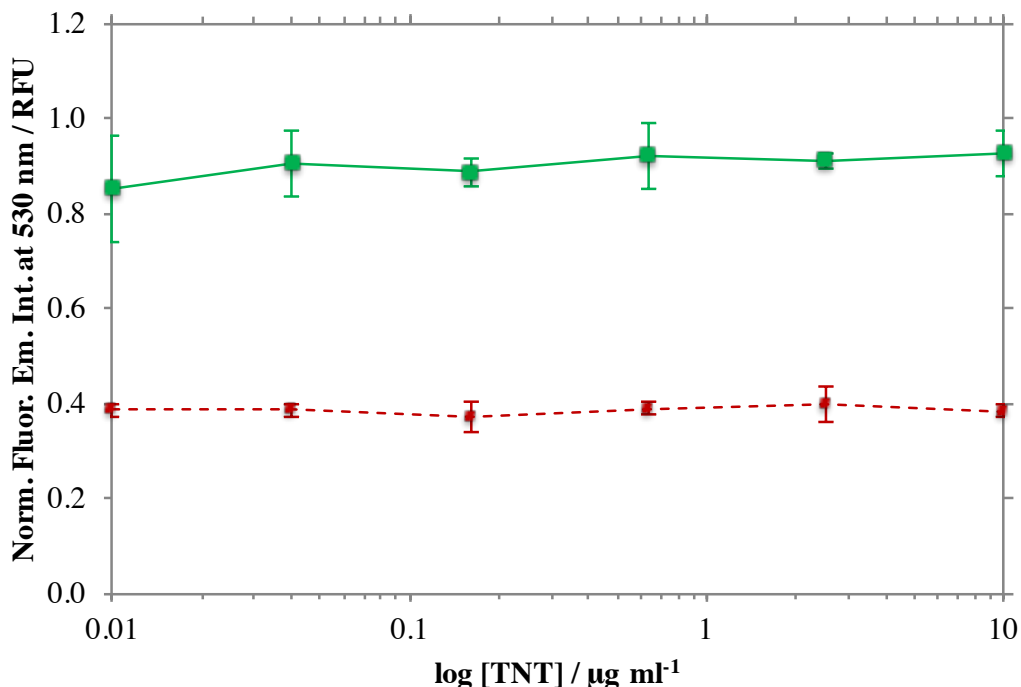


Figure 3.4: Assessment of the effect of the secondary antibody concentration on the sensitivity of the competitive immunoassay. The secondary antibody concentrations used were:  $10 \mu\text{g ml}^{-1}$  (red, dashed line) and  $50 \mu\text{g ml}^{-1}$  (green, solid line). The TNT concentration ranged between  $0\text{-}10 \mu\text{g ml}^{-1}$ . The anti-TNT antibody concentration used was  $25 \mu\text{g ml}^{-1}$ . Error bars represent standard deviation,  $n=3$ .

### 3.3.2 Anti-TNT Antibody Labelling

The AF488 dye used to label the anti-TNT antibody is the same fluorophore that was used to label the secondary antibody. An optimisation of the molar ratio of the number of dyes labelled to anti-TNT antibody was performed. The spectra obtained for each labelled anti-TNT antibody solution are shown in Figure 3.5. The moles of labelled dye per mole of antibody were calculated (see Section 2.5) giving rise to 13, 11, 9 and 3 moles of dye per 1 mole of anti-TNT antibody. These ratios will be referred to as 13:1, 11:1, 9:1 and 3:1, respectively for the remainder of this thesis. Table 3.1 summarises the conditions that were used to obtain the 13:1, 11:1, 9:1 and 3:1 labelled antibodies.

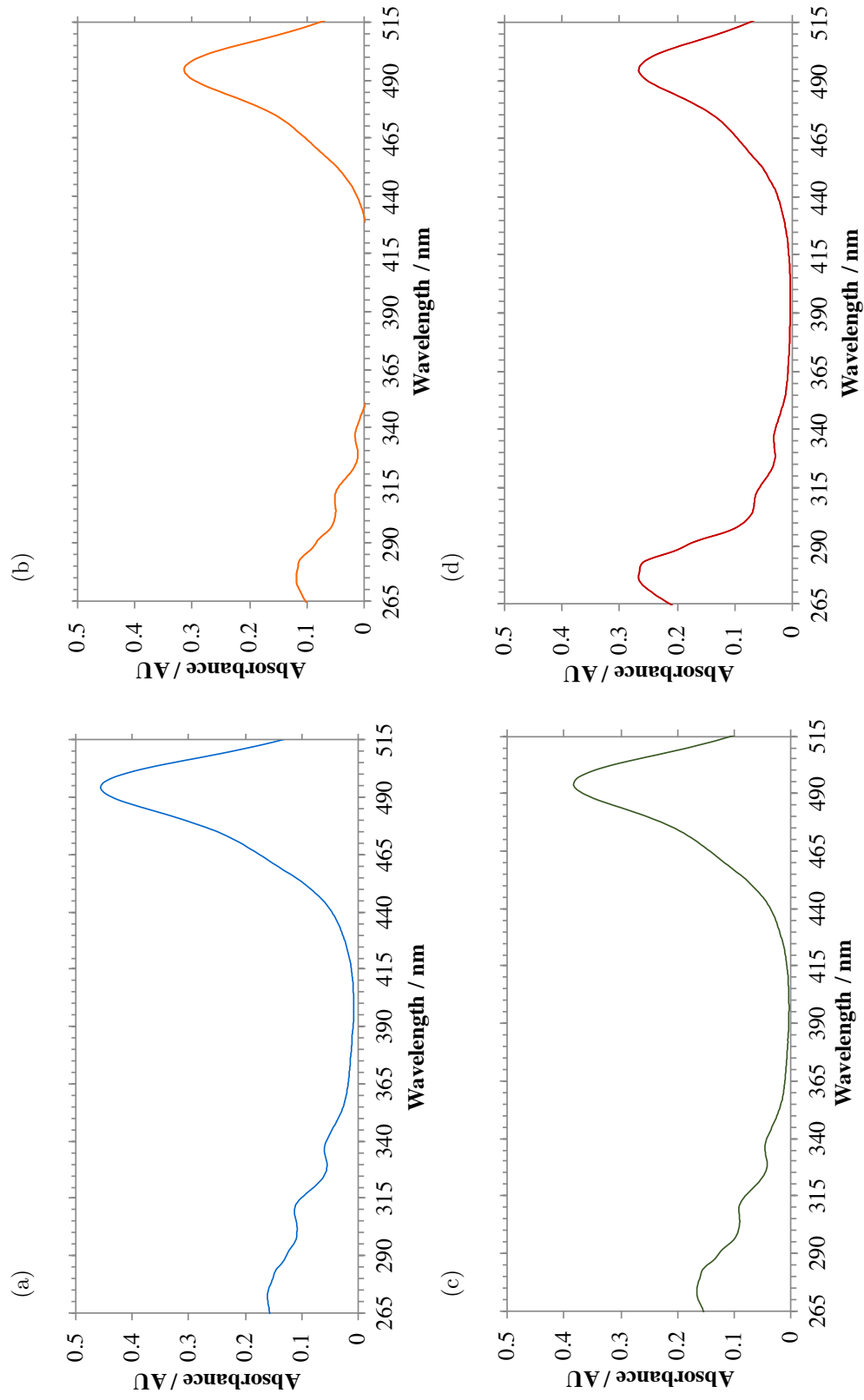


Figure 3.5: The absorbance spectra (265-515 nm) of the different AF488 labelled anti-TNT antibody solutions. The molar ratios of labelled dye per antibody of each solution are: (a) 13:1; (b) 11:1; (c) 9:1; and (d) 3:1. The labelled anti-TNT antibody solutions were measured at the following concentrations, based on the anti-TNT antibody concentration: (a) 0.07  $\mu\text{g ml}^{-1}$ ; (b) 0.06  $\mu\text{g ml}^{-1}$ ; (c) 0.09  $\mu\text{g ml}^{-1}$ ; and (d) 0.17  $\mu\text{g ml}^{-1}$ .

*Table 3.1: Summary of the conditions that provided the relative dye:antibody molar ratios.*

<b>Dye:Molar Ratio</b>	<b>[Dye] / <math>\mu\text{g ml}^{-1}</math></b>	<b>[Antibody] / <math>\text{mg ml}^{-1}</math></b>	<b>Time of Reaction / mins</b>	<b>Buffer</b>
13:1	10	1.67	60	SBB pH 9.5
11:1	5	0.85	60	SBB pH 9.5
9:1	5	1.85	60	SBB pH 9.5
3:1	0.5	1.9	60	SBB pH 8.02

It was important to assess the binding of the antibody after labelling as loss of specificity for the analyte, aggregation and fluorescence quenching can all occur. Loss of specificity would be as a result of the dyes attaching to the amino acids which are important to the structure of the binding site of the antibody, and is not necessarily restricted to those amino acids which comprise the binding site. The highly specific interaction between the antibody and its corresponding analyte can easily be lost if the structure and bonds are altered. The dye can also bind to the antibody in a manner which blocks the binding site from being able to access the analyte. Hence, binding of the dyes to the antibody can alter the antibody's specificity through chemical and physical interference. The AF488 dye is also highly hydrophobic and so over-labelling can lead to aggregation of antibodies. The aggregated antibodies could impose competition by binding to each other rather than the BSA-TNT and washing off the plate, consequently reducing the fluorescence signal. Over-labelling can also result in the fluorescence signal being quenched, due to the nature of the dyes self-quenching when in close proximity of each other. In the protein labelling kit manual<sup>[67]</sup> it is reported that the optimum moles of dye per mole of protein is 4-9:1. Therefore, the 13:1 and 11:1 labelled anti-TNT antibodies have slightly higher number of dyes than suggested. Consequently, it is important to confirm the specificity of the antibody and to ensure any competition shown isn't due to quenching effects.

The labelled antibodies were all tested in a competitive plate immunoassay, shown in Figure 3.6. The concentration of all antibodies was  $25 \mu\text{g ml}^{-1}$ , consistent with the previous unlabelled antibody studies. The labelled antibodies: 13:1, 11:1 and 9:1 all showed a significant decrease in fluorescence intensity as the TNT concentration increased, and hence demonstrated competition. The 13:1 and 11:1 labelled antibodies showed the steepest slopes and therefore, the highest sensitivity. The 13:1 and 11:1 labelled antibodies were consequently used for all future studies involving a labelled anti-TNT antibody. As stated above, the optimum dye per mole of protein is 4-9:1. This is not consistent with the results shown

in Figure 3.6, as the highest sensitivity was achieved with the 11:1 and 13:1, of which both are above the optimal moles of dye to protein ratio. However, the protein labelling kit manual also states that different antibodies react with the dye at different rates, along with the antibody binding specificity being maintained with different numbers of labelled dyes to that of the suggested labelled moles of dye to protein ratio (4-9:1)<sup>[67]</sup>. Hence, the 4-9:1 ratio may not be optimal for all antibodies. In the 'troubleshooting' section of the protein labelling kit manual, increasing the amount of labelling is suggested. Therefore, it is not an unusual result for a slightly higher moles of dye per mole of protein ratio, such as 11:1 and 13:1 to exhibit a higher sensitivity. In Figure 3.6, there is a trend of increasing antibody specificity for TNT as the number of labelled dyes are increased. This sensitivity plateaus at 11:1 and 13:1, as the antibodies have similar sensitivities.

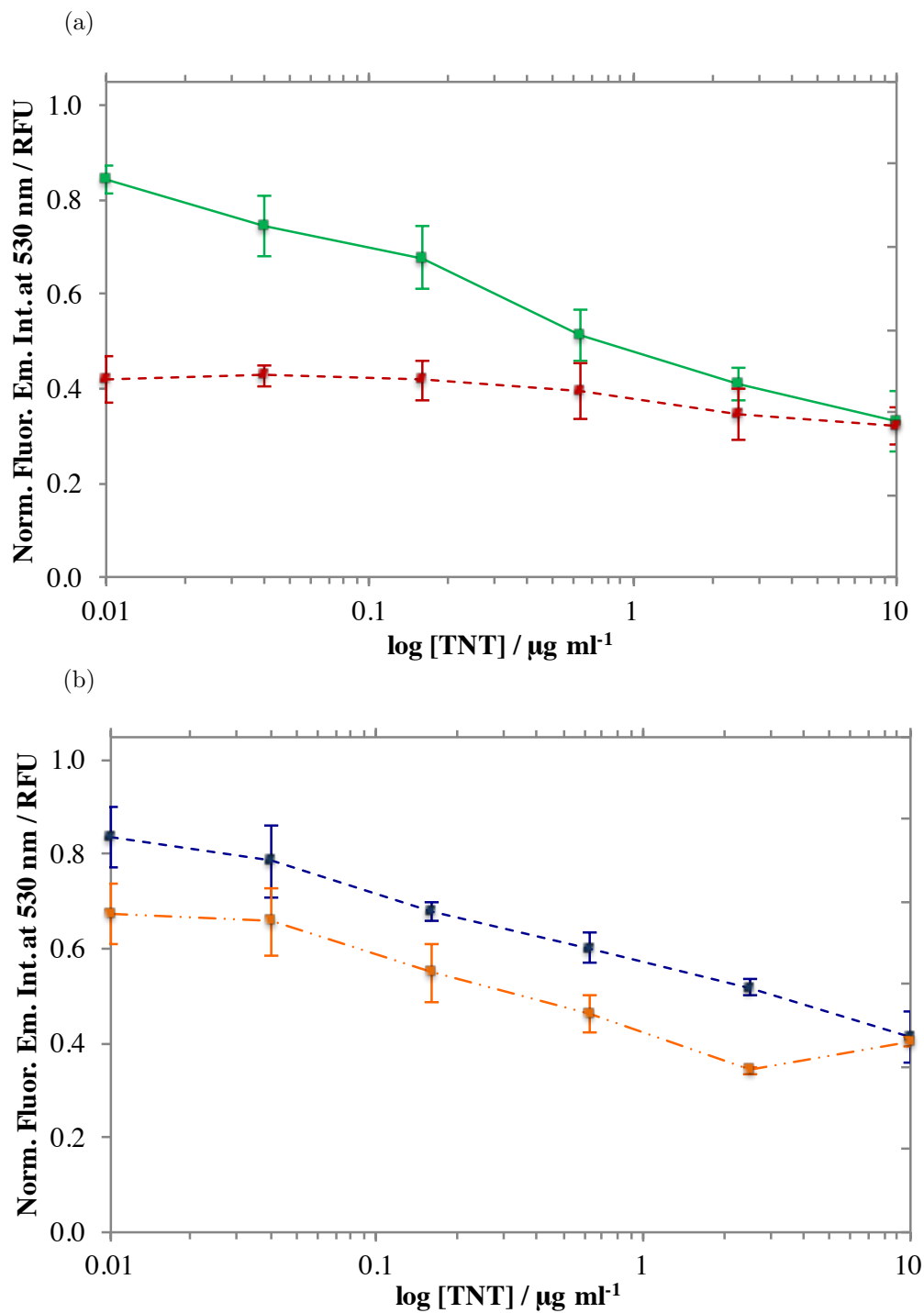


Figure 3.6: Optimisation of the moles of dye bound to the anti-TNT antibody. The ratios of moles of dye per mole of antibody were: (a) 13:1 (green, solid line) and 3:1 (red, dashed line); and (b) 11:1 (blue, dashed line) and 9:1 (orange, dashed and dotted line). The TNT reference concentration ranged from 0-10  $\mu\text{g ml}^{-1}$ . All antibodies were added to the plate at a concentration of 25  $\mu\text{g ml}^{-1}$ . Error bars represent standard deviation,  $n=3$ .



### **3.3.3 Labelling Effects on the Anti-TNT Antibody Binding Specificity**

Studies were first performed on the anti-TNT antibody's ability to recognise the bound form of the analyte, BSA-TNT. As shown in Figure 3.7, the anti-TNT antibody preferentially binds to the BSA-TNT conjugate over the BSA. The binding specificity of the unlabelled anti-TNT antibody to the BSA-TNT was compared against the AF488 labelled anti-TNT antibody (13:1), which showed similar results. These results signified that labelling did not diminish the antibody's ability to recognise BSA-TNT. Hence, the no competition seen with the unlabelled antibody studies (Section 3.3.1) was not due to the anti-TNT antibody binding to the BSA.

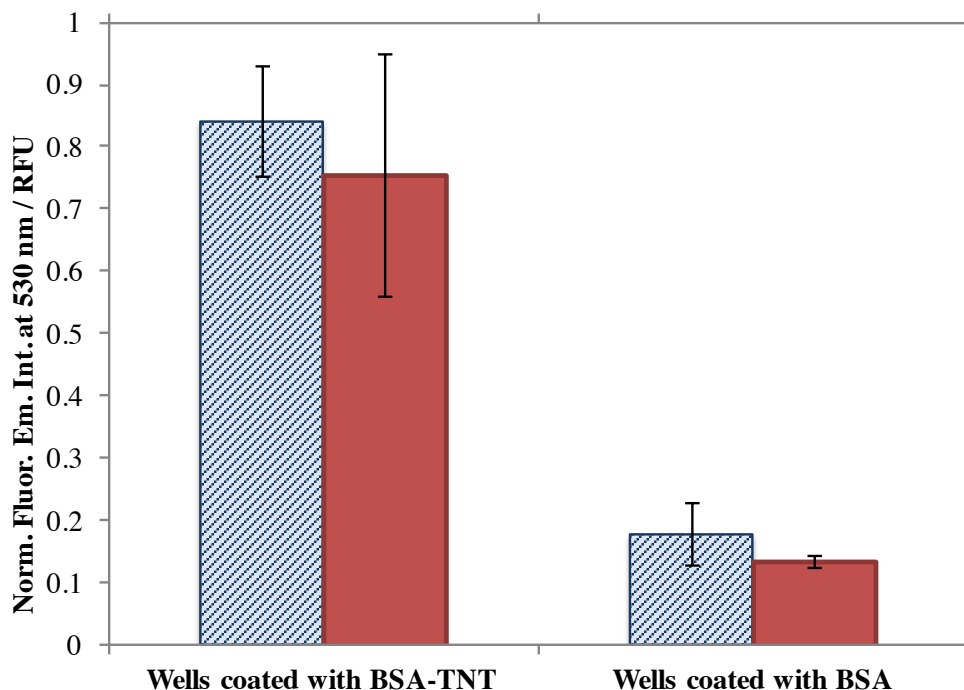


Figure 3.7: Assessment of the binding specificity of the anti-TNT antibody to the BSA-TNT, before and after labelling. Wells were coated with either  $1 \mu\text{g ml}^{-1}$  of BSA or BSA-TNT. Either  $25 \mu\text{g ml}^{-1}$  of unlabelled (red bars) or AF488 labelled (blue, dashed bars) anti-TNT antibody was added to the coated wells. The labelled antibody used had a molar dye to protein ratio of 13:1. For the unlabelled antibody,  $50 \mu\text{g ml}^{-1}$  of an AF488 labelled secondary antibody was added. Before addition of each antibody, the wells were washed with  $100 \mu\text{l}$  of  $10 \text{ mM}$  phosphate buffer,  $80 \text{ mM}$  NaCl and  $0.22 \text{ mM}$  Tween 20 (PBST) pH 7.4, three times. Error bars represent standard deviation,  $n=3$ .

### 3.3.4 Fluorescence Quenching Effects by TNT

Quenching studies were performed as described in Section 2.2.3. The highly electrophilic nature of the TNT molecule can result in its ability to quench fluorophores by accepting the excited electrons<sup>[75]</sup>. Additionally, it is possible that the TNT could bind to the BSA-TNT or the plate, or both, regardless of blocking steps. Therefore, there was a concern that the competition shown in Figure 3.6 was a result of the TNT quenching of the AF488 dye. If this were true, there would be a decrease in fluorescence signal emitted from the AF488 dye, as the TNT concentration increased. In Figure 3.8 there is no significant decrease in flu-

orescence intensity the TNT concentration was increased. Furthermore, as shown in Figure 3.6, competition is observed at 0.16-0.63  $\mu\text{g ml}^{-1}$  for the 13:1 labelled antibody. If this competition were a result of TNT quenching the fluorescence signal, it would be expected that a significant decrease of fluorescence at this concentration of TNT would be observed in Figure 3.8 as well. Since no fluorescence quenching is observed in Figure 3.8, the decrease in fluorescence signal shown in the competitive assays (Figure 3.6) is not due to quenching effects of the TNT. The quenching is instead due to the competitive binding of the antibody to the free TNT and bound TNT. This suggests that the labelling of the antibody has either increased the specificity of the anti-TNT antibody to detect TNT, reduced non-specific binding effects from the secondary antibody or, more likely, a mixture of both. Therefore, the labelled anti-TNT antibody will be used to optimise the conditions of the TNT competitive assay to increase the assay sensitivity.

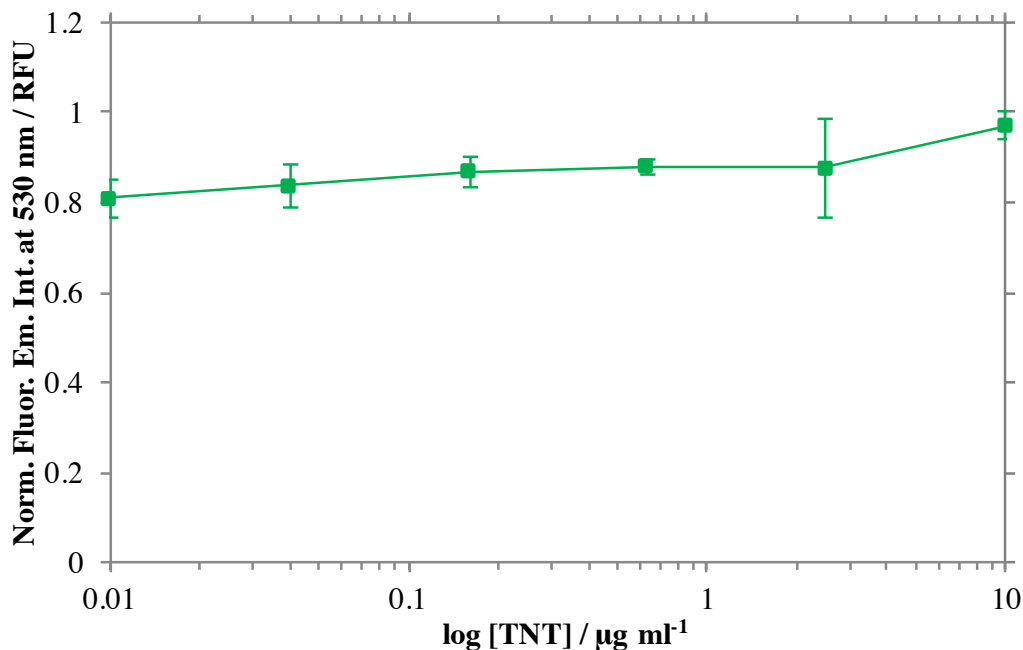


Figure 3.8: Assessment of the fluorescence quenching of the AF488 labelled anti-TNT antibody in the presence of increasing TNT concentrations (0-10  $\mu\text{g ml}^{-1}$ ). Labelled anti-TNT antibody (13:1) was added to the plate at 25  $\mu\text{g ml}^{-1}$ . Error bars represent standard deviation,  $n=3$ .

### 3.3.5 TNT Solubilisation Buffer Optimisation

The first step of the competitive immunoassay optimisation is to ensure that there is maximum solubilisation of the TNT, whilst maintaining a buffer that is compatible with the other components of the assay, such as prevention of antibody denaturation. If the TNT is solubilised then it is more accessible for binding by the antibody, which means that lower concentrations of TNT can be detected, *i.e.*, increased sensitivity. Note that for all optimisation experiments, the buffer providing the highest sensitivity was carried through for comparison against the following set of conditions. It has been shown in Chen et al.<sup>[76]</sup> that addition of methanol to TNT diluent can increase its solubility. Figure 3.9 shows the results from the competitive assays that have 10 mM phosphate buffer (PB) plus varying methanol concentrations (0%, 10% and 50%). It can be seen in Figure 3.9a that immunoassay competition occurs at 0.16-0.63  $\mu\text{g ml}^{-1}$  when TNT is solubilised in PBST (original conditions). However, solubilising the TNT in PB with 10% methanol increases the sensitivity of the assay to 0.04-0.16  $\mu\text{g ml}^{-1}$  (Figure 3.9b).

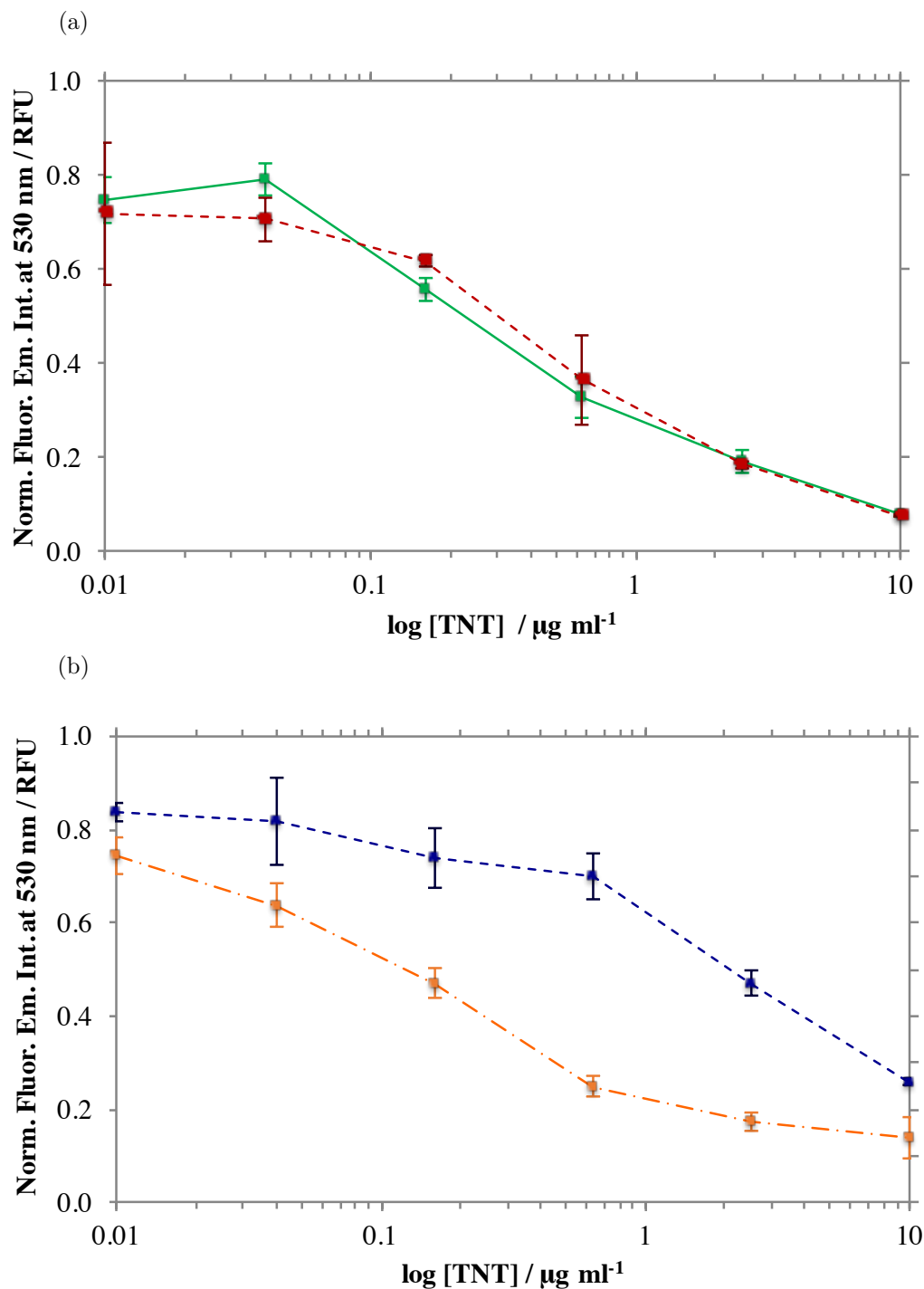


Figure 3.9: Optimisation of TNT reference solution diluent. Conditions in (a) represent phosphate buffer (red, dashed line) Vs. PBST (green, solid line) and (b) shows PB with 10% methanol (orange, dash dotted line) Vs. PB with 50% methanol (blue, dashed line). Labelled antibody (13:1) was added to the plates at  $25 \mu\text{g ml}^{-1}$ . All conditions were tested on the same plate but separated in Figures (a) and (b) for easier interpretation. Error bars represent standard deviation,  $n=3$ .

Next, different Tween 20 concentrations were tested against 10 mM PB with 10% methanol. Tween 20 is a non-ionic surfactant. As reported by Linke<sup>[77]</sup>, surfactants are used to lower a liquid's surface tension and the tension at the interface between two liquids. Surfactants are organic compounds with a hydrophobic 'tail' and hydrophilic 'head'. Tween 20 has a polysorbate head and a linear fatty acid chain tail. As the chain length is increased, so is the hydrophobicity of the surfactant. At a given concentration, the surfactant monomers aggregate into a spherical form, called a micelle. The concentration at which the surfactant forms micelles is called the critical micelle concentration (CMC)<sup>[78]</sup>. Micelles form around the hydrophobic molecules in aqueous solution, which can be a problem for small molecules, such as TNT, because the micelles may block the antibody from being able to access the TNT for binding. However, pH, temperature and salt concentration can all affect the CMC as well as directly affecting the solubility of the solute, *i.e.*, TNT, themselves. Therefore, it is important to test a range of surfactant concentrations to find the optimal solubility conditions. The Tween 20 concentration in the original solubilisation buffer, *i.e.*, PBST, was 0.22 mM. A range of Tween 20 concentrations were tested in 10 mM PB, these included: the CMC (0.06 mM), and then double (0.12 mM) and half (0.03 mM) the CMC of Tween 20. The different solutions were tested against the 10 mM PB with 10% methanol, and the results are shown in Figure 3.10. The conditions that provided the highest sensitivity was the 10 mM PB with 0.12 mM Tween 20, with immunoassay competition observed at 0.01-0.04  $\mu\text{g ml}^{-1}$ . Note that at this stage, to conserve antibody, the antibody concentration was reduced to 6.25  $\mu\text{g ml}^{-1}$ .

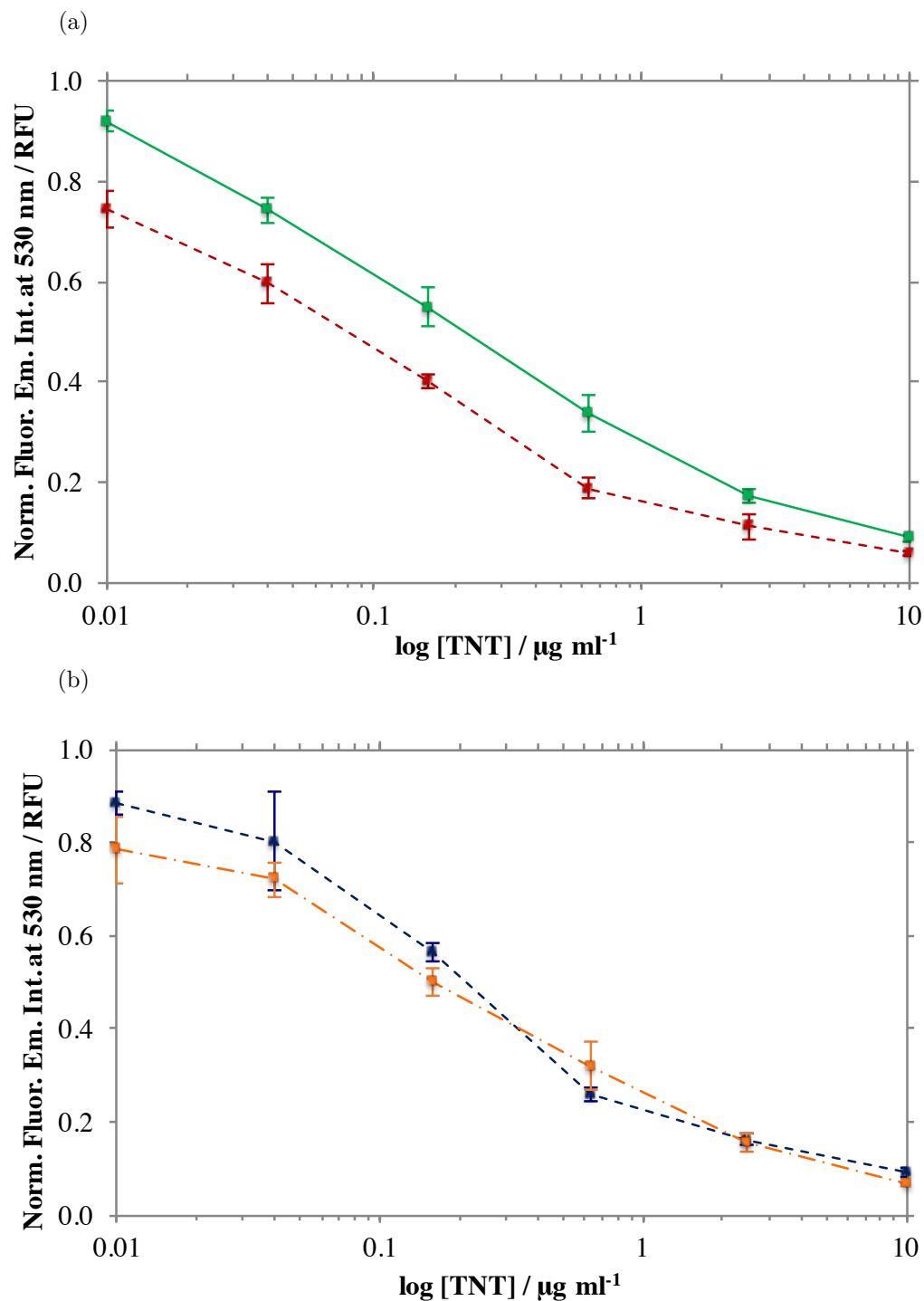


Figure 3.10: Optimisation of TNT reference solution diluent. Conditions in (a) represent 10 mM PB with 0.12 mM Tween 20 (green, solid line) Vs. 10 mM PB with 0.03 mM Tween 20 (red, dashed line) and (b) shows 10 mM PB with 0.06 mM Tween 20 (blue, dashed line) Vs. 10 mM PB with 10% methanol (orange, dash dotted line). Labelled antibody (13:1) was added to the plates at  $25 \mu\text{g ml}^{-1}$ . All conditions were tested on the same plate but separated in Figures (a) and (b) for easier interpretation. Error bars represent standard deviation,  $n=3$ .

The last component of the original PBST solution was sodium chloride (NaCl) at 80 mM. A range of NaCl concentrations were tested and the results are shown in Figure 3.11. The solutions tested were 10 mM PB with 0.12 mM Tween 20 and 0, 20, 40 or 80 mM NaCl. The optimal condition was 10 mM PB with 0.12 mM Tween 20 and 40 mM NaCl. This is because the buffer with 40 mM NaCl has the highest sensitivity, showing competition at 0.05-0.2  $\mu\text{g ml}^{-1}$ . It was shown by Luning Prak<sup>[79]</sup> that the addition of Tween 80 increased solubility of the TNT. Tween 80 is similar in structure to Tween 20, in that they both share a polysorbate head. However, Tween 80 has a longer, unsaturated fatty acid chain<sup>[77]</sup> making it a more hydrophobic surfactant. The Tween 80 was compared against Tween 20 in the TNT solubilisation buffer. The concentrations of Tween 80 were at the CMC (0.012 mM), half (0.006 mM) and double (0.024 mM) the CMC. The results are shown in Figure 3.12. It is difficult to see any improvement on the sensitivity with the addition of Tween 80. Therefore, the 10 mM phosphate buffer with 40 mM NaCl and 0.12 mM Tween 20 (pH 7.4) solubilisation buffer was taken through to the full plate optimisation studies.



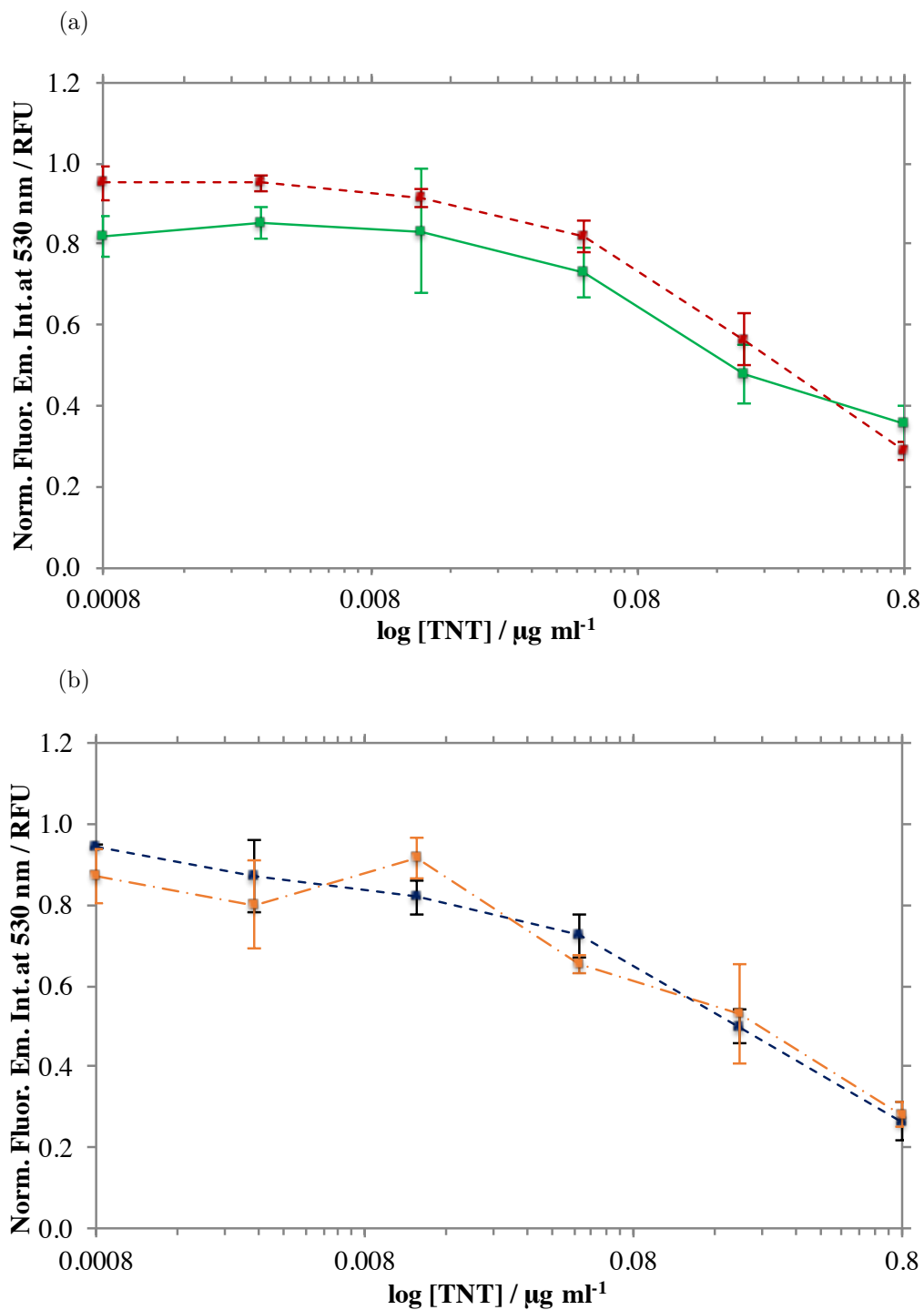


Figure 3.11: Optimisation of TNT reference solution diluent. Conditions in the figures represent 10 mM PB with 0.12 mM Tween 20 with different sodium chloride (NaCl) concentrations: (a) represent 0 mM (green, solid line) Vs. 40 mM (red, dashed line); and (b) shows 20 mM (orange, dash dotted line) Vs. 80 mM (blue, dashed line). Labelled antibody (13:1) was added to the plates at  $6.25 \mu\text{g ml}^{-1}$ . All conditions were tested on the same plate but Figures separated in (a) and (b) for easier interpretation. Error bars represent standard deviation,  $n=3$ .

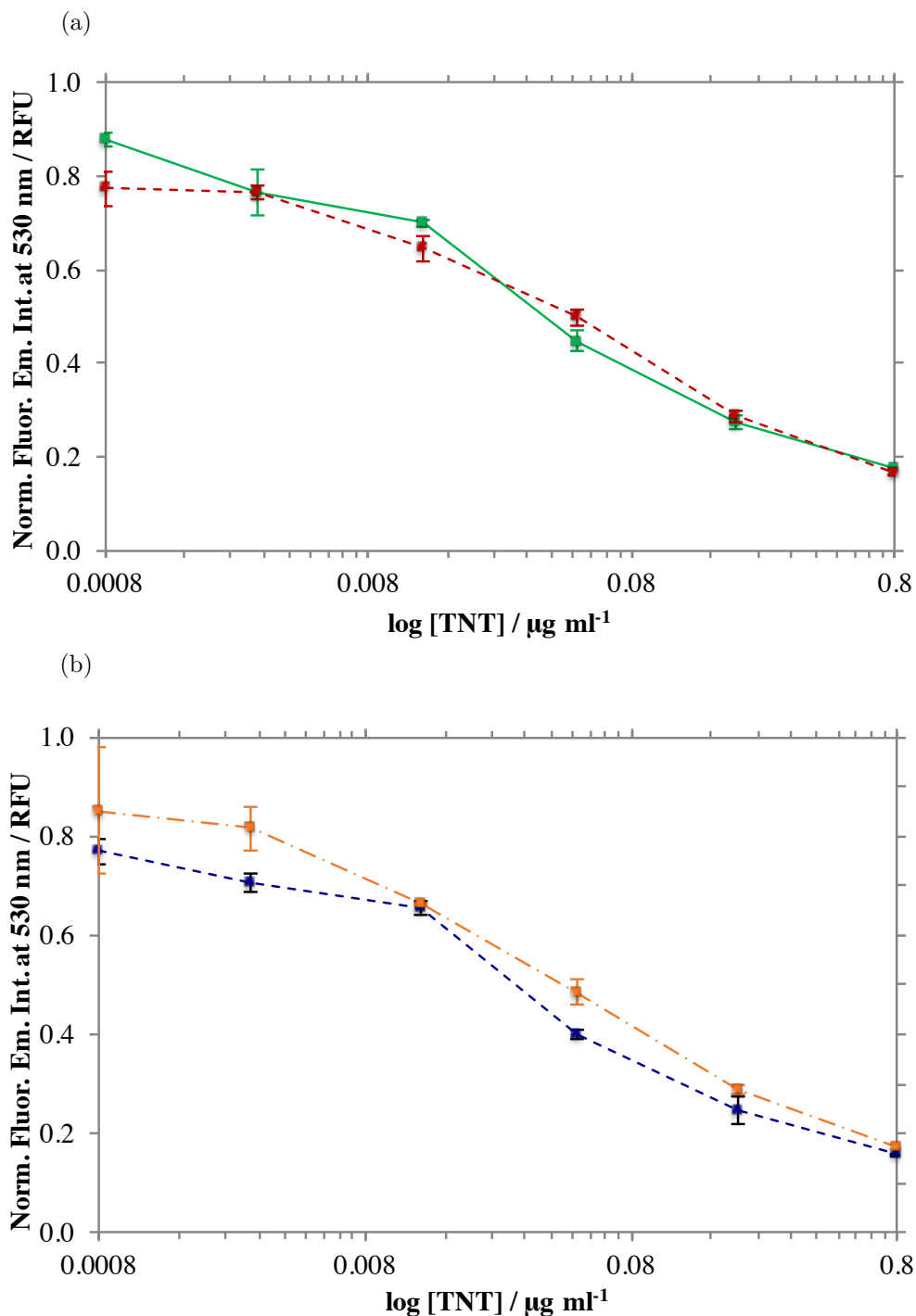


Figure 3.12: Optimisation of TNT reference solution diluent. The solubilisation buffers used were 10 mM PB with 40 mM NaCl with different concentrations of either Tween 20 or Tween 80: (a) represent 0.12 mM Tween 20 (red, dashed line) Vs. 0.006 mM Tween 80 (green, solid line); and (b) shows 0.012 mM Tween 80 (orange, dash dotted line) Vs. 0.025 mM Tween 80 (blue, dashed line). Labelled antibody (13:1) was added to the plates at  $6.25 \mu\text{g ml}^{-1}$ . All conditions were tested on the same plate but Figures separated in (a) and (b) for easier interpretation. Error bars represent standard deviation,  $n=3$ .

### 3.3.6 Plate Immunoassay Optimisation

Using the newly optimised solubilisation buffer (10 mM PB, 40 mM NaCl, 0.12 mM Tween 20, pH 7.4), a full optimisation of all plate immunoassay conditions was performed. This involved different BSA-TNT concentrations (0.25, 0.5, 1 and 2  $\mu\text{g ml}^{-1}$ ); different 13:1 antibody concentrations (0.39, 1.56 and 6.25  $\mu\text{g ml}^{-1}$ ) with a range of TNT concentrations (0 - 0.5  $\mu\text{g ml}^{-1}$ ). Figure 3.13 compares the set of plate immunoassay conditions used in the solubilisation buffer optimisation (BSA-TNT concentration at 1  $\mu\text{g ml}^{-1}$ ; anti-TNT antibody concentration at 6.25  $\mu\text{g ml}^{-1}$ ) against the set of the conditions from the full plate immunoassay optimisation that shows the highest sensitivity (BSA-TNT concentration at 0.5  $\mu\text{g ml}^{-1}$ ; anti-TNT antibody concentration at 6.25  $\mu\text{g ml}^{-1}$ ). Both sets of conditions provide a limit of detection at 0.03  $\mu\text{g ml}^{-1}$ . Hence, there is no difference in sensitivity between the conditions used in the solubilisation buffer optimisation studies and the best conditions from the full plate immunoassay conditions.

The BSA-TNT and anti-TNT antibody concentrations were fine tuned with one another to provide optimal results. It is worth noting that lower anti-TNT antibody concentrations provide more sensitive results. As stated previously, in order to detect a fluorescence signal, the anti-TNT antibody must be bound to the BSA-TNT to prevent the anti-TNT antibody from being washed off the plate. If there are lower antibody concentrations, lower TNT concentrations are required to occupy the antibody binding sites, lowering the available anti-TNT antibody that can bind to the BSA-TNT. Hence, lower antibody concentrations require lower TNT concentrations to demonstrate a significantly lower fluorescence signal, and therefore improved sensitivity. However, lowering the antibody concentration too far can result in low fluorescence intensities, with undetectable fluorescence intensity changes. On top of this, the BSA-TNT concentration can also affect the fluorescence intensity and the sensitivity of the assay. The higher the BSA-TNT concentration, the more sites available for the antibody to bind too. This means

there is higher fluorescence signals with higher BSA-TNT concentrations. Increasing the BSA-TNT concentration above a certain point can improve sensitivity, as there are greater differences in fluorescence signals with increasing TNT concentrations. However, lower BSA-TNT concentrations result in lower available sites for the unoccupied anti-TNT antibody to bind too, which again can improve sensitivity of the assay. Hence, the results shown in Figure 3.13 suggest that the original conditions using the optimised solubilisation buffer, provide optimal conditions as sensitivity was not significantly improved with any other conditions tested. Hence these conditions were taken forward.

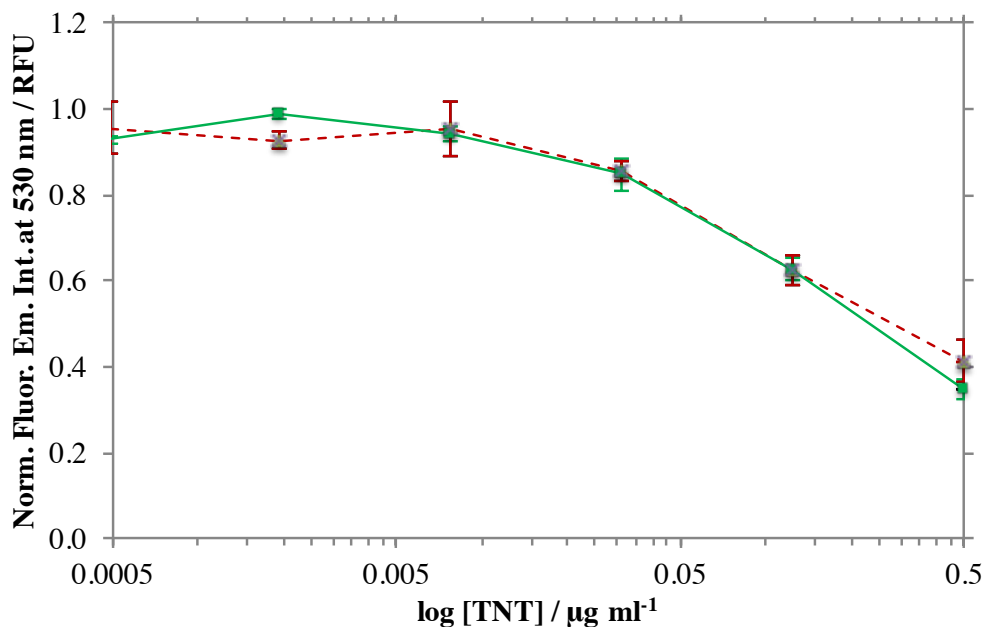


Figure 3.13: Optimisation of the TNT competitive plate assay conditions. The set of conditions used in the optimised solubilisation buffer studies are represented by the red, dashed line (BSA-TNT and anti-TNT antibody concentrations were  $1 \mu\text{g ml}^{-1}$  and  $6.25 \mu\text{g ml}^{-1}$ , respectively). The set of conditions which provided the highest sensitivity in the full plate immunoassay studies are represented by the green, solid line (BSA-TNT and anti-TNT antibody concentrations were  $0.5 \mu\text{g ml}^{-1}$  and  $6.25 \mu\text{g ml}^{-1}$ , respectively). Error bars represent standard deviation,  $n=3$ .

### 3.3.7 Competitive Plate Assay using TNT Spiked Fingerprints

In this research, the final immunoassay should be able to detect TNT from a contaminated, deposited fingerprint. Fingerprints were introduced to check that the fingerprint deposit does not interfere with the assay, for instance the anti-TNT antibody may non-specifically bind to components in the fingerprint deposit. Any interference caused by the fingerprint can result in loss of sensitivity or 'false' positives, and hence, it is important to test at an early stage in the assay development. As described in Section 2.2.4, non-contaminated fingerprints were deposited onto glass slides and then extracted. Known TNT reference solutions ( $0-8 \mu\text{g ml}^{-1}$ ) were added to the extracted fingerprint solutions. Fingerprints that have the addition of a known concentration of TNT are referred to as 'spiked' fingerprints. A control set of TNT standards (without fingerprint addition) were tested alongside. The results are shown in Figure 3.14. The data was analysed with the four parameter logistic nonlinear regression model using SigmaPlot and the  $\text{IC}_{50}$  was calculated. The  $\text{IC}_{50}$  of the TNT solutions in the presence of fingerprints was  $0.19 \mu\text{g ml}^{-1}$  of TNT; whereas, the  $\text{IC}_{50}$  with the TNT solutions in the absence of fingerprints was  $0.38 \mu\text{g ml}^{-1}$  of TNT. The lower  $\text{IC}_{50}$  value of the TNT solution in the presence of fingerprints means that lower concentrations of TNT are required to cause 50% inhibition of the anti-TNT antibody binding. Therefore, lower  $\text{IC}_{50}$  value demonstrates that the fingerprint does show some interference of the immunoassay. The interference is likely to be from non-specific binding by the anti-TNT antibody to the components in the fingerprint residue. The implication of non-specific binding of the anti-TNT antibody to the fingerprint residue is that the use of this antibody in a test could provide false positives. The non-specific binding effect should be taken into account when developing the lateral flow immunoassay test. Larger sample sizes, testing the variability and effect of the non-specific anti-TNT antibody should be assessed.

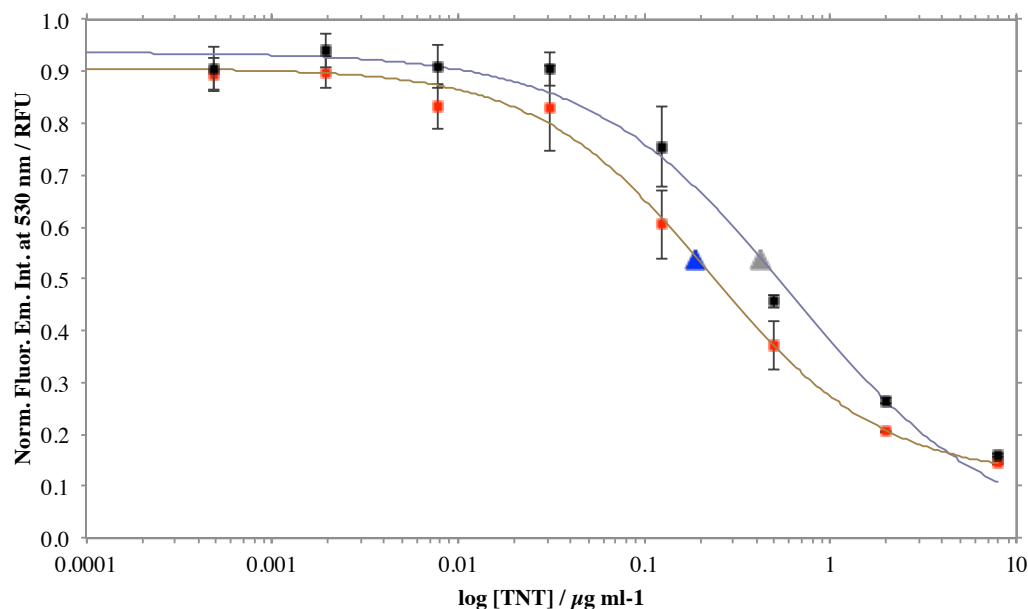


Figure 3.14: Testing the effect of the addition of fingerprints on the sensitivity of the TNT competitive assay. The TNT reference solutions either contained extracted fingerprint (red squares) or no fingerprint (black squares). Error bars represent standard deviation,  $n=3$ . The fitted curves for the TNT reference solutions containing extracted fingerprints (green line) and without fingerprints (purple line) were calculated with a four parameter logistic nonlinear regression model using SigmaPlot. The  $IC_{50}$  of the TNT solution containing fingerprints is represented by a blue triangle and the  $IC_{50}$  of the TNT solutions without fingerprints is represented by a grey triangle.

### 3.4 Conclusions

The primary aim of the research presented in this chapter was to demonstrate that TNT can be detected in a competitive plate fluoroimmunoassay. This aim has been achieved successfully. The anti-TNT antibody was first shown to recognise the bound form of TNT, *i.e.*, BSA-TNT. The next step demonstrated issues with the anti-TNT antibody recognising the free form of the TNT. The anti-TNT antibody was labelled with Alexa Fluor 488 dye to remove the requirement of the secondary antibody. This was done to reduce any effects of non-specific binding from the secondary antibody, which could mask any competition. The removal of the secondary antibody also reduced error from decreasing the number of steps

required in the assay. It was found that sensitivity of the assay was improved with removal of the secondary antibody, and increasing the ratio of moles of labelled dye to mole of anti-TNT antibody. The optimal ratio of moles of labelled dye to anti-TNT antibody was found to be between 11-13:1, both displaying the same limit of detection in the presence of TNT at  $0.63 \mu\text{g ml}^{-1}$ . The binding specificity for the BSA-TNT conjugate was assessed after labelling, where no statistically significant difference in binding specificity was observed before and after labelling. TNT was then tested for any fluorescent quenching effects on the AF488 dye that is used to label the anti-TNT antibody. No fluorescence quenching was observed, which meant that any decrease in fluorescence seen with the addition of TNT is due to the competitive binding of the anti-TNT antibody for the BSA-TNT and TNT. Consequently, higher TNT concentrations resulted in lower anti-TNT antibody concentrations bound to the BSA-TNT. To improve sensitivity, the solubilisation buffer composition, BSA-TNT and anti-TNT concentrations, *i.e.*, the immunoassay reagents, were optimised. Firstly, different compositions of the TNT solubilisation buffer were tested, including different surfactants (Tween 20 and Tween 80), salt (NaCl) and methanol concentrations. The optimal solubilisation buffer composition was found to be 10 mM phosphate buffer, 40 mM NaCl and 0.12 mM Tween 20, pH 7.4, as the solubilisation buffer provided the results with the lowest limit of detection at  $0.05 \mu\text{g ml}^{-1}$ . After this, the anti-TNT antibody and BSA-TNT concentrations were optimised, to provide the optimal sensitivity. The concentrations which provide the highest sensitivity were  $6.25 \mu\text{g ml}^{-1}$  for the anti-TNT antibody and  $1 \mu\text{g ml}^{-1}$  for the BSA-TNT. This provided a limit of detection at  $0.03 \mu\text{g ml}^{-1}$ .

The immunoassay developed in this research is to be used in the detection of TNT in fingerprints. However, a critical finding from the fingerprint studies showed that lower concentrations of TNT were required to inhibit anti-TNT antibody binding to BSA-TNT by 50% in the presence of fingerprints when compared to TNT solutions without fingerprints. Therefore, the presence of fingerprints would falsey

imply more TNT was present in the sample than there would be. The non-specific binding of the anti-TNT antibody to the fingerprint residue should be taken into consideration during development of the lateral flow immunoassay (LFIA).



## Chapter 4

# Developing a Lateral Flow Immunoassay Test Using a Competitive Binding Format

The plate immunoassay studies described in Chapter 3 have demonstrated that the antibody recognises TNT with a limit of detection of  $0.03 \mu\text{g ml}^{-1}$ . The TNT sample volume used in the competitive plate immunoassay is  $10 \mu\text{l}$ , and so that equates to a sensitivity of around  $300 \text{ pg}$  per fingerprint deposit. Therefore, Chapter 3 has demonstrated that TNT can be detected with a competitive immunoassay technique. However, the plate immunoassay method does not offer the many advantages of the lateral flow immunoassay (LFIA) format; which are that the LFIA is quick, portable, cheap and easy to use. There are elements that can be carried forward from the plate immunoassay studies in Chapter 3 to the LFIA. Firstly, a functioning, labelled anti-TNT antibody that recognises the BSA-TNT and TNT has been demonstrated for use in a competitive immunoassay format. Secondly, the solubilisation buffer has shown to be compatible for anti-TNT antibody and TNT solubilisation, and so, can be used for solubilisation of the reagents in the LFIA. However, different volumes of the reagents are required for the LFIA along with different materials; and hence, further optimisation of the

competitive immunoassay in the LFIA format will be required.

The research described in this chapter begins by employing a direct wick format. This simplifies the test set-up, only using a test strip and adsorbent pad, which may remove possible interference challenges that may arise with the full, LFIA assembly. Firstly, the test strip blocking conditions were optimised, testing different compositions. Secondly, there was comparison between the plate immunoassay and direct wick format to ensure the reaction could occur using the same conditions as the direct wick, *i.e.*, at room temperature and within four minutes. Next, the optimal BSA-TNT concentration was selected to provide maximum sensitivity. Finally, the conditions optimised on the test strip were tested using a LFIA system, *i.e.*, with full assembly of components and in a cassette. The fluorescence of the test (BSA-TNT) and control (horse anti-mouse antibody) lines were measured using a Qiagen Lateral Flow Reader, and the test strip was fluorescently imaged in an Optical Breadboard Imaging Device designed by EG Technology.

This chapter will begin with an introduction to the LFIA technique used in the research and the strengths of the LFIA format over the plate immunoassay. This will be followed by a brief look at the research published and then the aims of this chapter. The results obtained during the research will be discussed and finally a section on the conclusions drawn from the research findings.

## 4.1 Introduction

A LFIA simplifies the competitive immunoassay procedure shown in the plate immunoassay studies in Chapter 3. The test is performed along a single axis with the use of a porous membrane and designed to demonstrate if the analyte of interest (TNT) is present in a sample<sup>[80]</sup>. In LFIA, the solution moves through the system via capillary action, described as 'wicking' from here on in<sup>[81]</sup>. The LFIA format

is often used for diagnostic and detection tests, due to the many advantages it can offer. The high affinity nature of the interaction between the antibody and its corresponding analyte can result in a sensitive detection method. The sensitivity between different immunoassays can vary, as the sensitivity is largely determined by the binding affinity of the antibody with the analyte. As different immunoassays employ different antibodies with varying binding affinities, the sensitivity of an immunoassay differs between different analytes. The highly specific interaction between the antibody and its analyte means that sample preparation is usually not required, as other components in the sample should not interfere with the functioning of the assay. Without the need for sample preparation, the procedure and equipment required for testing is simplified, allowing non-specialised personnel to operate the test. It is important for a test to be easy-to-use if the test is to be applicable for use in a diverse range of environments. Although the primary use for the TNT LFIA test may be in security settings, the test could also be used in health monitoring applications. For example, one situation may be to monitor employees who are based in the manufacture of TNT products, such as munition factories, to ensure they have not been exposed to dangerous levels or accidental contamination of TNT.

In this research, the LFIA is composed of a number of materials: a sample pad, conjugate pad, test strip and adsorbent pad. The assembled components are encased in a plastic cassette (see Figure 2.3 in Section 2.4). A TNT-contaminated fingerprint is deposited onto the sample pad. Solubilisation buffer is then added to the sample pad. The buffer wicks through the sample pad solubilising the TNT in the fingerprint deposit. The conjugate pad contains the AF488 labelled anti-TNT antibody. The solubilised TNT moves with the buffer into the conjugate pad, where the anti-TNT antibody is solubilised. The TNT and anti-TNT antibody then move along the test strip. The test strip is a porous membrane (nitrocellulose) that has a test line (BSA-TNT) and a control line (horse anti-mouse antibody) deposited. As the anti-TNT antibody and the TNT wick along

the test strip, the anti-TNT antibody binds the TNT. As the solubilisation buffer passes over the test and control lines, any unbound anti-TNT antibody binds to the BSA-TNT (test line). The control line is composed of horse anti-mouse which binds any mouse antibody, TNT occupied or not. Therefore, the control line is used to confirm that the antibody has passed through the system. Note that the adsorbent pad functions to draw up the liquid through the test and prevent flow back down the strip<sup>[62]</sup>. The LFIA therefore employs the same principle as the plate immunoassay; as the free TNT concentration is increased, the lower the fluorescent signal emitted. Figure 4.1 summarises the LFIA mechanism. Note that 4.1 is shown without the cassette for easier interpretation; in the LFIA studies described in this chapter, the LFIA components are encased in a plastic cassette. In the LFIA reported in this chapter, the fluorescence signal is measured with a Qiagen ESEQuant Lateral Flow Reader. This uses a light emitting diode (LED) excitation and a photodiode detector. Hence, the fluorescence intensity corresponds to the voltage produced for the area measured ( $\text{mm}^2 \cdot \text{mV}$ ) on the test strip.

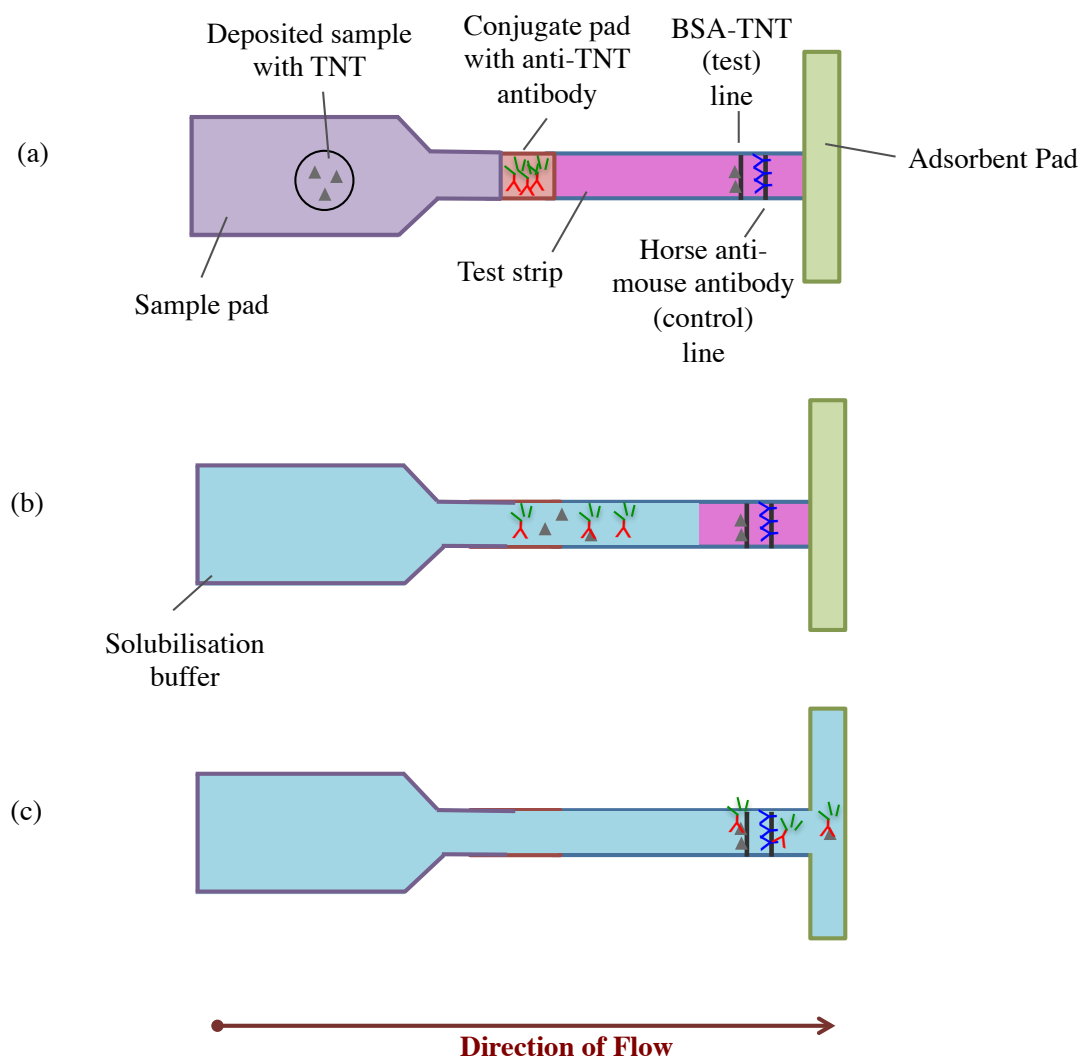


Figure 4.1: A schematic diagram summarising the LFIA mechanism used in this research. Note that in the LFIA studies described in Chapter 4, the LFIA components will be encased by a cassette. The assembled test is shown in (a). In (b), the solubilisation buffer has been added to the sample pad and has wicked along the test, solubilising the TNT in the deposited sample and anti-TNT antibody from the conjugate pad. The solubilised antibody and TNT interact as they move along the test strip. Three possible results from the LFIA have been shown in (c): the antibody bound to the test line (BSA-TNT); the antibody bound to the control line (horse anti-mouse antibody); and the antibody bound to the free TNT in the deposited sample, that has wicked through the adsorbent pad.

In comparison to the plate immunoassay format, the LFIA provides a better option for a test. Firstly, the plate immunoassay takes  $\sim 3$  hours for completion and involves a more complicated, laboratory-based procedure, that would require a higher level of training in comparison to the LFIA. The simplicity of the LFIA test will also improve the speed at which the test can be carried out, together with requiring minimal training. The design of the LFIA means that the test is portable, and hence allows for the test to be used in a wide range of settings. Results can also be obtained in minutes with a LFIA test, obtaining results in 8 minutes within the research described in this chapter. It is important for the test be fast if it is to be used in environments where large sample sets need to be tested as quick as possible, such as airports. The LFIA also has the added advantage of being relatively cheap to produce<sup>[81]</sup>.

With reference to this research, the LFIA test developed aims to detect TNT through a fingerprint deposit. As stated in Chapter 3, this mechanism is non-invasive, and through fingerprint identification, it can provide a method of linking the handler to the deposited TNT-contaminated fingerprint. Although there has been research conducted for the detection of TNT through LFIA, to date, there have been no literature reports demonstrating the detection of explosive materials in fingerprints using a LFIA mechanism. The focus of the LFIA research for explosive detection has been with contaminated environmental samples or from swabbed samples. In 2009, Maiolini et al.<sup>[82]</sup> developed a chemilluminiscent based LFIA for the detection of TNT, also using a secondary antibody labelled with gold nanoparticles. The LFIA developed by Maiolini et al.<sup>[82]</sup> had a detection limit of  $1 \mu\text{g ml}^{-1}$ . In 2010, Girotti et al.<sup>[83]</sup> demonstrated a LFIA test using a secondary antibody labelled with colloidal gold. The assay used swabbed samples containing TNT, and achieved a sensitivity of  $1 \mu\text{g ml}^{-1}$ . In 2012, Mirasoli et al.<sup>[84]</sup> developed an enzyme-based chemilluminiscent LFIA<sup>[84]</sup>, that obtained a limit of detection of  $0.2 \mu\text{g ml}^{-1}$ . The enzyme-based chemilluminiscent LFIA was also field deployable as the chemilluminiscent signal was measured by an imaging device that

was portable<sup>[84]</sup>. In 2015, Romolo et al.<sup>[85]</sup> demonstrated the use of the LFIA techniques developed by Girotti et al.<sup>[83]</sup> and Mirasoli et al.<sup>[84]</sup> for the detection of TNT in contaminated soil samples and swabbed hand samples. The technique developed by Girotti et al.<sup>[83]</sup> achieved a limit of detection of 1  $\mu\text{g ml}^{-1}$ , and the technique developed by Mirasoli et al.<sup>[84]</sup> achieved a limit of detection of 0.5  $\mu\text{g ml}^{-1}$ , with the extracted TNT contaminated soil and hand swab samples. An excellent review by Smith et al.<sup>[81]</sup> discusses the immunoassay techniques developed for the detection of explosive materials. In the review by Smith et al.<sup>[81]</sup>, a LFIA technique by DSTL is described that utilises a LFIA technique to detect TNT from swabbed samples, however the immunoassay sensitivity is not discussed.

## 4.2 Aims of the Research Described in this Chapter

In this chapter, the first aim was to demonstrate that the competitive immunoassay optimised in the plate immunoassay (see Chapter 3) can be applied to a lateral flow mechanism, *i.e.*, demonstrate using the direct wick method. The second aim was to introduce the LFIA components to produce a portable LFIA test for the detection of TNT in fingerprint deposits.

## 4.3 Results and Discussion

### 4.3.1 Direct Wick Studies

The LFIA format uses different stationary phase materials, *e.g.*, nitrocellulose, which have different treatments and therefore different properties compared to the plate assay. This can mean that a re-optimisation of the conditions are required for the analyte to remain soluble and accessible for binding by the antibody. The direct wick format was employed to remove all materials (sample pad, conjugate pad) except for the nitrocellulose, *i.e.*, the test strip and the adsorbent

pad. There are different materials that can be used for the sample pad and the conjugate pad. The role of the sample pad is to provide a platform for analyte deposition and then solubilisation of the analyte. The conjugate pad contains the antibody. Both the analyte and the antibody have to be combined in the solubilisation buffer to allow for interaction and binding. This requires the analyte to be solubilised and moved through the sample pad and then through the conjugate pad, where the antibody can be solubilised so that they can interact whilst moving through the test strip. These factors can require additional optimisation to ensure the analyte can be efficiently solubilised from the sample pad, such as alteration to the solubilisation buffer. Therefore, the direct wick format removes these additional factors as the antibody and analyte solution are premixed before being added to the test strip. As the premixed antibody and analyte solutions are added directly to the test strip, this also removes interactions which affect analyte or antibody solubility and ease of movement through the assay components.

Firstly, the optimised plate assay conditions (see Table 4.1) were replicated in the direct wick format, which can be seen in Figure 4.2. Neither a control line nor a test line was observed, yet a fluorescent area can be seen at the bottom of the test strip. The fluorescent area was the antibody, which suggests the premixed solution has not moved through the test strip. One reason for the solution unsuccessfully wicking along the test strip may be because of non-specific binding to the test strip by the antibody and the analyte in the premixed solution.

*Table 4.1: Optimised Plate Assay Conditions*

Reagent	Optimised Condition
[BSA-TNT]	1 $\mu\text{g ml}^{-1}$
[Labelled Anti-TNT Antibody]	6.25 $\mu\text{g ml}^{-1}$
Solubilisation Buffer	10 mM PB, 40 mM NaCl, 0.12 mM Tween 20 (pH 7.4)



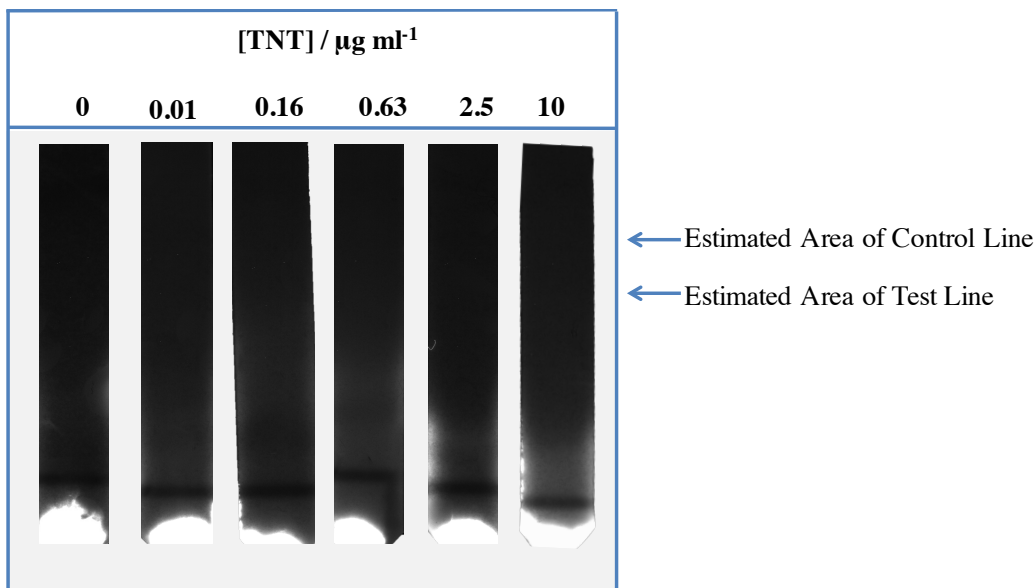


Figure 4.2: Fluorescent images of the test strips from the direct wick assay with the optimised plate assay conditions is measured using the Optical Breadboard Imaging Device designed by EG Technology. The exposure of the images was at 1 s. TNT concentration increases from 0 to 10  $\mu\text{g ml}^{-1}$ , from left to right. The estimated areas of the control (HAM) and test (BSA-TNT) lines are indicated with arrows.

Nitrocellulose is a membrane that binds proteins and so non-specific binding by the antibody is an expected effect. Wetting agents may also need to be employed to encourage movement of the solution through the test strip. Wetting agents, such as surfactants, lower the surface tension and allow the solution to spread more easily across the surface<sup>[86]</sup>. As reported by Liu et al.<sup>[87]</sup> and Mirasoli et al.<sup>[84]</sup>, BSA was used in the TNT solubilisation buffer at 0.1% and 3%, respectively. BSA is used as a blocking agent by physically blocking non-specific binding by binding to the membrane itself. A wetting agent that also has blocking properties is polyvinylpyrrolidone (PVP). Therefore, a number of different conditions were tested. The nitrocellulose was blocked with 10 mM phosphate buffer with either 0.1% BSA, 0.1% PVP or 3% PVP (pH 7.4) for 20 minutes; or the nitrocellulose received no treatment, denoted as 'None' in Figure 4.3. Each condition was then tested with either the original solubilisation buffer (Table 4.1); or solubilisation buffer with the addition of 3% BSA, denoted <sup>a</sup> in Figure 4.3. The results are

summarised in Figure 4.3. There were only two blocking conditions that did not display a control line, both used the original solubilisation buffer: the nitrocellulose that did not receive any blocking application; and nitrocellulose blocked with 0.1 % BSA. Although, the fluorescent area (antibody) has clearly wicked further along the nitrocellulose with the addition of 0.1% BSA as a blocking buffer. The remaining conditions all displayed a control line. No test line was observed with any of the conditions, suggesting that the BSA-TNT concentration was too low to produce a detectable signal. Increasing the BSA-TNT concentration should provide more binding sites for the unoccupied anti-TNT antibody to bind too, therefore increasing the fluorescence signal from the test line. Three of the conditions were taken forward for further investigation: 10 mM phosphate buffer with either 0.1% BSA, 0.1% PVP and 3% PVP.

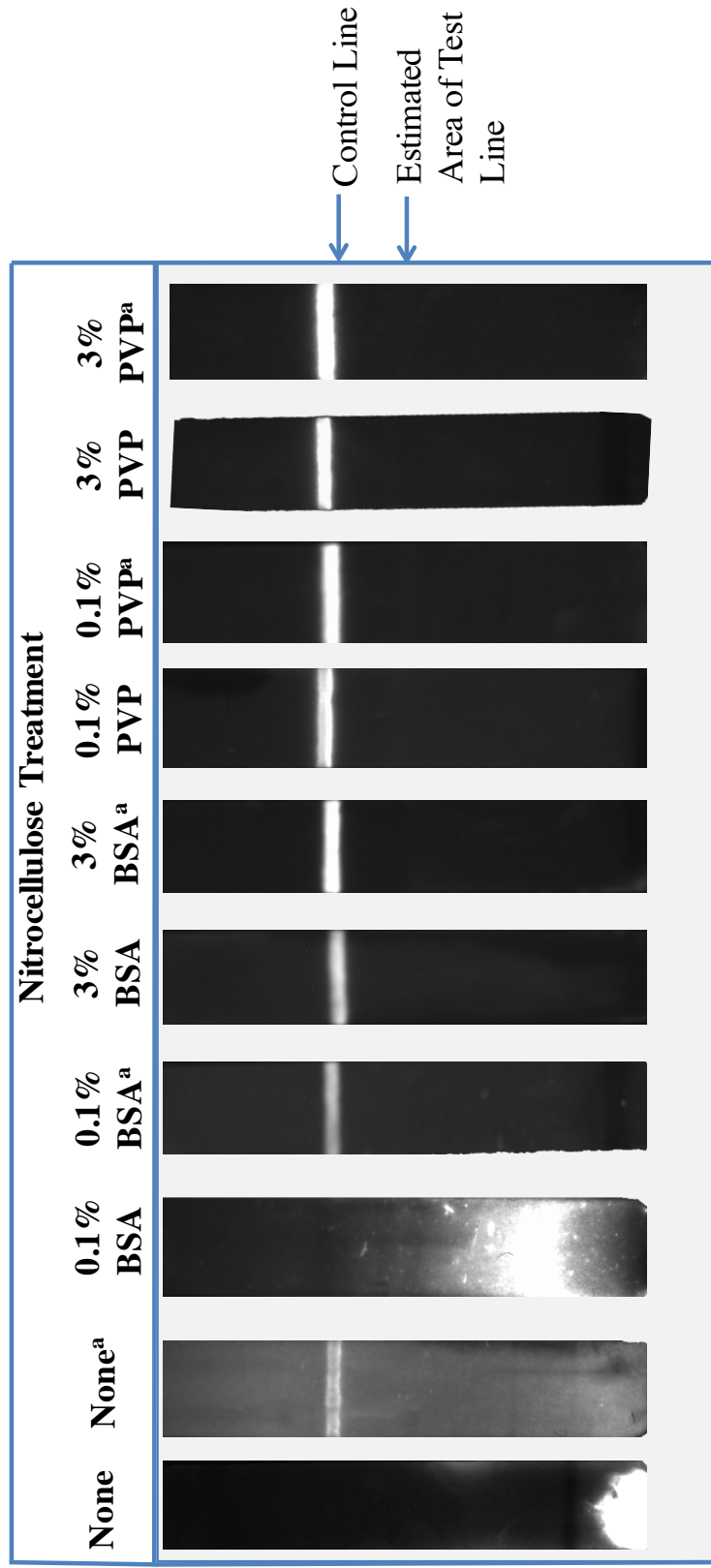


Figure 4.3: Fluorescent images of the test strips from the direct wick assay testing different nitrocellulose treatments as measured using the Optical Breadboard Imaging Device designed by EG Technology. The blocking conditions used are 10 mM PB with BSA or PVP at 0.1% or 3%, indicated above the image. Each treatment has been tested with solubilisation buffer, with and without 3% BSA. Those conditions which use solubilisation buffer with 3% BSA are indicated by <sup>a</sup>. The exposure of the images was at 1 s. The control (HAM) and test (BSA-TNT) lines are indicated with arrows.

The faintness or absence of the test line signal from Figure 4.3 suggested that the BSA-TNT concentration was too low. The anti-TNT antibody binds to the BSA-TNT. Lower BSA-TNT concentrations result in lower concentrations of anti-TNT antibodies being able to bind to the test line. As the labelled dye is bound to the anti-TNT antibody, lower concentrations of anti-TNT antibody bound to the test line result in a lower fluorescence signal detected. When the BSA-TNT concentration is too low, a fluorescence signal can not be detected above the background level, as in Figure 4.3. Therefore, the BSA-TNT concentration was increased from  $1 \mu\text{g ml}^{-1}$  (as in the plate assay) to  $5 \mu\text{g ml}^{-1}$ . From the results presented in Figure 4.3, the following nitrocellulose blocking conditions were taken forward: 10 mM PB with either 0.1% PVP, 3% PVP or 3% BSA, pH 7.4. Premixed solutions containing  $6.25 \mu\text{g ml}^{-1}$  anti-TNT antibody (13:1) with different TNT concentrations (0, 0.63, 2.5 and  $10 \mu\text{g ml}^{-1}$ ) were wicked along the test strips and the results are shown in Figure 4.4. The optimal nitrocellulose blocking condition was the 10 mM PB with 3% PVP as this provided more consistent background levels when compared to 0.1% PVP, and higher test line signals when compared to the 3% BSA blocked strips. The reduced test line signals that occurred when the nitrocellulose was blocked with 10 mM PB with 3% BSA, may be a result of the BSA physically blocking the binding between the antibody to the test line. Therefore, the nitrocellulose blocking conditions used from this point forward were: 10 mM PB with 3% PVP, pH 7.4. From the fluorescent images obtained with the Optical Breadboard Imaging Device (designed by EG Technology) and shown in Figure 4.4, it is clear that both the control and test lines are visible in all of the conditions. However, there was not a significant decrease of the test line fluorescence signal observed with increasing TNT concentrations with the readings from the ESEQuant Lateral Flow Reader.

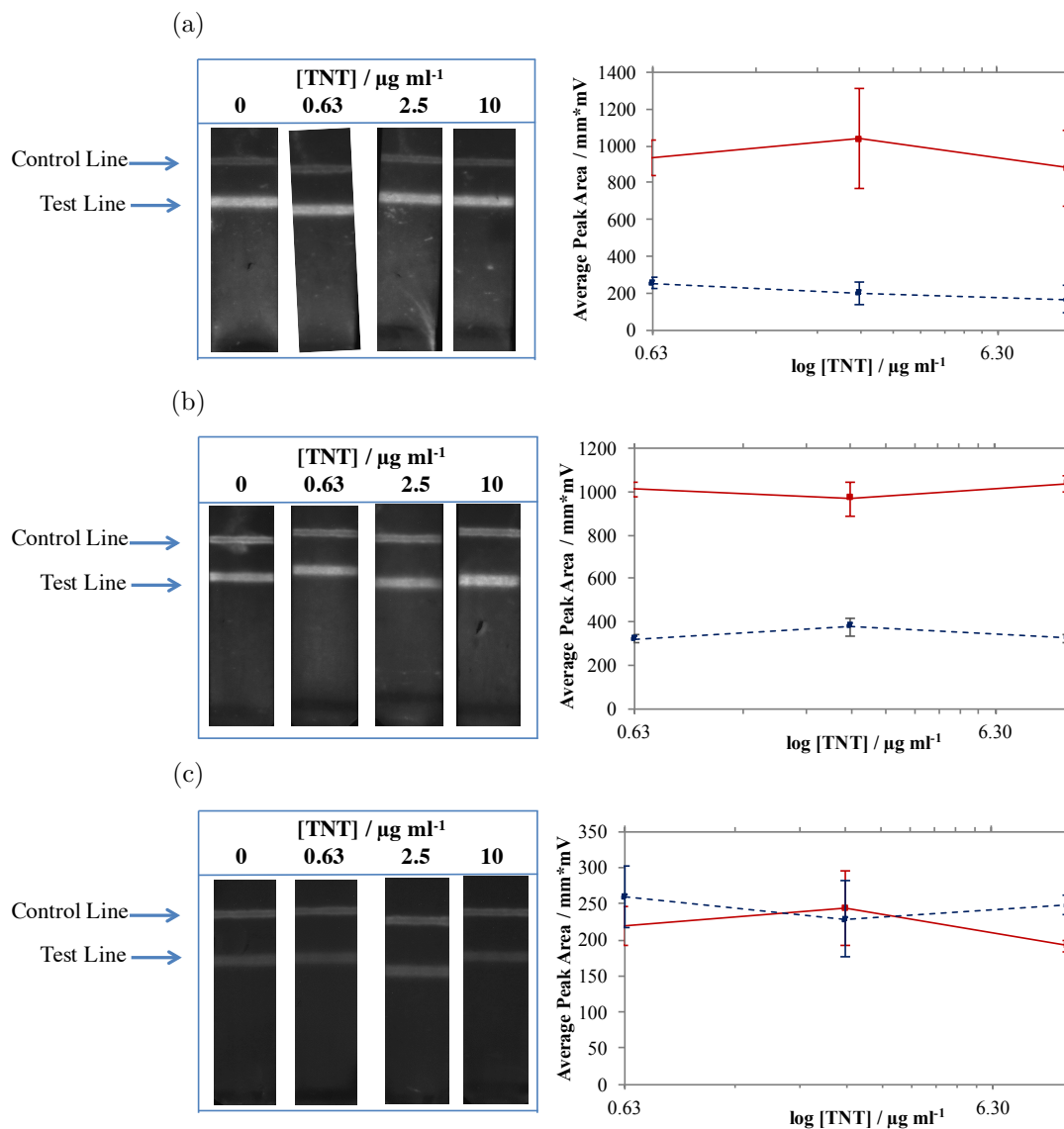


Figure 4.4: Fluorescent images of the test strips measured with the Optical Breadboard Imaging Device (EG Technology) and readings using the ESEQuant Lateral Flow Reader of the test strips from the direct wick assay results, with an increased BSA-TNT concentration of  $10 \mu\text{g ml}^{-1}$ . Different nitrocellulose blocking solution were tested, which consisted of  $10 \text{ mM PB}$  with: (a)  $0.1\% \text{ PVP}$ ; (b)  $3\% \text{ PVP}$  and (c)  $3\% \text{ BSA}$ . The control line (horse anti-mouse antibody) is the blue, dashed line and the test line (BSA-TNT) is the red, solid line on the graphs. Image exposure =  $1 \text{ s}$ . Error bars representing standard deviation,  $n=3$ .

One possibility for the loss of competition in the direct wick format may be the different temperature and time available for the reagents (antibody and analyte) to interact. In comparison to the plate immunoassay, the direct wick format is performed at a lower temperature (room temperature as oppose to 37°C in the plate immunoassay) and the reagents have a shorter time period (four minutes as oppose to one hour in the plate assay) to interact, which may affect the binding kinetics between the anti-TNT antibody and the TNT, and account for the loss of sensitivity in the direct wick experiment. The research described in Chapter 3 demonstrated that a competitive plate immunoassay format could successfully detect TNT. To test whether the loss of sensitivity in the direct wick format is due to the time and temperature at which the anti-TNT antibody and TNT interact, a plate immunoassay was performed under direct wick conditions. The competitive plate immunoassay procedure followed the same format as described in Section 2.2.2, except that 20  $\mu\text{l}$  of a premixed solution (containing anti-TNT antibody and TNT) was added to the wells for four minutes (instead of one hour, as in the competitive plate immunoassay format described in Section 2.2.2) and at room temperature (instead of 37°C, as in the competitive plate immunoassay format described in Section 2.2.2). A range of BSA-TNT concentrations were tested in the plate immunoassay. A direct wick experiment was performed at the same time as the plate immunoassay and the results are shown in Figure 4.5. The test strips from the direct wick experiment were fluorescently imaged using an Optical Breadboard Imaging Device (EG Technology) and the fluorescence of the test and control lines were measured in the ESEQuant Lateral Flow Reader. The plate from the plate immunoassay was measured in a CLARIOStar Plate Reader. The results in Figure 4.5 show that a significant decrease in fluorescence signal in the presence of 10  $\mu\text{g ml}^{-1}$ , *i.e.*, competition, was observed in the plate immunoassay but not in the direct wick format. The anti-TNT antibody and TNT solution interacted for four minutes at room temperature in both the direct wick and plate immunoassay, therefore, the loss of sensitivity in the direct wick experiments was not due to a difference in binding kinetics between the two assay formats. An

important finding from these results is that the competition seen in the plate immunoassay demonstrates that, in principle, a test can be performed at room temperature and within four minutes. However, in practice, the immunoassay would take a longer time since the wash solution is required to also elute along the nitrocellulose strip.

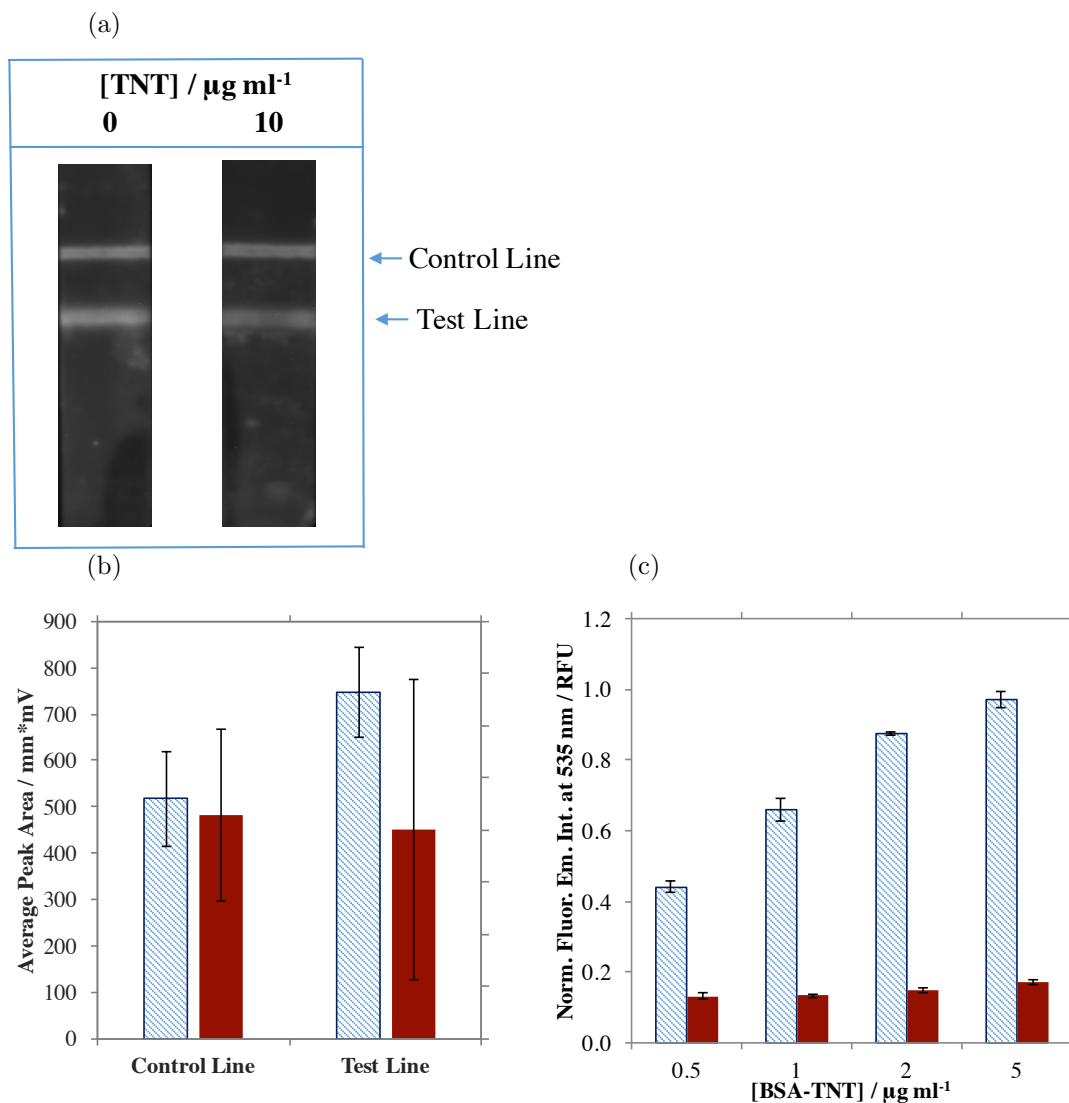


Figure 4.5: Assessment of the binding kinetics between direct wick and the plate immunoassay format, both performed under direct wick conditions (4 mins at room temperature). A) shows the fluorescent images obtained from the Optical Breadboard Imaging Device (EG Technology) of the test strips. Exposure = 1 s. Conditions are tested with 0 µg ml<sup>-1</sup> and 10 µg ml<sup>-1</sup> TNT. Test strips have a BSA-TNT concentration of 5 µg ml<sup>-1</sup>. B) shows the corresponding fluorescent readings from the ESEQuant Lateral Flow Reader of the control and test lines of the test strips, with 0 µg ml<sup>-1</sup> (blue, dashed bars) and 10 µg ml<sup>-1</sup> (red, solid bars). C) shows the plate immunoassay results performed under direct wick conditions, i.e., adding a premixed solution to the BSA-TNT coated wells (0.5, 1, 2 or 5 µg ml<sup>-1</sup> of BSA-TNT) for 4 mins at room temperature. Each condition was tested with 0 µg ml<sup>-1</sup> (blue, dashed bars) or 10 µg ml<sup>-1</sup> (red, solid bars) of TNT. Error bars representing standard deviation, n=3.



For the results shown in Figure 4.5c, the plate contained wells coated with different BSA-TNT concentrations (0.5, 1, 2 and 5  $\mu\text{g ml}^{-1}$ ) because the exact area and amount of BSA-TNT that interacts with the premixed solution is unknown, and hence can not be replicated from the plate immunoassay to the direct wick assay. Therefore, a range of BSA-TNT concentrations were tested. All BSA-TNT concentrations on the plate immunoassay demonstrated competition, which suggested that the loss of sensitivity in the direct wick format may be due to the antibody being in such excess that it saturates the BSA-TNT test line. Saturation of the test line is a result from the antibody binding to all the free TNT in solution and still having sufficient remaining antibody to bind to the sites available (BSA-TNT) on the test line, giving a high fluorescence signal. Hence, no competition will be observed. This can be resolved by increasing the BSA-TNT concentration in the test line on the test strips, so that the antibody is no longer in such excess. Another option is to lower the antibody concentration, however, this will result in loss of fluorescent signal. Therefore, a range of BSA-TNT concentrations were tested which include: 10, 50, 100, 200 and 400  $\mu\text{g ml}^{-1}$ . The results are shown in Figure 4.6. As can be seen from the images in Figure 4.6a, all BSA-TNT conditions showed at least one test strip showing competition. There was a statistically significant decrease in fluorescence signal of the test line, measured with the ES-EQuant Lateral Flow Reader, at BSA-TNT concentrations at 10, 100 and 400  $\mu\text{g ml}^{-1}$  (Figure 4.6b). The variability from the results is likely to be from the direct wick format which can have an uneven flow and loss of solution to the surrounding material, *i.e.*, the 2 ml tube. A cassette is employed in the fully assembled, LFIA format, which is designed to direct the flow of the solution so that neither sample nor antibody are lost to the surrounding material. Therefore, variability of the test and control line fluorescent signals should be reduced when using the LFIA format.

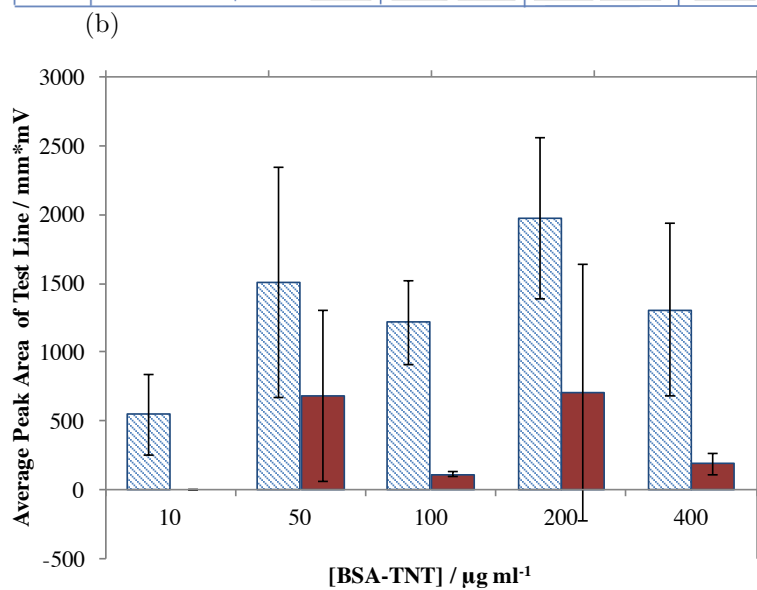
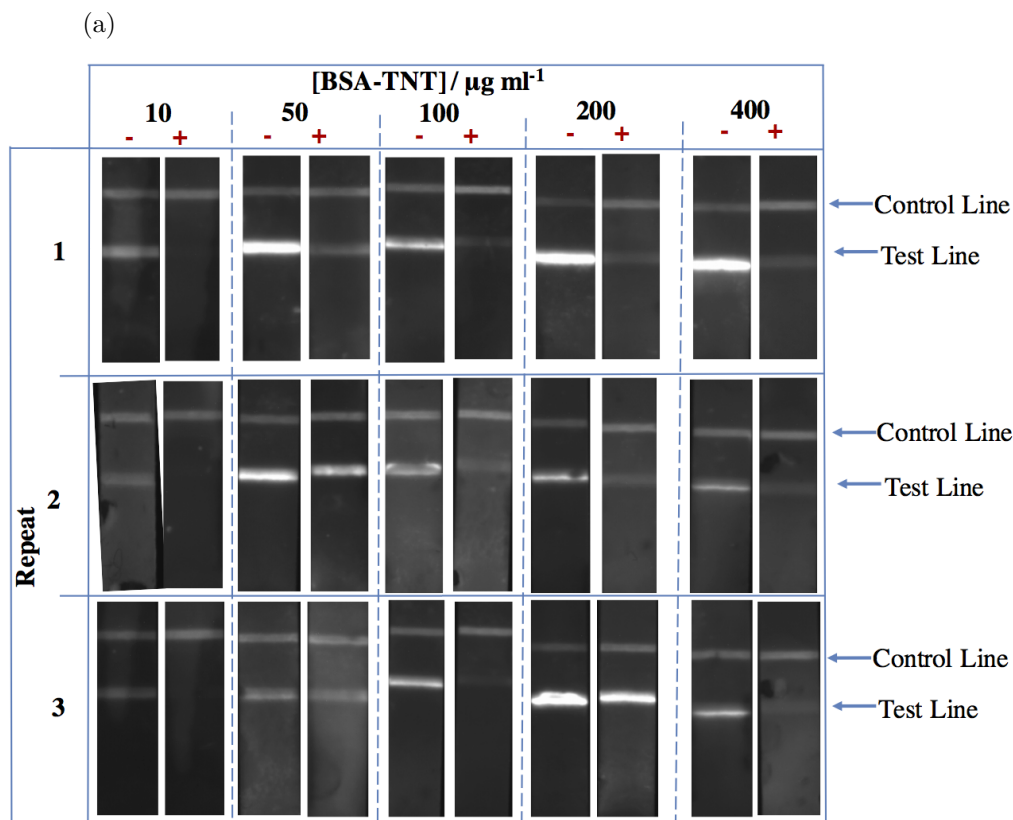


Figure 4.6: Assessment of increased BSA-TNT concentrations to improve sensitivity of direct wick assay format. The fluorescent images of the test strips obtained using an Optical Breadboard Imaging Device (EG Technology) are shown in (a). Exposure = 1 s. Conditions were tested with 0  $\mu\text{g ml}^{-1}$  (-) and 10  $\mu\text{g ml}^{-1}$  (+) of TNT. BSA-TNT concentrations tested were 10, 50, 100, 200 and 400  $\mu\text{g ml}^{-1}$ . The corresponding readings (obtained using the ESEQuant Lateral Flow Reader) of the test lines on the test strips from (a) are shown in (b). Error bars representing standard deviation,  $n=3$ .

The optimal condition for the results shown in Figure 4.6 were the strips deposited with  $10 \mu\text{g ml}^{-1}$  of BSA-TNT, because there was complete obliteration of the test line signal, seen in both the fluorescent images (obtained with the Optical Breadboard Imaging Device, EG Technology) and the readings of the test line (measured with the Qiagen ESEQuant Lateral Flow Reader) of the test strips. Therefore, test strips were deposited with  $10 \mu\text{g ml}^{-1}$  of BSA-TNT and tested with a range of TNT concentrations to establish the sensitivity of the assay. The results are shown in Figure 4.7. It is clear from both the fluorescent images (Figure 4.7a) and ESEQuant readings (Figure 4.8b) that there was high variability with the test line fluorescence signals between repeats of the same TNT concentration. At each TNT concentration from  $0.63$  to  $10 \mu\text{g ml}^{-1}$ , there are test strips which show competition, *i.e.*, loss of fluorescence signal, and strips that do not. This can be seen from the loss of test line fluorescent intensity in the images in Figure 4.7a. As stated previously, from observations when performing the direct wick, it is likely that the lack of consistency may be due to loss of liquid to the underneath of the test strip and surrounding tube. This results in insufficient and inefficient movement of the solution through the test strip. Inefficient movement of the premixed solution through the test strip could result in lower concentrations of antibody reaching the test and control lines. It is important to note that inefficient movement of the solution through the test strip did not necessarily result in the loss of fluorescence signal at the test line. Hence, those test strips which demonstrate competition are not a result of a loss of solution and reduced antibody concentrations reaching the test lines. To reduce variability, the competitive TNT immunoassay was tested in the LFIA format.

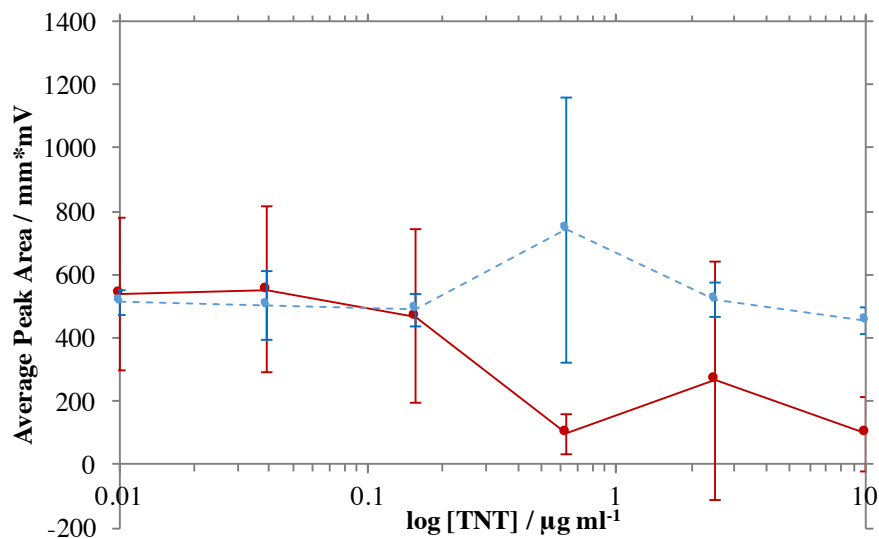
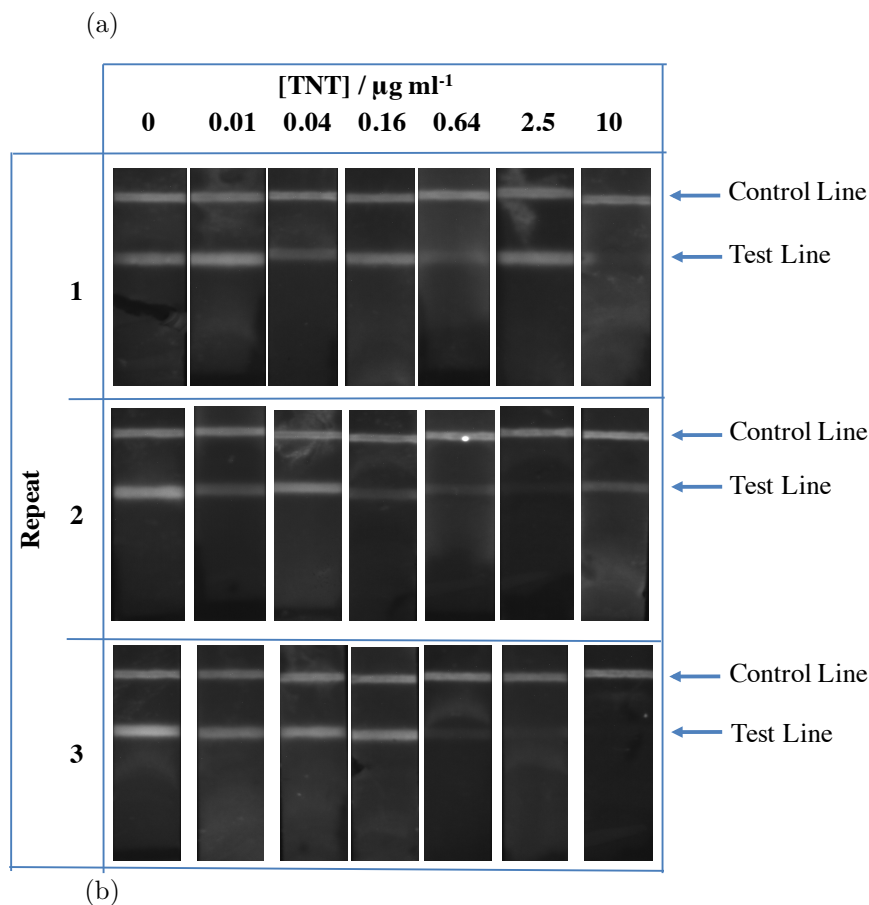


Figure 4.7: Measurement of the sensitivity of the TNT assay using a range of TNT concentrations ( $0\text{-}10 \mu\text{g ml}^{-1}$ ). The fluorescent images obtained using an Optical Breadboard Imaging Device (EG Technology) of the test strips are shown in (a). Exposure = 1 s. The corresponding fluorescent readings (measured on the Qiagen ESEQuant Lateral Flow Reader) of the control (blue, dashed line) and test (red, solid line) lines of the test strips are shown in (b). Error bars representing standard deviation,  $n=3$ .

### 4.3.2 LFIA Studies

The LFIA format was used with the aim to reduce the variability issues that arose from the direct wick method. In the LFIA, the materials are enclosed within a cassette and are assembled so that the flow is directed through the system to prevent loss of solution. The results from the LFIA can be seen in Figure 4.8, and fluorescent images of the test strips were obtained from an Optical Breadboard Imaging Device (EG Technology) and the fluorescent signals of the test and control lines were measured in the Qiagen ESEQuant Lateral Flow Reader. Unfortunately, neither the fluorescent images nor the readings from the ESEQuant Lateral Flow Reader demonstrated competition, as there was no significant decrease in fluorescence intensity at the test line with increasing levels of TNT. This could be due to a number of reasons. Firstly, sensitivity may have been lost due to the addition of different materials (sample pad and conjugate pad), and larger volumes of solubilisation buffer used in the LFIA, compared to the direct wick method. This would mean that the BSA-TNT and anti-TNT antibody concentrations may need further optimisation. Secondly, it is important to remember the stages involved in the LFIA system to understand the problems which may arise. The sample containing TNT is deposited onto the sample pad. The solution wicks along the sample pad, solubilising the TNT. The solution containing the TNT then moves into the conjugate pad, which contains the anti-TNT antibody. As the solution passes through the conjugate pad, it solubilises the anti-TNT antibody. The solution which contains the TNT and the anti-TNT antibody moves onto the test strip, where the anti-TNT antibody and TNT interact. As the solution moves along the test strip, the anti-TNT antibody binds the TNT. As the solution moves over the test line, any anti-TNT antibody which is not occupied by TNT can bind to the BSA-TNT. With this in mind, the TNT may be interacting or binding to the sample pad material, making it more difficult to solubilise the TNT than the anti-TNT antibody, which could mean that the anti-TNT antibody and TNT do not have an opportunity to interact before they reach the test line.

There are different approaches to overcome this problem. Different materials for the sample pad and conjugate pad could be tested, along with different blocking solutions, to encourage movement of the TNT through the system. However, one important finding from the results presented in Figure 4.8 is that both the test and control lines were observed in the fluorescent images (obtained with an Optical Breadboard Imaging Device) and fluorescent readings (measured with the Qiagen ESEQuant Lateral Flow Reader) of the test strips. In order for there to be fluorescent signals detected at the test and control lines, the anti-TNT antibody must have been solubilised by the solubilisation buffer and successfully wicked along the test strip, suggesting that the cassette design and assembly of the components enables successful flow of the solution and reagents through the LFIA system.

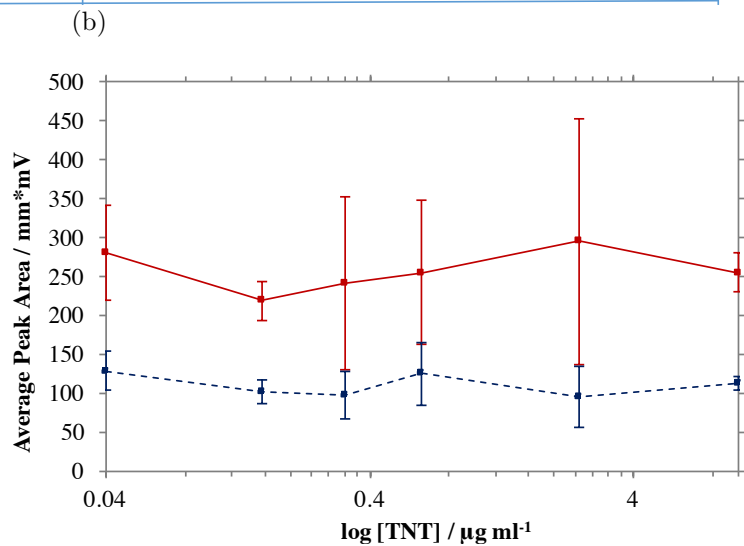
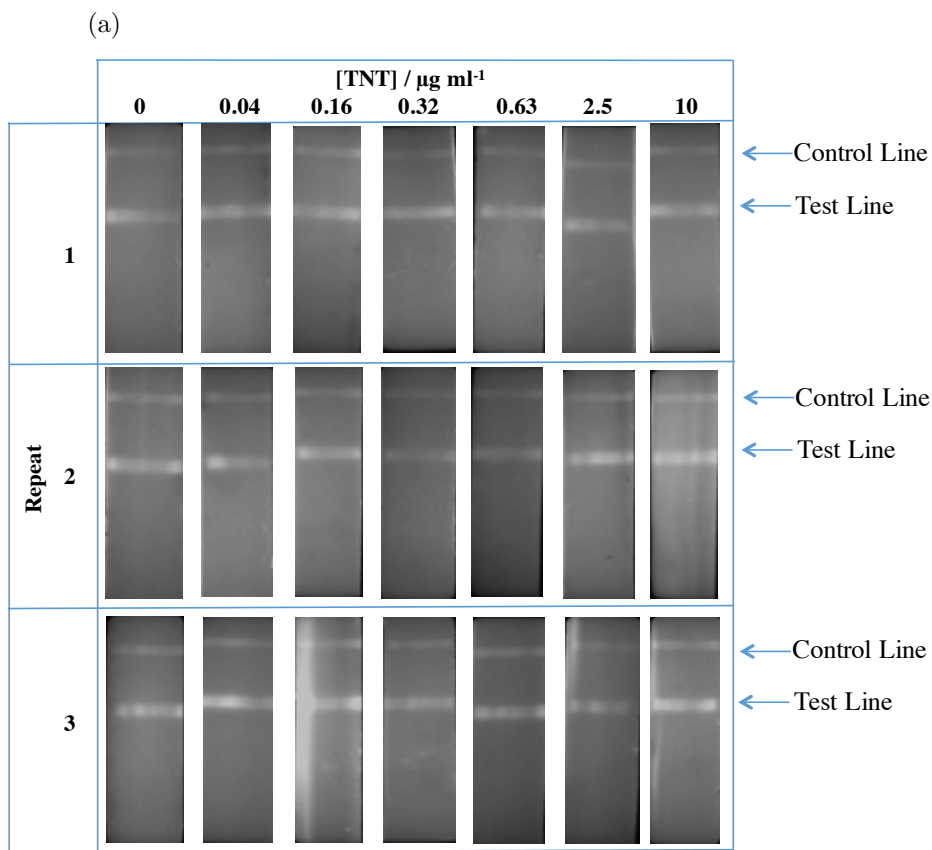


Figure 4.8: Measurement of the sensitivity of the TNT assay with a range of TNT concentrations ( $0\text{-}10 \mu\text{g ml}^{-1}$ ). The fluorescent images obtained with an Optical Breadboard Imaging Device (EG Technology) of the test strips are shown in (a). Exposure = 1 s. The corresponding fluorescent readings (measured with a Qiagen ESEQuant Lateral Flow Reader) of the control (blue, dashed line) and test (red, solid line) lines of the test strips are shown in (b). Error bars representing standard deviation,  $n=3$ .

## 4.4 Conclusions

The research described in this chapter begins with the direct wick experiments. The optimised conditions were taken from the plate immunoassay (Chapter 3) for the direct wick experiments. Firstly, it was highlighted that the nitrocellulose test strip required a blocking step since the antibody-TNT solution was not able to move through the test strip, as control and test lines were not observed. Therefore, it was likely that the antibody or TNT were non-specifically binding to the nitrocellulose. A range of conditions involving BSA and PVP were tested. It was found that the optimal conditions, *i.e.*, those conditions which had successful movement of the solution through the nitrocellulose test strip, were 10 mM phosphate buffer with either 0.1% BSA, 0.1% PVP or 3% PVP. These conditions all displayed control lines and had high fluorescent signals. No test lines were observed on any of the conditions, suggesting that the BSA-TNT concentration was too low for a signal to be detected. Therefore, the three best blocking conditions were taken forward for further testing. The BSA-TNT concentration was increased from 1  $\mu\text{g ml}^{-1}$  to 5  $\mu\text{g ml}^{-1}$ , and a range of TNT concentrations were tested to find the sensitivity of the assay. Both a test line and control line were observed in all test strips. However, no decrease in fluorescent signal was observed with increasing TNT concentration, *i.e.*, no competition. The condition with the lowest background signal was 10 mM phosphate buffer with 3% PVP, which suggested that this condition provided the lowest levels of non-specific binding. Therefore, the optimal blocking conditions selected were 10 mM phosphate buffer with 3% PVP for all future studies.

The lack of competition observed may have been due to the time and temperature for which the anti-TNT antibody and TNT interact, which was different between the direct wick (four minutes at room temperature) and plate immunoassay (one hour at 37°C). The difference in time and temperature, between the direct wick and plate immunoassay formats, could affect the binding kinetics of the reaction,



and hence, account for the lack of sensitivity in the direct wick format. Therefore, a plate immunoassay was performed alongside a direct wick experiment, using the same time and temperature conditions that the anti-TNT antibody and TNT interact at in the direct wick format. The results showed that the plate immunoassay displayed competition under direct wick conditions, suggesting the lack of sensitivity in the direct wick was due to binding kinetic differences. Therefore, different BSA-TNT concentrations were tested on the test strips, ranging from 10-400  $\mu\text{g ml}^{-1}$ . The optimal conditions were found to be 10  $\mu\text{g ml}^{-1}$  showing complete obliteration of the test line signal in the presence of 10  $\mu\text{g ml}^{-1}$  of TNT. The sensitivity of the assay was then tested by using a range of TNT concentrations. There was a trend with increasing TNT concentration and decreasing fluorescence signal, however, the results were variable so that there could be no statistical significant decrease. The high variability was likely to be an error of the direct wick method, with solution being lost to the tube and inefficient wicking of the solution. Therefore, the optimised conditions were applied to the LFIA.

The LFIA is designed to direct the flow of the solution through the system, reducing error and the variability of the results. The results from the LFIA did have reduced variability but no competition of the immunoassay was observed, which could be because the TNT was not able to move through the different materials fast enough to interact with the anti-TNT antibody. Hence, there needs to be further screening of materials used for the sample and conjugate pads; and/or treatment to the materials.

# Chapter 5

## Conclusions and Future Work

### 5.1 Conclusions

Detection of TNT has been shown in a competitive immunoassay (plate immunoassay format) at a limit of detection of around  $0.03 \mu\text{g ml}^{-1}$ . The assay sensitivity was achieved through optimisation of various components of the immunoassay. Firstly, the anti-TNT antibody was labelled with an AF488 dye to remove the need for a secondary antibody, which reduces the number of steps required in the assay and consequently reduces error. The moles of dye labelled to one mole of anti-TNT antibody was optimised, testing a range of ratios that included: 3:1, 9:1, 11:1 and 13:1. The optimal moles of dye per mole of anti-TNT antibody was 11-13:1, both providing similar sensitivity. It was clear that as the number of moles of labelled dye increased, so did the sensitivity of the assay. Labelling an antibody can result in alterations to the tertiary structure. This could involve alterations to the binding site of the antibody, which could have either a positive, neutral or negative affect on the antibody's ability to recognise the TNT. In this case, the labelling of the anti-TNT antibody was thought to result in a positive effect, as sensitivity improved with high moles of dyes labelled per mole of anti-TNT antibody.

The next stage of the TNT plate immunoassay optimisation was to ensure the solution used to solubilise the TNT, *i.e.*, the solubilisation buffer, provided optimal solubilisation of TNT so that it was accessible to the antibody. It was important to ensure the solubilisation buffer was suitable for the TNT, anti-TNT antibody and lateral flow immunoassay (LFIA) materials that would be used during this research. Different compositions of the solubilisation buffer were tested, involving the addition of methanol; different surfactants (Tween 20 and Tween 80) and different salt (NaCl) concentrations. The solubilisation buffer which provided the highest sensitivity ( $0.03 \mu\text{g ml}^{-1}$ ) was 10 mM phosphate buffer with 40 mM NaCl and 0.12 mM Tween 20 at pH 7.4. Addition of a dissolved fingerprint was tested with the optimised conditions to ensure that a fingerprint residue did not interact with the functioning of the assay. It was shown that the fingerprint did interfere with the sensitivity of the immunoassay, as lower concentration of TNT were required to inhibit 50% of binding of the BSA-TNT by the anti-TNT antibody. During development of the LFIA test, a larger sample size to measure the effect and variability of the fingerprint residue should be studied. It may be necessary to screen different anti-TNT antibodies to aim to improve binding specificity for the TNT by the anti-TNT antibody.

The competitive immunoassay principle relies on competitive binding between the bound and free form of TNT by the anti-TNT antibody. Lower antibody concentrations improve assay sensitivity because lower TNT concentrations are required to occupy the anti-TNT antibody and prevent binding of the antibody to the BSA-TNT, *i.e.*, competition. However, when the anti-TNT antibody concentrations are too low, the fluorescence signal is difficult to detect. Hence, there is balance between sensitivity and signal. Increasing the BSA-TNT concentration can provide more molecules for the anti-TNT antibody to bind to, and thus increase the fluorescence signal. The balance between the anti-TNT antibody and BSA-TNT needs careful optimisation to provide a sensitive and detectable assay. The optimal conditions were found to be with the anti-TNT antibody at a

concentration of  $6.25 \mu\text{g ml}^{-1}$  and the BSA-TNT at  $1 \mu\text{g ml}^{-1}$ , in the plate assay. These conditions were taken forward to the direct wick method.

The LFIA (lateral flow immunoassay) test requires different materials and volumes of solutions, as compared to the plate immunoassay. Analytes can interact with the materials used in the LFIA, which can interfere with the functioning of the assay. Therefore, the direct wick method was employed first as it only uses the most basic components of the test, which are the nitrocellulose test strip and the adsorbent pad. The direct wick method aims to show that the basic principle of the competitive immunoassay can function in the LFIA format, as well as to show that the analyte and antibody do not interact with the nitrocellulose. It was shown that the nitrocellulose required to be blocked before adding the TNT and anti-TNT antibody as it was difficult for the reagents to move along the test strip, which may have been due to non-specific binding as the nitrocellulose is known to bind proteins. The optimal blocking buffer was found to be 10 mM PB with 3% PVP at pH 7.4. It was then observed that the BSA-TNT concentration was too low at  $1 \mu\text{g ml}^{-1}$ , as a test line was difficult to detect. As the control line produced a high fluorescence signal, it was thought that the immunoassay was functioning properly. A range of BSA-TNT concentrations were then tested, and the optimal concentration selected was  $10 \mu\text{g ml}^{-1}$ . The limit of detection using the direct wick method was likely to be  $0.16 \mu\text{g ml}^{-1}$  but was not statistically significant due to the large variability from the results, shown by the error bars. The variability was likely to be due to the error in the method of the direct wick assay. It was observed that there was insufficient wicking of the solubilisation buffer along the test strip, with some solution being lost to the surrounding tube and resulted in two out of the three test strips tested demonstrating competition at  $2.5 \mu\text{g ml}^{-1}$ . However, competition was observed with all three repeats for the lower TNT concentration of  $0.63 \mu\text{g ml}^{-1}$ . As the lack of consistency may be due to the direct wick method, the TNT competitive immunoassay was taken forward to be tested in the LFIA.

The LFIA aims to reduce inconsistency as the test is designed to direct the flow of the solution and reagents through the system. Although reduced variability was demonstrated in the LFIA, suggested by the reduced standard deviation, competition was not observed with increasing concentrations of TNT. As stated previously, the TNT analyte could interact with the different materials and components used in the LFIA, such as the sample pad and the conjugate pad. As a control and test line were both observed, the anti-TNT antibody clearly moved through the test as expected. However, the TNT and anti-TNT antibody may not have come into contact with each other, which would mean that the TNT was more difficult to solubilise after deposition on the Fusion 5 sample pad.

## 5.2 Future Work

There would be a number of studies that would be completed to obtain a working LFIA. Firstly, different BSA-TNT and anti-TNT antibody concentrations would be tested to see if the sensitivity of the assay could be improved. The LFIA requires larger volumes of solubilisation buffer to move through the system, as there is a larger distance for the buffer to travel, and more components compared to the direct wick assay. Although the anti-TNT antibody and TNT would interact for the same distance in the direct wick assay and the LFIA, *i.e.*, along the test strip length, more solubilisation buffer is required as the solubilisation buffer must travel along the sample pad and conjugate pad before reaching the test strip. Therefore, the TNT and anti-TNT antibody may become more dilute in the LFIA method, as the LFIA requires a larger volume of solubilisation buffer than the direct wick method. The anti-TNT antibody and BSA-TNT concentration could be tested at a range of concentrations to find optimal sensitivity. It is also possible that the anti-TNT antibody and TNT interact with the materials in the LFIA, such as the sample pad or conjugate pad, which could result in the antibody or TNT being more difficult to solubilise in the solubilisation buffer

and lower the concentration of the reagents passing through the system. Two approaches could be taken to overcome the problem of efficient TNT solubilisation. Firstly, the sample pad and conjugate pad could be tested with different blocking conditions to improve the movement of the TNT and anti-TNT antibody through the system. Secondly, a range of materials could be tested for use as the sample pad or conjugate pad, to assess whether a different material could be more easily solubilised than from the current material (Fusion 5). If these conditions resulted in a functioning and detectable LFIA, volunteer fingerprints would be tested to determine whether TNT residue can be detected.

Once a functioning LFIA test for the detection of TNT has been developed, the LFIA could be applied to different explosive materials. The LFIA test developed in this research is based on the high affinity and highly specific interaction between an antibody and its complimentary analyte. Therefore, the LFIA test could be applied for use in the detection of other explosive materials, such as RDX and PETN, as anti-RDX and anti-PETN antibodies are available.

## Chapter 6

## References

- [1] M Kücken and A C Newell. Fingerprint formation. *Journal of theoretical biology*, 235(1):71–83, 2005.
- [2] S Cadd, M Islam, P Manson, and S Bleay. Fingerprint composition and aging: a literature review. *Science & justice*, 55(4):219–238, March 2015.
- [3] J R Vanderkolk. Forensics: identical twins don’t share fingerprints. *Nature*, 499(7456):29, 2013.
- [4] D A Garzón-Alvarado and A M Ramírez Martínez. A biochemical hypothesis on the formation of fingerprints using a turing patterns approach. *Theoretical biology & medical modelling*, 8(1):24, 2011.
- [5] A R W Jackson and J M Jackson. Trace and contact evidence part II: fingerprints and other marks and impressions. In C Holden, R Woodward, and G Hall, editors, *Forensic science*, chapter 4, pages 87–89. Prentice Hall, New Jersey, 3rd edition, 2008.
- [6] J R Vanderkolk. Examination process. In E Holder, L Robinson, and J Laub, editors, *The fingerprint sourcebook*, chapter 9, page 26. U.S. Department of Justice, Office of Justice Programs, National Institute of Justice, Washington DC, 1st edition, 2011.
- [7] A C Weaver. Biometric authentication. *Computer*, 39(2):96–97, 2006.
- [8] H S Kahn. Fingerprint ridge-count difference between adjacent fingertips (dR45) predicts upper-body tissue distribution: evidence for early gestational programming. *American journal of epidemiology*, 153(4):338–344, 2001.



- [9] K Wilke, A Martin, L Terstegen, and S S Biel. A short history of sweat gland biology. *International journal of cosmetic science*, 29(3):169–179, 2007.
- [10] A M Porter. Why do we have apocrine and sebaceous glands? *Journal of the royal society of medicine*, 94(5):236–237, 2001.
- [11] E Boelsma, L van de Vijver, R A Goldbohm, I A Klopping-Ketelaars, H Hendriks, and L Roza. Human skin condition and its associations with nutrient concentrations in serum and diet. *The american journal of clinical nutrition*, 77(2):348–355, 2003.
- [12] R S Croxton, M G Baron, D Butler, T Kent, and V G Sears. Variation in amino acid and lipid composition of latent fingerprints. *Forensic science international*, 199:93–102, 2010.
- [13] M Frick, S K Modi, S J Elliott, and E P Kukula. Impact of gender on fingerprint recognition. In *5th international conference on information technology and applications*, pages 717–721, 2008.
- [14] S K Modi, S J Elliott, J Whetsone, and H Kim. Impact of Age Groups on Fingerprint Recognition Performance. In *Workshop on Automatic Identification Advanced Technologies*, pages 19–23. IEEE, 2007.
- [15] R Merkel, J Dittmann, and C Vielhauer. How contact pressure, contact time, smearing and oil/skin lotion influence the aging of latent fingerprint traces: first results for the binary pixel feature using a CWL sensor. In *International workshop on information forensics and security*, pages 1–6. IEEE, 2011.
- [16] J S Day, H G M Edwards, S A Dobrowski, and A M Voice. The detection of drugs of abuse in fingerprints using Raman spectroscopy I: latent fingerprints. *Spectrochimica acta part a: molecular and biomolecular spectroscopy*, 60:563–568, 2004.
- [17] L Senesac and T G Thundat. Nanosensors for trace explosive detection. *Materials today*, 11(3):28–36, 2008.

- [18] S Singh. Sensors—an effective approach for the detection of explosives. *Journal of hazardous materials*, 144(1-2):15–28, 2007.
- [19] R K. Eckhoff. Explosives, pyrotechnics, and propellants. In *Explosion hazards in the process industries*, chapter 6, pages 313–352. Gulf Publishing Company, Texas, 2005.
- [20] J Pichtel. Distribution and fate of military explosives and propellants in soil: A review. *Applied and environmental soil science*, 2012, 2012.
- [21] J A Conkling and C Mocella. *Chemistry of pyrotechnics: basic principles and theory*. CRC Press, Florida, 2nd edition, 2010.
- [22] P O K Krehl. *History of shock waves, explosions and impact - a chronological and biographical reference*. Springer Berlin Heidelberg, Berlin, 2009.
- [23] J Yinon. *Toxicity and metabolism of explosives*. CRC Press, Florida, 1990.
- [24] S Letzel, T Göen, M Bader, J Angerer, and T Kraus. Exposure to nitroaromatic explosives and health effects during disposal of military waste. *Occupational and environmental medicine*, 60(7):483–488, 2003.
- [25] P Lucena, I Gaona, J Moros, and J J Laserna. Location and detection of explosive-contaminated human fingerprints on distant targets using standoff laser-induced breakdown spectroscopy. *Spectrochimica acta part b: atomic spectroscopy*, 85:71–77, 2013.
- [26] J R Verkouteren. Particle characteristics of trace high explosives: RDX and PETN. *Journal of forensic sciences*, 52:335–340, 2007.
- [27] J R Verkouteren, J L Coleman, and I Cho. Automated mapping of explosives particles in composition C-4 fingerprints. *Journal of Forensic Sciences*, 55(2):334–340, 2010.

- [28] A Kraj, D M Desiderio, and N M Nibbering. *Mass spectrometry: instrumentation, interpretation, and applications*. John Wiley & Sons, New York, 2008.
- [29] D R Ifa, N E Manicke, A L Dill, and R G Cooks. Latent fingerprint chemical imaging by mass spectrometry. *Science*, 321(5890):805, 2008.
- [30] F Rowell, J Seviour, A Y Lim, C G Elumbaring-Salazar, J Loke, and J Ma. Detection of nitro-organic and peroxide explosives in latent fingerprints by DART- and SALDI-TOF-mass spectrometry. *Forensic science international*, 221(1-3):84–91, 2012.
- [31] K Clemons, J Dake, E Sisco, and G F Verbeck. Trace analysis of energetic materials via direct analyte-probed nanoextraction coupled to direct analysis in real time mass spectrometry. *Forensic science international*, 231:98–101, 2013.
- [32] S N Cross, E Quinteros, and M Roberts. Surface modification for the collection and identification of fingerprints and colorimetric detection of urea nitrate. *Journal of forensic sciences*, 60(1):193–196, 2015.
- [33] G A Eiceman and J A Stone. Ion mobility spectrometers in national defense. *Analytical chemistry*, 76(21):390 A–397 A, 2004.
- [34] G A Eiceman, Z Karpas, and H H Jr. Hill. *Ion mobility spectrometry*. CRC Press, Florida, 3rd edition, 2013.
- [35] J L Staymates, S Orandi, M E Staymates, and G Gillen. Method for combined biometric and chemical analysis of human fingerprints. *International journal for ion mobility spectrometry*, 17(2):69–72, 2014.
- [36] H Hill and G Simpson. Capabilities and limitations of ion mobility spectrometry for field screening applications. *Field analytical chemistry and technology*, 1(13):119–134, 1997.

- [37] W Brown, B Iverson, E Anslyn, and C Foote. *Organic chemistry*. Brooks/Cole, California, 7th edition, 2013.
- [38] M Á F Fernández de la Ossa, J M Amigo, and C García-Ruiz. Detection of residues from explosive manipulation by near infrared hyperspectral imaging: a promising forensic tool. *Forensic science international*, 242:228–35, 2014.
- [39] M Á Fernández de la Ossa, C García-Ruiz, and J M Amigo. Near infrared spectral imaging for the analysis of dynamite residues on human handprints. *Talanta*, 130:315–321, 2014.
- [40] G G Hammes. *Spectroscopy for the biological sciences*. John Wiley & Sons, New Jersey, 2005.
- [41] R Bhargava, R Perlman, D C Fernandez, I W Levin, and E G Bartick. Non-invasive detection of superimposed latent fingerprints and inter-ridge trace evidence by infrared spectroscopic imaging. *Analytical and bioanalytical chemistry*, 394(8):2069–2075, 2009.
- [42] T Chen, Z D Schultz, and I W Levin. Infrared spectroscopic imaging of latent fingerprints and associated forensic evidence. *The analyst*, 134(9):1902–1904, 2009.
- [43] Y Mou and J W Rabalais. Detection and identification of explosive particles in fingerprints using attenuated total reflection-Fourier transform infrared spectromicroscopy. *Journal of forensic sciences*, 54(4):846–850, 2009.
- [44] P M Fredericks. Forensic analysis of fibres by vibrational spectroscopy. In J M Chalmers, H G M Edwards, and M D Hargreaves, editors, *Infrared and raman spectroscopy in forensic science*, chapter 4.4, page 163. John Wiley & Sons, New Jersey, 2012.
- [45] G Mogilevsky, L Borland, M Brickhouse, and A W Fountain III. Raman spectroscopy for homeland security applications. *International journal of spectroscopy*, 2012:1–12, 2012.

- [46] I Malka, A Petrushansky, S Rosenwaks, and I Bar. Detection of explosives and latent fingerprint residues utilizing laser pointer-based Raman spectroscopy. *Applied physics b*, 113(4):511–518, 2013.
- [47] Q Wang, K Liu, H Zhao, C H Ge, and Z W Huang. Detection of explosives with laser-induced breakdown spectroscopy. *Frontiers of physics*, 7(6):701–707, 2012.
- [48] C López-Moreno, S Palanco, J J Laserna, F DeLucia Jr, A W Miziolek, J Rose, R A Walters, and Andrew I. Whitehouse. Test of a stand-off laser-induced breakdown spectroscopy sensor for the detection of explosive residues on solid surfaces. *Journal of analytical atomic spectrometry*, 21:55, 2006.
- [49] F C De Lucia, J L Gottfried, C A Munson, and A W Miziolek. Double pulse laser-induced breakdown spectroscopy of explosives: initial study towards improved discrimination. *Spectrochimica acta part b: atomic spectroscopy*, 62(12):1399–1404, 2007.
- [50] J Moros, J Serrano, F J Gallego, J Macías, and J J Laserna. Recognition of explosives fingerprints on objects for courier services using machine learning methods and laser-induced breakdown spectroscopy. *Talanta*, 110:108–117, 2013.
- [51] M. Abdelhamid, F. J. Fortes, M. A. Harith, and J. J. Laserna. Analysis of explosive residues in human fingerprints using optical catapulting-laser-induced breakdown spectroscopy. *Journal of analytical atomic spectrometry*, 26(7):1445–1450, 2011.
- [52] L M Dorozhkin, V A Nefedov, A G Sabelnikov, and V G Sevastjanov. Detection of trace amounts of explosives and/or explosive related compounds on various surfaces by a new sensing technique/material. *Sensors and actuators b: chemical*, 99:568–570, 2004.

- [53] R Burns. Immunochemical techniques. In K Wilson and J Walker, editors, *Principles and techniques of biochemistry and molecular biology*, chapter 7, pages 263–299. Cambridge University Press, New York, 7th edition, 2010.
- [54] F Miroslav. Biosynthesis of antibodies. In *Handbook of immunochemistry*, chapter 7, page 154. Springer Science & Business Media, New York, 2012.
- [55] K D Blaney and P R Howard. Immunology: basic principles and applications in the blood bank, 1. In *Basic & applied concepts of blood banking and tranfusion particles*, chapter 1, page 3. Elsevier, Missouri, 3rd edition, 2008.
- [56] S R Mikkelsen and E Corton. *Bioanalytical chemistry*. John Wiley & Sons, New Jersey, 2004.
- [57] C A Janeway, P Travers, M Walport, and M J Shlomchik. Antigen recognition by B-cell and T-cell receptors. In P Austin and E Lawrence, editors, *Immunobiology: the immune system in health and disease*, chapter 3, pages 93–123. Garland Science, New York, 5th edition, 2001.
- [58] R F Venn. Immunoassay techniques. In *Principles and practice of bioanalysis*, chapter 8, pages 151–176. CRC Press, Florida, 2nd edition, 2008.
- [59] A K Abbas, S Pillai, and A H Lichtman. Antibodies and antigens. In *Cellular and molecular immunology*, chapter 5, pages 89–108. Elsevier/Saunders, Philadelphia, 7th edition, 2012.
- [60] P Englebienne. Immuno- and receptor-assay design. In *Immune and receptor assays in theory and practice*, chapter 5, pages 181–226. CRC Press, Florida, 1999.
- [61] S S Deshpande. Immunoassay classification and commercial technologies. In *Enzyme immunoassays from concept to product development*, chapter 8, pages 240–242. Chapman and Hall, New York, 1996.

- [62] M Sajid, A Kawde, and M Daud. Designs, formats and applications of lateral flow assay: a literature review. *Journal of saudi chemical society*, pages 1–17, September 2014.
- [63] J R Albani. Fluorescence spectroscopy principles. In *Principles and applications of fluorescence spectroscopy*, chapter 7, pages 88–113. Blackwell Publishing, Oxford, 2007.
- [64] J R Lakowicz. *Introduction to fluorescence*. Springer, New York, 3rd edition, 2006.
- [65] I D Johnson and M T Z Spence. Fluorophores and their amine-reactive derivatives. In *Molecular probes handbook: a guide to fluorescent probes and labeling technologies*, chapter 1, pages 11–91. Life Technologies, Inc., California, 11th edition, 2010.
- [66] Thermo Fisher Scientific Alexa Fluor<sup>®</sup> 488 Antibody Labeling Kit. [online] available at: <https://www.thermofisher.com/order/catalog/product/a20181> [accessed 25-08-2015].
- [67] Invitrogen Alexa Fluor<sup>®</sup> 488 Protein Labeling Kit. [online] available at: <https://tools.thermofisher.com/content/sfs/manuals/mp10235.pdf> [accessed 20-08-2015].
- [68] GE Healthcare PD-10 desalting columns handbook. [online] available at: [https://www.gelifesciences.com/gehcls\\_images/gels/related\\_content/files/1314723116657/litdoc52130800bb\\_20110830191706.pdf](https://www.gelifesciences.com/gehcls_images/gels/related_content/files/1314723116657/litdoc52130800bb_20110830191706.pdf) [accessed 26-08-2015].
- [69] F A Costanzo. Underwater explosion phenomena and shock physics. In T Proulx, editor, *Structural dynamics, volume 3*, page 919. Springer, New York, 2011.
- [70] L Wang, Y Hung, H Lo, and C Yapijakis, editors. *Handbook of industrial and hazardous wastes treatment*. Marcel Dekker, New York, 2nd edition, 2004.

- [71] J Yinon. Field detection and monitoring of explosives. *Trends in analytical chemistry*, 21(4):292–301, 2002.
- [72] A Esteve-Núñez, A Caballero, and J L Ramos. Biological degradation of 2,4,6-trinitrotoluene. *Microbiology and molecular biology reviews*, 65(3):335–352, 2001.
- [73] K K Kartha, S S Babu, S Srinivasan, and A Ajayaghosh. Attogram sensing of trinitrotoluene with a self-assembled molecular gelator. *Journal of the american chemical society*, 134(10):4834–4841, 2012.
- [74] D D Fetterolf, J L Mudd, and K Teten. An enzyme-linked immunosorbent assay (ELISA) for trinitrotoluene (TNT) residue on hands. *Journal of forensic sciences*, 36(2):343–349, 1991.
- [75] Y Ma, S Wang, and L Wang. Nanomaterials for luminescence detection of nitroaromatic explosives. *Trends in analytical chemistry*, 65:13–21, 2015.
- [76] L Chen, F Zhou, and J Wang. Solubilities of 2,4,6-trinitrotoluene in methanol and binary mixtures of methanol + water from 293.15 to 333.15 K. *Journal of Solution Chemistry*, 43(12):2163–2169, 2014.
- [77] D Linke. Detergents: an overview. *Methods in enzymology*, 463:603–617, 2009.
- [78] A Chattopadhyay and E London. Fluorimetric determination of critical micelle concentration avoiding interference from detergent charge. *Analytical biochemistry*, 139(2):408–412, June 1984.
- [79] D J Luning Prak. Solubilization of nitrotoluenes in micellar nonionic surfactant solutions. *Chemosphere*, 68(10):1961–1967, 2007.
- [80] G A Posthuma-Trumpie, J Korf, and A van Amerongen. Lateral flow (immuno)assay: its strengths, weaknesses, opportunities and threats. A literature survey. *Analytical and bioanalytical chemistry*, 393(2):569–582, 2009.



- [81] R G Smith, N D'Souza, and S Nicklin. A review of biosensors and biologically-inspired systems for explosives detection. *The analyst*, 133(5):571–584, 2008.
- [82] E Maiolini, S Girotti, E Ferri, P Caputo, G Guarnieri, S Eremin, A Montoya, M Moreno, and M D'elia. Development of chemiluminescent methods for explosives detection. *Ovidius university annals of chemistry*, 20(1):57–60, 2009.
- [83] S Girotti, S Eremin, A Montoya, M J Moreno, P Caputo, M D'Elia, L Ripani, F S Romolo, and E Maiolini. Development of a chemiluminescent ELISA and a colloidal gold-based LFIA for TNT detection. *Analytical and bioanalytical chemistry*, 396(2):687–695, 2010.
- [84] M Mirasoli, A Buragina, L S Dolci, M Guardigli, P Simoni, A Montoya, Elisabetta Maiolini, Stefano Girotti, and Aldo Roda. Development of a chemiluminescence-based quantitative lateral flow immunoassay for on-field detection of 2,4,6-trinitrotoluene. *Analytica chimica acta*, 721:167–172, 2012.
- [85] F S Romolo, E Ferri, M Mirasoli, M D'Elia, L Ripani, G Peluso, R Risoluti, E Maiolini, and Stefano Girotti. Field detection capability of immunochemical assays during criminal investigations involving the use of TNT. *Forensic science international*, 246:25–30, 2015.
- [86] N V Churaev and V D Sobolev. Wetting of low-energy surfaces. *Advances in colloid and interface science*, 134-135:15–23, 2007.
- [87] J L Liu, D Zabetakis, G Acevedo-Vélez, E R Goldman, and G P Anderson. Comparison of an antibody and its recombinant derivative for the detection of the small molecule explosive 2,4,6-trinitrotoluene. *Analytica chimica acta*, 759:100–104, 2013.